The Synthesis of Azides from Alcohols using Sulfonyl Azides

By

Brian J. Dobosh

Submitted in Partial Fulfillment of the Requirements

for the Degree of

Masters of Science

in the

Chemistry

Program

YOUNGSTOWN STATE UNIVERSITY

August, 2008

The Synthesis of Azides from Alcohols using Sulfonyl Azides

Brian J. Dobosh

I hereby release this thesis to the public. I understand that this thesis will be made available from the OhioLINK ETD Center and the Maag Library Circulation Desk for public access. I also authorize the University or other individuals to make copies of this thesis as needed for scholarly research.

Signature: _____

Brian J. Dobosh Date

Approvals:

_____

Dr. Peter Norris Date
Thesis Advisor

_____

Dr. John Jackson Date
Committee Member

_____

Dr. Howard Mettee Date
Committee Member

_____

Dr. Peter J. Kasvinsky Date
Dean of Graduate Studies

Thesis Abstract

The following thesis deals with the synthesis of azide products from their alcohol starting materials, utilizing sulfonyl azides as the azide nucleophile source. The reactions were carried out in a microwave (MW) reactor. It also deals with the attempted MW assisted synthesis of *N*-Sulfonylamides in aqueous solutions in the presence of copper sulfate and ascorbic acid, as well as the synthesis of a possible monomer for use as an artificial knee cartilage.

Acknowledgements

I would first off like to thank my family who have supported me throughout my master's and undergraduate career at YSU. Secondly, I would like to thank Dr. Peter Norris for helping me to grow and mature as both a chemist and a person. Also, I would like to thank other committee members, Dr. John Jackson and Dr. Howard Mettee for their insights and suggestions. Dr. Matthias Zeller deserves a special thanks for solving the crystal structures that appear in this thesis, as well as for the help he offered in other aspects of research. Finally, I would like to thank all the members of the Norris research group that I have known throughout the years. You have all impacted my life in numerous ways. A special thanks goes to Lucas Beagle, who instructed me in many life lessons, and to always strive for "little victories".

Table of Contents

List of Tables

List of Schemes

List of Equations

List of Equations (cont'd)

List of Figures

List of Figures (cont'd)

List of Figures (cont'd)

Introduction

Microwave-Assisted Synthesis of Organic Azides

Azides are a broad and diverse class of organic compounds. They serve as useful building blocks in natural product synthesis, are easily converted to other functional groups, and prove to be useful industrial and pharmaceutical reagents. Upon the synthesis of the first organic azide, phenyl azide, by Peter Grieβ (Griess) in 1864, interest in azides waned considerably due to their potentially dangerous nature.[1,2] All azides, particularly hydrogen azide and azides of the heavy metals, are potentially explosive; sensitive to physical and thermal shock, releasing nitrogen gas upon exitation.[2] It was not until the 1950s and 1960s, when safety technology caught up with chemical curiosity, that the interest in azides re-emerged, and numerous applications of, and new synthetic routes towards, were realized.

The common representation of an organic azide is R-N_3, where the central nitrogen carries a formal positive charge and the negative charge delocalizes between the terminal nitrogens as shown in Figure 1.[2]

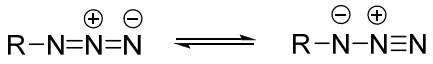

Figure 1: Depiction of a generic organic azide

A classic method of azidation is through nucleophilic substitution (S_N2-like) with the highly nucleophilic N_3^- species.[2] With alcohol starting materials, this usually involves a two step methodology (Scheme 1) where the alcohol is first activated with a suitable leaving group, and then reacted with an azide ion source. The leaving groups and azide

source can be varied according to experimental evidence. However, the traditional source of azide is sodium azide.[2]

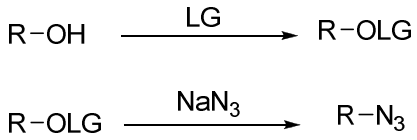

Scheme 1: General scheme for synthesis of azides with leaving group.

There are, however, many "one-pot" syntheses for the azidation of alcohols. A common method is the use of Mitsunobu reaction conditions. Papeo and associates performed a nicotinoyl azide (NCA)-mediated Mitsunobu reaction (Equation 1) to convert secondary alcohols into the corresponding azides.[3] Similarly, Viaud and Rollin performed a Mitsunobu reaction on secondary alcohols, involving this time zinc azide as the nucleophile source (Equation 2).[4]

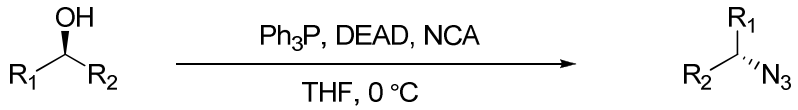

Equation 1: NCA-mediated azide synthesis

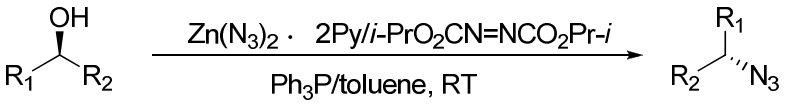

Equation 2: Mitsunobu conditions for the synthesis of azides from alcohols.

Further research shows that there are other one-pot methodologies besides the

Mitsunobu. Researchers at Merck Research Laboratories developed a one-pot scheme for azidation of secondary alcohols that did not involve Mitsunobu conditions. Instead, they reacted a secondary alcohol with diphenyl phosphorazidate (DPPA) and 1,8-diazabicyclo[5.4.0]undec-7-ene (DBU) (Equation 3).[5] Mizuno and Shioiri performed a similar reaction, using bis(*p*-nitrophenyl)phosphorazidate instead of DPPA.[6]

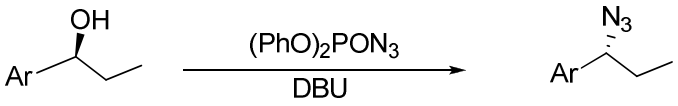

Equation 3: Synthesis of azides using bis(*p*-nitrophenyl)phosphorazidate.

Researchers at Rutgers University found the Merck team's methods lacking for their own particular need and developed a new one-pot scheme where the hydroxyl group of the alcohol is activated by bis(2,4-dichlorophenyl) phosphate before being transformed into their azides (Equation 4).[7] The researchers concluded that the methodology developed at Merck did not provide a good enough leaving group for less reactive alcohols.

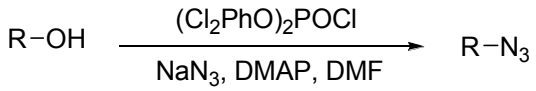

Equation 4: Synthesis of azides by activation of alcohol with bis(2,4-dichlorophenyl) phosphate.

More recently, new one-pot methodologies have been published in the literature that can give the chemist more ways to convert alcohols into azides. Rad and co-workers

published a method to convert alcohols into azides directly using *N*-(*p*-toluenesulfonyl) imidazole (TsIm, Figure 2), in the presence of triethylamine (TEA), sodium azide, and a catalytic amount of tetra-*n*-butylammonium iodide (TBAI) in DMF.

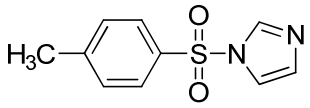

Figure 2: Structure of TsIm.

Using this route (Equation 5), the researchers reported fairly high yields (41-93%) of various azides from primary, secondary, and tertiary starting materials. However, the times for reaction ranged from five to twelve hours under reflux.[9]

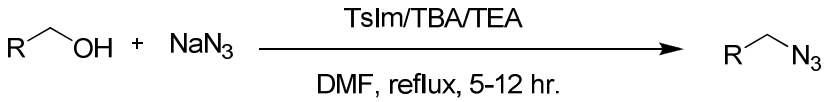

Equation 5: Synthesis of azides using TsIm and aodium azide.

Jayanthi, Gumaste, and Deshmukh describe their synthesis of allyl azides from allyl alcohols en route to the synthesis of *N*1-cinnamyl azetidin-2-ones, using triphosgene and sodium azide at room temperature over 12 hours (Equation 6) with yields ranging from 46-91%.[10]

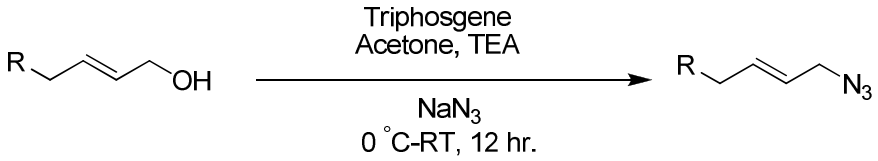

Equation 6: Synthesis of allyl azides from allyl alcohols.

While all of these synthetic routes are proven in the literature, for the most part, they still require an external azide source. This means that while the addition of a leaving group and azidation of the alcohol takes place in one pot, they still require two distinct reagents to work correctly. The reaction that the proposed research focuses on uses sulfonyl azides as the azide source for the S_N2 displacement. These compounds can be thought of as both the leaving group and attacking nucleophile all in the same molecule (Figure 3).

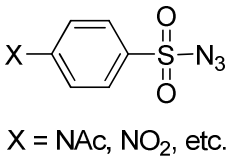

Figure 3: Possible sulfonyl azides.

Use of sulfonyl azides allows for the *in situ* generation of the N_3^- nucleophile *via* displacement from the sulfonyl group upon attack of the alcohol. The general reaction is shown in Equation 7. DBU acts as the base in the reaction, and *p*-acetamidobenzenesulfonyl azide (*p*-ABSA) is the azide source.

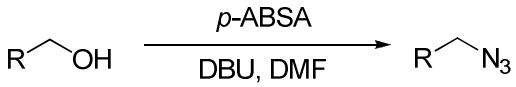

Equation 7: Description of general reaction of the research.

The reaction is carried out in a basic environment with a polar aprotic solvent, dimethyl formamide (DMF). These are classic S_N2 conditions. However, in recent years the rates of substitution reactions of this type[11] and many others [11,12] have been greatly increased when heated with microwave (MW) radiation. Microwave reactors have proven to be extremely useful tools in the synthetic laboratory, allowing researchers to expand new "green" techniques since they impart so much energy[13,14] to the reaction even without the use of solvents.[15] While this research will still use an organic solvent, the reaction, which takes an overnight reflux to go to completion,[8] can be refined to run in reasonable time periods, showing thrift with reagents and good product yield.

Microwave-Assisted Synthesis of *N*-Sulfonyl amides

The one pot azidation of alcohols is not the only microwave-assisted synthesis that this research will be focusing on, however. Another reaction to be investigated is the Cu(I)-catalyzed synthesis of sulfonamides from terminal alkynes and sulfonyl azides in aqueous solution (Equation 8).[16,17] In this reaction, the Cu(I) is generated *in situ* from the copper sulfate and ascorbic acid. Chemistry occurs in the aqueous solution because the *tert* butanol is soluble in water and the starting materials and other reagents are soluble in it. Upon completion of the reaction, the solid product precipitates out of solution in good yields requiring very little purification.

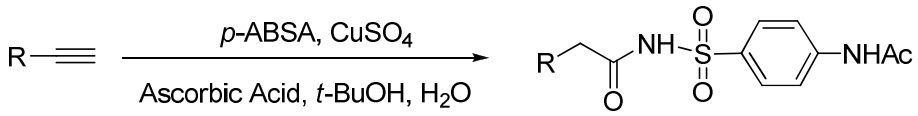

Equation 8: Copper-catalyzed synthesis of sulfonylamides.

Reaction conditions from Equation 8 are based on the work done by Sharpless and co-workers in 2002.[18] This reaction has proven to be applicable across many fields of chemistry and is a powerful example of a "click" reaction.[19] The proposed research will focus partly on this click reaction, in aqueous solution, carried out under MW conditions with yield optimization and diverse product formation being the goal.

Polymers in Medicine; Towards Artificial Cartilage

The use of polymers by living organisms is well known. Biology has used polymeric molecules as methods of support (proteins and celluloses), defensive mechanisms (chitin in insect and arthropod exoskeletons), energy sources (starches and other polysaccharides), and means of reproduction (DNA and RNA in the cell).[20] Mankind, however, has only recently begun to realize and tap into the potential of polymers in the last century, when advances in polymer chemistry affected nearly all aspects of modern life including, but not limited to, medicine. Polymers have found numerous applications in medicine from bio-absorbable stitches to artificial heart valves.[20] The types of polymers and their properties are numerous and have been well studied,[21] but the main property of interest concerning the use of polymers as biomaterials is that of biocompatibility. Biocompatibility deals broadly with how the

artificial material reacts once inside the body, and there are many guidelines on how to judge specifically if a material is biocompatible or not.[22]

For brevity, if a biomaterial is rejected outright by the host immune system, it is a poor candidate for *in vivo* use. However, if it remains inert, or is integrated with cells of the surrounding region with no effect on its integrity or function, the biomaterial is successful. Biocompatibility can be designed by chemists at a molecular level, and biochemical and biomedical research has given synthetic chemists numerous target molecules, along with their hypothesized chemical interactions inside the body. If one can synthesize a biomimetic compound that closely resembles the target molecule in its gross structure, overall function, and interactions with the cellular environment, the subject of biocompatibility becomes much more manageable.

A goal of this research is to design a new polymer to serve as a replacement for the articular cartilage of the knee. Cartilage can be looked at as an engineering marvel that few, if any, synthetic materials can perfectly replicate. It can handle and redistribute shearing and compressive forces while maintaining its elastic and anti-friction properties all while being in constant use for over 80 years or more.[23] Cartilage is produced by cells called chondrocytes[23,24] that also comprise bone as well. The structure of articular cartilage is well known,[24,25] but it is important to know that it is composed of six layers or zones.

These zones are comprised mainly of proteins, especially collagen, and numerous proteo- or peptidoglycans (PG) which form comb- or bristle-like structures, with the central protein core having numerous “bristles” of sulfated saccharide subunits hanging off of it.[26] The chondrocytes, which synthesize the PG’s constantly, make up only a

small percentage of the cartilage[24] and the most abundant material is actually water, in the form of the synovial fluid. Cartilage can therefore be thought of as a sophisticated sponge that takes in and releases the water it is saturated with based on the stresses placed on it.[26] The pressure and release of this water is very important to the proper functioning of the chondrocytes,[25] and it also accounts for why cartilage is so slippery under friction and stress.[25, 26]

Based on these facts, any biomaterials that wish to serve as a replacement for articular cartilage must either act as a scaffold for the growth of new chondrocytes seeded onto them, which can then rebuild the zones of the normal cartilage, or behave in such a way that it responds similarly to the fluid pressures placed on it under load. Numerous biodegradable scaffolds have been discussed in the literature that foster cell growth when placed in the body,[24,27] but the goal of this research is to create a biomaterial for a full replacement of the damaged cartilage in the joint.

One type of material that has been studied for this purpose are hydrogels. As their name suggests, these materials can absorb and release large amounts of water. Many kinds of hydrogels have been studied for cartilage replacements, but those that show most promise are copolymers of two biocompatible monomers. Katta and co-workers from Drexel University looked at the friction and wear behavior of poly(vinyl alcohol)/poly (vinyl pyrrolidone) hydrogels.[28] Poly(vinyl alcohol) (PVA) is a common co-polymer in many hydrogels, but it can also be used alone as replacements for the meniscus.[29, 30]

These double-network polymers seem to show the most promise in mimicking the wear patterns of cartilage, which gives chemists a large number of options, as it is a simple matter of changing the co-polymers. Gong et.al. at Hokkaido University

conducted numerous studies on varying networks of hydrophilic polymers from completely artificial to naturally occurring polymers such as collagen, agarose, and Bacterial Cellulose.[31] They concluded that these double-networks allow for the best manipulation of properties of each of the co-polymers, allowing two monomers that may be mechanically weak to combine into a network that is amenable to use inside of the body. Further studies of similar double-network hydrogels in 2006 by another group from Hokkaido focused on the biodegradation of the materials *in vivo*.[32]

This research however focuses on using a methacrylate polymer as the potential artificial cartilage. Poly(ethylmethacrylate) (PEMA), tetrahydrofurfuryl methacrylate (THFMA), and hydroxyethyl methacrylate (HEMA) are three commonly studied methacrylate monomers for use as artificial cartilage. Usually, this research focuses on varying different ratios of these three monomers and studying the properties of the corresponding polymer.

Hutcheon and co-workers examined the water absorption and surface properties of these polymers in 2000.[33] Additionally, Hutcheon, Downes, and Davies looked at how chondrocytes interact with these polymers, concluding that they attached easily and the material could be used as a potential artificial cartilage.[34] Wyre and Downes looked at PEMA/THFMA polymers *in vitro* examining how chondrocyte cells attach to them compared to Thermanox, a substance whose cell adhesion properties are well known. The researchers chose the PEMA/THFMA system due to its physical properties, but also because it absorbs water and proteins easily, which may lead to its high degree of biocompatibility.[35] Finally, in 2008, another group of researchers from Spain, led by Sanchis, studied the water sorbtion of polymers composed exclusively of THFMA, due to

the considerable interest in the monomer for use as a biomaterial.[36] These versatile polymers can also be used as scaffolds,[37] and as double-network polymers with the other network being made of biotic cellulose.[38] The proposed research will focus on the synthesis of a possible methacrylate monomer, with carbohydrate pendant groups synthesized from Bisphenol A Diglycidyl Ether (BADGE) in the following synthesis (Scheme 2).

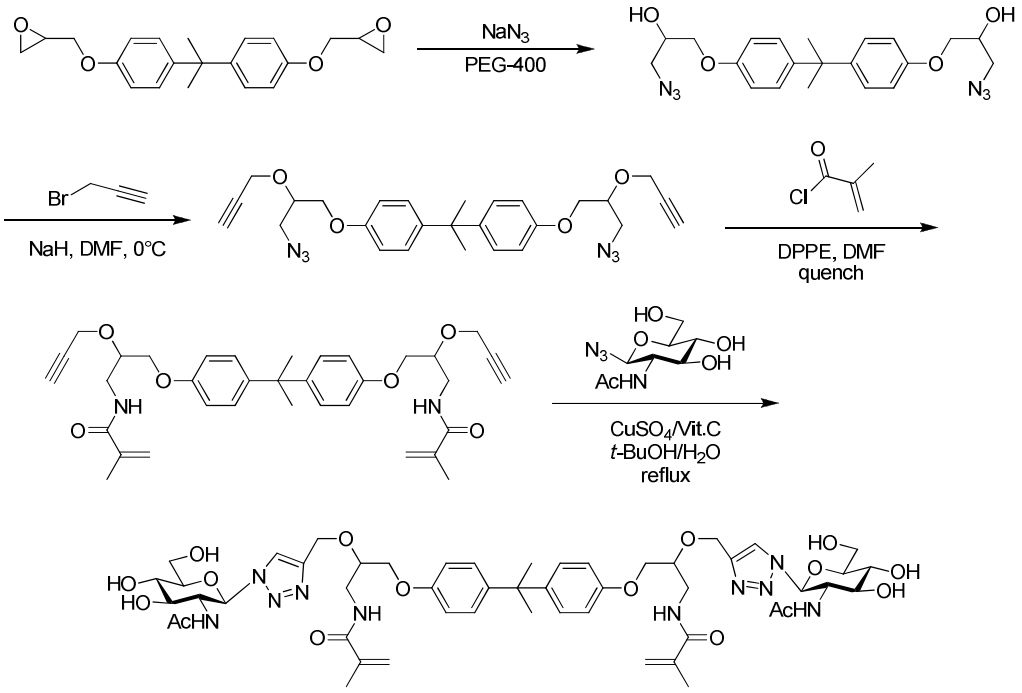

Scheme 2: Proposed synthetic pathway towards artificial cartilage.

Statement of Problem

The previously described preparation of aliphatic and aryl azides from alcohols *via* an *in situ* generated N_3^- species will be further studied in a "one-pot" microwave-(MW) assisted synthetic reaction. Special attention will be paid to optimization of azide yield through manipulation of reaction conditions. Chief among these are: base used, equivalents of reagents, heating times and temperatures, and azide sources. A second reaction the research will examine is the versatile Cu(I)-catalyzed "click" reaction of terminal alkynes and sulfonyl azides in aqueous solution. This well-known reaction type will be examined under MW-irradiation and modified for maximal yield of the sulfonamide product. The final part of the proposed research will focus on the synthesis of a potential artificial cartilage synthesized from Bisphenol A Diglycidyl Ether (BADGE).

Results and Discussion

Microwave-Assisted Synthesis of Organic Azides

This research performed in the first section of this thesis is a continuation of the work done by Iulia Sacui on her master's thesis,[8] when she showed that *p*-ABSA, in the presence of a base, could convert an alcohol to an azide. However, the reactions were only performed on carbohydrate systems. This research was conducted to explore the generalities of the reaction on non-carbohydrate based primary and secondary alcohols, while designing a procedure that allowed for complete conversion of the hydroxyl-containing starting material to the azide product. The general reaction conditions are shown in Equation 9. The main question at the beginning of the research was how well do these conditions translate into the microwave (MW) reactor? Ms. Sacui used acetonitrile, boiling point 81-82 °C, as her solvent. This, however, can be too low of a boiling point to use efficiently in the MW reactor, as high pressures can quickly build up inside of the reaction vessel. A new solvent was chosen, DMF, due to its similar properties to acetonitrile (polar aprotic), yet higher boiling point (153 °C).

Once this new solvent was selected, the reaction shown in Equation 8 was chosen as the "test" reaction, on which different conditions and their effects could be monitored against reaction completeness.

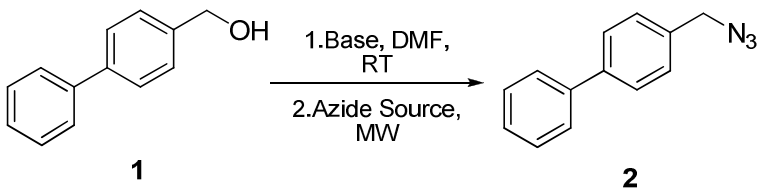

Equation 9: Synthesis of 4-(azidomethyl)biphenyl (**2**), from 1,4-biphenylmethanol (**1**).

This reaction was chosen for three reasons. First, it is a primary system, and if the reaction truly is S_N2-like, then it would work best on this type. Second, the starting material is inexpensive and readily available from commercial sources. And third, the benzene rings in the molecule allow for easy detection of compounds with a UV lamp. Since the azide sources to be tested were also UV- active, it would be easy and efficient to monitor any changes in the reaction *via* TLC. The only drawback, as it could be seen, to running this reaction in the microwave reactor is that such small quantities of material had to be used. The tubes used in the CEM Microwave Reactor have a very limited volume of 10 mL. As a result, the reactions in the tests, and subsequently further on in the research were all run on 100 mg scales. While it was straightforward to monitor during the reaction, subsequent workup and purification steps led to losses in overall yield.

The first attempts at the reaction were run with the azide source from previous work *p*-ABSA, and the base, DBU, at room temperature. The reason for starting the tests at room temperature arose from the fact that **1** is a primary system in participating in what is believed to be an S_N2-type reaction, which should be favorable even at ambient temperature. This, however, was not shown to be the case. These initial reactions with 1.0 equivalent each of *p*-ABSA and DBU indicated that while some product was formed

after one hour, this was the extent of the reaction, with no more product formation occurring even after 15 hours of stirring at room temperature with monitoring *via* TLC.

Now faced with the prospect of heating, the reaction was again run with 1.0 equivalent of azide and base but heated in the microwave, first for 10 minutes at 40 °C, then for 30 minutes at 100 °C. It was believed that by ramping the temperature in this fashion, the reaction would run to completion, but the temperatures would still be far enough below the boiling point of the solvent as to avoid any decomposition in the reaction. Again the reaction failed to produce complete conversion to product as monitored *via* TLC. It was then proposed that the temperature should be increased even more, and the same reaction with the same equivalents was run in the MW reactor at 140 and 150 °C for 10 and 40 minutes respectively. This did produce some product, but the majority of the starting material remained in the reaction mixture. These high temperatures were seen as not conducive to high yields, and left the starting material prone to decomposition so they were abandoned temporarily to study the effects of different bases, equivalents of azide source, and heating times had on the reaction.

Since DBU had served as the model base, it was kept for the first extensive series of tests, summarized in Table 1, where the equivalents of DBU were held at 1.0 and the temperature and times were varied. These tests showed that 1.0 equivalents of base did not seem to be enough to afford complete conversion to product. While some product was indeed forming, the majority was left as starting material, as had been observed with the reactions at room temperature. The next phase of testing would hold the equivalents of *p*-ABSA at 3.0, and the temperature at 120 °C, shown in Table 2.

Equivalents Azide	MW Temperature (°C)	Time (minutes)	Complete Conversion?
1.5	100	60	No
2.0	100	120	No
3.0	100	120	No
2.0	130	30	No
2.0	130	30	No
2.0	130	30	No
2.0	130	50	No
3.0	120	60	No
4.0	120	60	No
5.0	120	60	No
6.0	120	60	No

Table 1: Constant equivalents of DBU.

Equivalents Base	Time (minutes)	Complete Conversion?
1.5	60	No
3.0	60	No
2.5	60	No
5.0	60	No

Table 2: Reactions with *p*-ABSA 3.0 eq, 120 °C.

Armed with the results of these first two rounds of tests, it was concluded that equivalents of azide, equivalents of base, time in the MW reaction, or MW temperature had little, if any, bearing on the completeness of the reaction. At best, there was only a minimal amount of azide produced, as observed *via* TLC. TLC plates were an efficient method for determining crude reaction completeness when stained with *para*-anisaldehyde, which causes any azide to appear yellow against a red background upon heating.

The next plan of attack on the methodology was to begin researching different bases. The strength of the base is important in determining how effectively it de-protonates the alcohol. In doing so, it makes the oxygen more nucleophilic, and increases the likelihood of attack on the sulfur atom of that azide source. Once attacked, this sulfur

releases the azide nucleophile *in situ* as shown in Figure 4, where "BASE" represents a generic base.

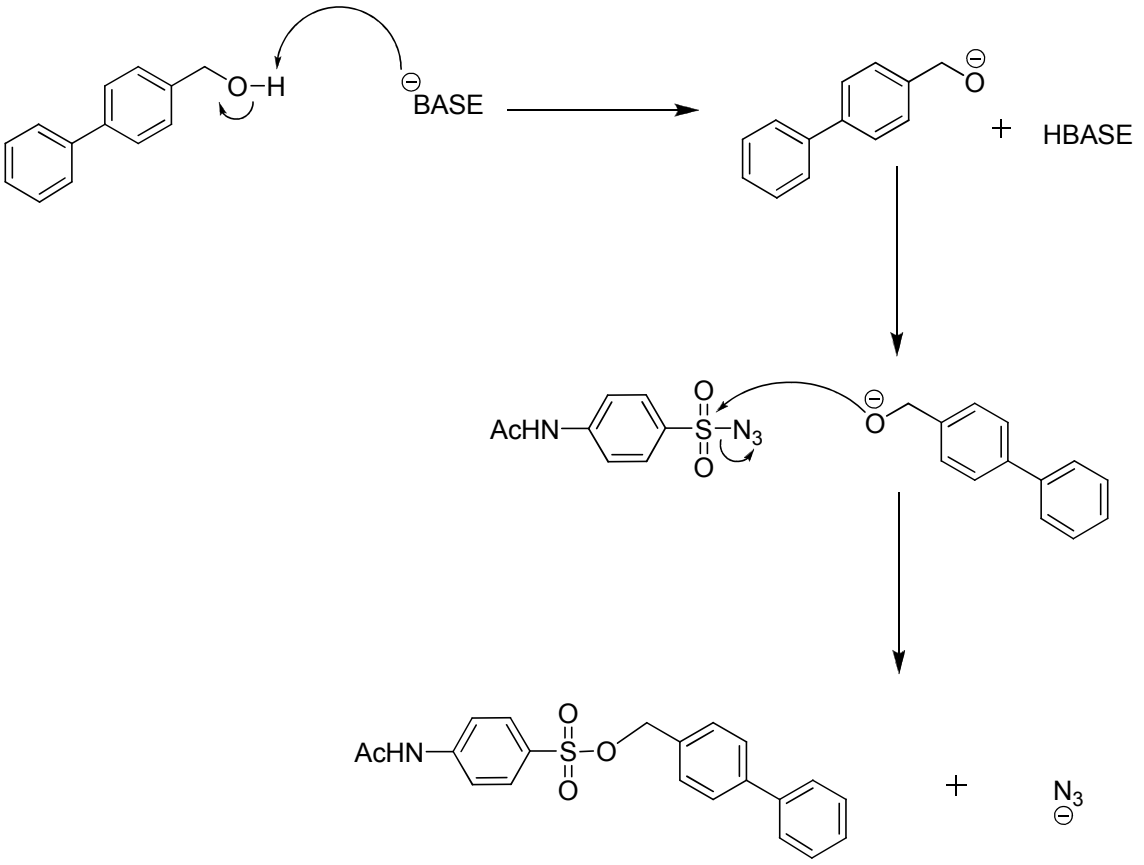

Figure 4: Proposed mechanism for the generation of the azide nucleophile.

This left us with a daunting task. There were numerous bases to explore for optimization of the reaction, ranging from organic in nature, such as pyridine, to wholly inorganic bases, such as potassium hydroxide. It was even speculated that the strong, hindered phosphorazine bases might be useful, but these proved prohibitive from both a cost and safety point of view. In light of this, the next base to be tried in the reaction conditions was *N*,*N*-diisopropylethylamine (DIEA). DIEA is hindered around the

nucleophilic nitrogen, making it more favorable to attack the most accessible, and acidic proton available, which in our reaction is the hydroxyl proton. However, in the few trials run with DIEA, no reaction occurred as monitored by TLC. Another organic base tried under these reaction conditions was 1,4-diazabicyclo[2.2.2]octane (DABCO), also a hindered base similar to DIEA. But DABCO proved ineffective as well towards the conversion of alcohols to azides.

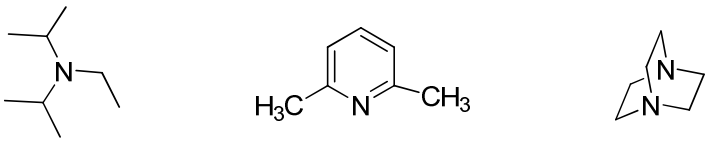

Figure 5: Structure of DIEA (left), 2,6-Lutidine (center), and DABCO (right).

A third and final hindered nitrogenous base, 2,6-lutidine, was then tested for effectiveness in the reaction. But, from what were at first promising experiments turned out like the other hindered, nitrogen-containing bases, i.e. no reaction occurred at all (Table 3).

After trying these stronger, hindered bases, the original procedure from Ms. Sacui's thesis was then examined in more detail. In the methodology outlined in her thesis, the azide source and alcohol were put into solution, and the base was then added before refluxing overnight. Then, upon examination for completeness by TLC, "some more base or *p*-ABSA was added as needed".[8] When weighed against the proposed mechanism for the generation of the azide nucleophile shown in Figure 3, this procedure began to look less appealing. Perhaps, it was thought, if the alcohol and base were stirred together first, before the addition of the azide source, it would ensure complete de-

protonation of the alcohol and expedite the process of nucleophile generation. With this in mind, a new procedural order was performed with 2,6-lutidine again, holding the equivalents of azide constant and increasing the reaction times to one hour at 100 °C and one hour at 130 °C. Unfortunately, the results of these reactions, summarized in Table 4, were similar to the original procedure.

After trying these different bases, as well as the base from the original work on the reaction, DBU, it was decided to go in the opposite direction: a small, strong, non-hindered base. The base chosen as the first test subject was sodium hydride. The first reactions with sodium hydride, however, were similar to those performed with the previous bases. It was decided that 5.0 equivalents of sodium hydride would be used in each reaction to ensure complete de-protonation of the alcohol starting materials. In spite of this, it was observed that the early reactions performed with sodium hydride were all incomplete even when heating at 100 and 130 °C for 30 minutes respectively. At this point, however, the research received a breakthrough, in the form of a reaction that when run for 15 minutes at 100 °C, 1.5 equivalents *p*-ABSA, and 5.0 equivalents sodium hydride showed complete consumption of starting material, and positive identification *via* TLC that the azide had formed. The reaction was run again with the same amount of reagents but for only 10 minutes at 100 °C, and again showed complete consumption of the starting material. It now seemed that the equivalents of azide, temperature and reaction time, as well as the proper base had been found. However, the reactions were inconsistent, so a new azide source was examined and tried in the reaction.

Base	Equivalents Base	Equivalents Azide	Temperature (°C)	Time (minutes)	Complete Conversion?
DIEA	1.0	1.5	100	60	No
DIEA	1.0	1.5	110	60	No
DIEA	1.0	1.5	120	60	No
DABCO	1.0	1.5	110	30	No
2,6-Lutidine	1.0	1.0	100	60	No
2,6-Lutidine	1.5	1.0	100	60	No
2,6-Lutidine	2.0	1.0	100	60	No

Table 3: Hindered nitrogen base reactions.

Equivalents Base	Temperature (°C)	Time (minutes)	Complete Conversion?
1.0	100	60	No
2.0	100	60	No
3.0	100	60	No
4.0	100 130	60 60	No
5.0	100 130	60 60	No

Table 4: New procedure with 2,6-lutidine.

In Ms. Sacui's thesis, she discussed another azide source that would be a good candidate for use in the reaction, *para*-nitrobenzenesulfonyl azide (*p*-NBSA), Equation 10. The synthesis of *p*-NBSA proceeded smoothly and the product was obtained as a white solid with a m.p. 95-98 °C, whose structure was confirmed by X-ray structure analysis, Figure 6, and the NMR data agreed with Ms. Sacui's thesis. With this new azide source in hand, the reaction was again attempted with 5.0 equivalents of NaH, and 1.5 equivalents of *p*-NBSA.

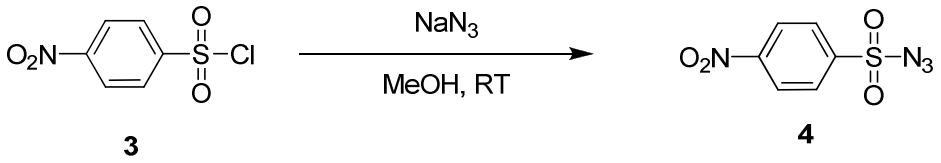

3 **4**

Equation 10: Synthesis of *para*-nitrobenzenesulfonyl azide (**4**) from *para*-nitrobenzenesulfonyl chloride (**3**).

It was then heated at 100 °C in the MW reactor. After such time, the reaction showed complete consumption of starting material and formation of **2** after 10 minutes *via* TLC. However, the appearance of the spots on the TLC plate was different than it had been in the previous trials using alcohol **1** and *p*-ABSA. The top spots,which had turned a deep yellow upon heating, now did not change color at all. And under UV light, there appeared to be a bright, blue top spot where the azide spot would normally be found.

When these top spots were separated from the crude reaction mixture by column chromatography and the infrared (IR) spectrum taken, there was no absorbance ~2100 cm^{-1}. IR analysis proved useful for an initial test of the reactions since azides have a distinct absorbtion, ranging between 2000-2200 cm^{-1} in the infrared range.[39] When NMR analysis was performed on the top spots it was clear why no IR absorbance in the azide range had been observed for the product. There was a singlet worth one proton observed at 10.06 ppm, indicating that an aldehyde was present. Examination of the ^{13}C NMR also confirmed the presence of a carbonyl carbon with a singlet at 193.16 ppm. Mass spectroscopy (MS) also validated the evidence for the production of an aldehyde in the reaction. However, analysis of the spectrum taken on azide **2** revealed an *m*/*z* of 181.0. The *m*/*z* calculated for the aldehyde of **1** is 182.07, within one mass unit of the target.

Undeterred by this result, the reaction was run with another primary alcohol, 2,3-dimethoxybenzyl alcohol, illustrated in Equation 11. Unlike the first reaction with 4-biphenylmethanol, after treating **5** under the reaction conditions, azide product was initially formed in the reaction after the heating cycle of 10 minutes in the microwave reactor at 100 °C. Initial analysis by TLC indicated near complete consumption of the starting material, and IR spectroscopy of the reaction showed an absorbance at 2105 cm^{-1}, validating the formation of the azide product **6**. The mass spectrum of the column-purified product, **6** verified the presence of the azide with an *m*/*z* of 151.8, indicating the loss of N_2 from the product.

Azide **6** has not been synthesized in the literature before, so it provided an opportunity to show that the reaction conditions could successfully synthesize a unique azide. This proved to be the first example that indicated that the reaction conditions proposed could, in fact, synthesize azides from alcohol starting materials.

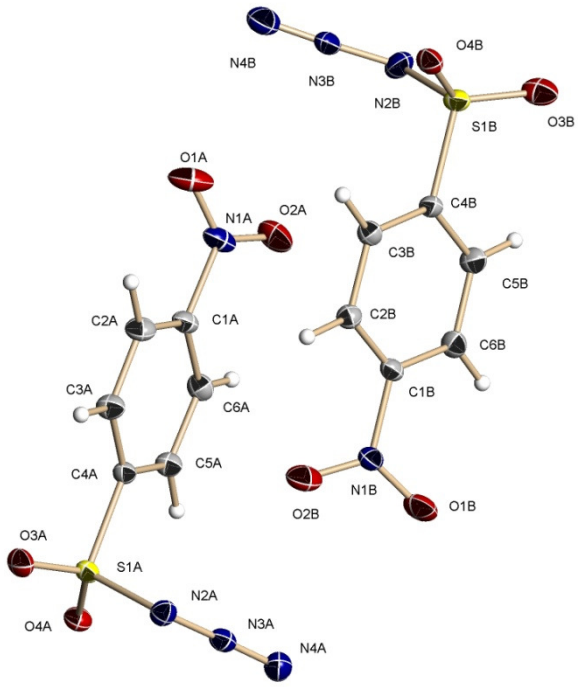

Figure 6: The X-Ray structure of *p*-NBSA.

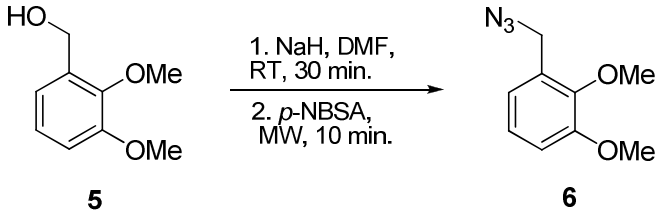

5 **6**

Equation 11: Synthesis of 1-(azidomethyl)-2,3-dimethoxybenzene (**6**) from 2,3-dimethoxybenzyl alcohol (**5**).

The next primary alcohol tested under the new conditions was piperonyl alcohol, illustrated in Equation 12. Piperonyl alcohol required 20 minutes of heating in the MW at 100 °C, but showed complete conversion when observed *via* TLC to form azide **8**. IR spectroscopy showed an absorbance at 2100 cm^{-1}, in good agreement with the literature.[40]

Mass spectrometry also showed an *m/z* of 135.1, indicating the loss of N_3 from **8**. NMR spectroscopy provided no conclusive data towards the structural determination of the azide.

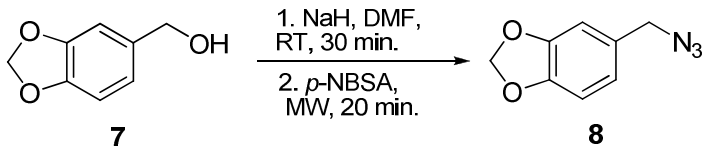

Equation 12: Synthesis of 5-(azidomethyl)benzo[*d*][1,3]dioxole (**8**) from Piperonyl alcohol (**7**).

The final primary alcohol-derived azide came from 1,4-benzenedimethanol to form azide **10**, illustrated in Equation 13. The use of this diazide has been reported in the literature, specifically in the field of "click" chemistry-derived triazoles.[41] The only difference in the standard reaction procedure when performed on this particular starting material was to double the equivalents of azide source since there were two hydroxyl functional groups in the molecule. As with **5**, this alcohol required 20 minutes of heating at 100 °C for complete conversion of the starting material to be observed *via* TLC. The reaction looked very clean with a trace, if any, starting material present after the heating cycle. Therefore, the NMR was taken of the crude product without any further column purification. The IR spectrum taken of the product revealed an absorbance at 2102 cm^{-1}, indicating that the azide had been formed in the reaction; mass spectrometry also confirmed azide production, detecting an *m/z* of 185.9, when the calculated *m/z* was 188.03.

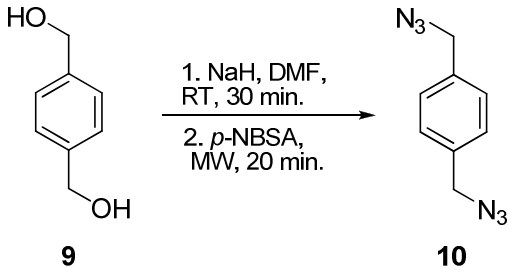

9 **10**

Equation 13: Synthesis of 1,4-bis(azidomethyl)benzene (**10**) from (1,4-benzenedimethanol (**9**).

The next stage of the research involved performing the new methodology on secondary alcohols. Because the reaction is believed to go through an S_N2 mechanism, reactions of secondary alcohols should still be possible, though perhaps with reduced yields due to the increased steric bulk around the reaction center in the molecule, and thus competition with other processes such as elimination. The alcohols in question would also have to be solids at room temperature and contain a benzene ring or other conjugated moiety to facilitate monitoring the reaction progress *via* TLC during heating in the microwave.

The first secondary alcohol attempted with the new methodology was 1-indanol. After heating the reaction mixture for 20 minutes, examination *via* TLC showed complete consumption of the starting material and conversion into **12** (Equation 14). ^{1}H NMR reinforced this with the shift of the CH_2 signal to 5.0 ppm when placed next to the azide, and MS showed an experimental *m*/*z* of 158.9, while the *m*/*z* calculated was 159.08, IR spectroscopy showed an absorbance at 2094 cm^{-1}.

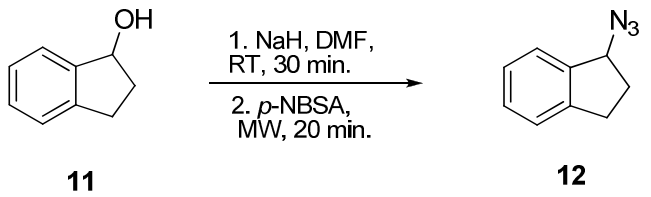

Equation 14: Synthesis of 1-azido-2,3-dihydro-1*H*-indene (**12**) from 1-indanol (**11**).

Upon closer examination of the TLC plate, an interesting observation was made. As well as the single azide spot at R_f = 0.64, there was another spot below that, at R_f = 0.48. This lower spot did not burn like an azide, but subsequent heating, or changes in azide equivalents did not force all of the starting material towards the formation of the desired azide product. Therefore, the two spots were separated and purified by column chromatography. Fortunately, the bottom spot was able to be recrystallized and its structure determined by X-Ray crystallography as very few of the other azides were able to be crystallized; the structure is shown in Figure 7.

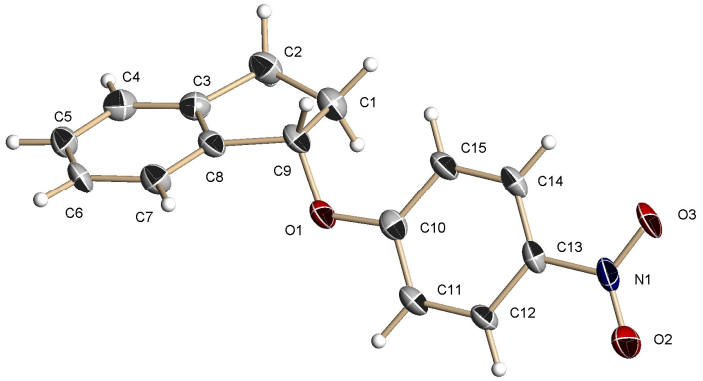

Figure 7: Structure of by-product from 1-indanol.

This structure came as a surprise for three reasons. One, the large $-SO_2N_3$ group was missing from the *p*-NBSA. Two, there was an ether bond formed between the oxygen of our alcohol and the aryl ring from the *p*-NBSA. And third, was the complete loss of N_3 from anywhere in the molecule, forcing us to speculate about what had happened to the azide.

The most logical explanation for the formation of this by-product is that it is formed *via* the S_NAR mechanism. The electron-withdrawing effects of the NO_2 group *para* to the $-SO_2N_3$ contributes directly to the ease of the substitution, as outlined in the mechanism from March[42], where one of the resonance forms in the sigma complex has the negative charge directly next to the nitro group, thus allowing for an additional resonance form and therefore more stability. Another factor contributing is the rather large sulfonyl azide leaving group. This group is stabilized by electron resonance between the sulfur and the oxygens which disperses the extra electron density created by breaking the carbon-sulfur bond, making it a "good" leaving group. This type of minor S_NAR product would continue to show up in most of the secondary alcohols attempted; however, due to the small amount of product formed, it was not always isolated in pure form.

The next reaction, shown in Equation 15, was performed on a similar alcohol, 2-indanol. Like 1-indanol, it was heated in the MW reactor for 20 minutes at 100 °C until TLC showed nearly complete consumption of the starting material. IR spectroscopy showed an absorbtion at 2101 cm^{-1}, indicating that the azide had been formed, and MS showed an *m*/*z* of 158.9, within one mass unit of the calculated *m*/*z* further validating that

the azide had been synthesized. Again, the S_NAR product spot was seen on TLC, but the product was not isolated.

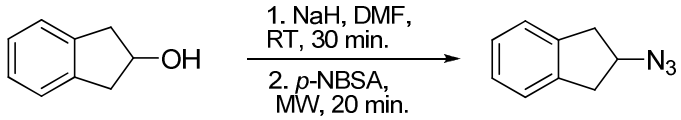

13 **14**

Equation 15: Synthesis of 2-azido-2,3-dihydro-1*H*-indene (**14**) from 2-indanol (**15**).

The final reaction on a secondary alcohol that worked in a straightforward manner is illustrated in Equation 16, where (±)-α-methyl-2-naphthalenemethanol was reacted according to the methodology developed, and reacted in the microwave for 20 minutes instead of the 10 required for primary alcohols. After column chromatography, the IR spectrum indicated absorbance at 2105 cm^{-1}, suggesting that the azide had been formed, and MS data further confirmed that the product had been formed, but that it had lost N_2 during the ionization process with an *m*/*z* of 167.0, and 154.0 from the loss of N_3.

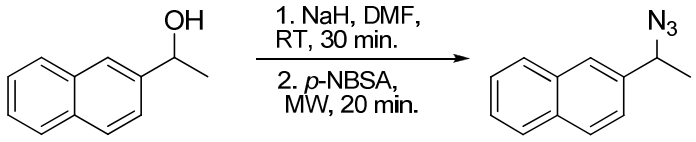

15 **16**

Equation 16: Synthesis of 2-(1-azidoethyl)naphthalene (**16**) from α-methyl-2-naphthalenemethanol (**15**).

At this point we knew that the methodology would work on primary and secondary alcohols. However, as indicated in the reactions with 4-biphenylmethanol, unexpected products could be formed. Another possible example of this is shown in

Equation 17, with the reaction of 9-hydroxyfluorene (**17**) in the microwave according to reaction conditions. Examination *via* TLC showed that after 10 minutes of heating, some kind of reaction had occurred. However, the top spot (R_f = 0.46) did not burn yellow as it usually should in *p*-anisaldehyde as had been observed previously for **2**. A column was run on the crude mixture and the top spot was separated and purified. When an IR spectrum was taken, it showed no azide absorbances around 2100 cm^{-1}. Since the product formed as a yellow solid, it was recrystallized from methanol and a structure was found. However, when the structure was elucidated, it was determined to be 9-fluorenone (**18**). Mass spectrometry confirmed this with a *m*/*z* found of 181.1, corresponding to the ketone product whose calculated *m*/*z* is 180.6, and ^{13}C NMR indicated a signal at 194.0 ppm further indication that a ketone carbonyl was present in the product.

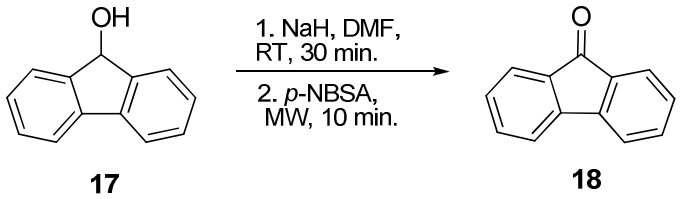

Equation 17: Synthesis of 9-fluorenone (**18**) from 9-hydroxyfluorene (**17**).

Microwave-Assisted Synthesis of *N*-Sulfonyl amides

The next area that this research dealt with was the microwave-assisted synthesis of *N*-sulfonyl amides. Unlike the previous section on the conversion of alcohols to azides, this part of the research met with no success. It was the overall goal of the research to replicate the reaction shown in Equation 8. However, when this reaction was

attempted in the microwave reactor no reaction was observed. The article that served as the source of the method describes the products of the reaction as forming as solids that could then be easily separated from the rest of the reaction mixture easily in high yields. Yet when the reaction was first attempted in the microwave reactor with phenylacetylene as the alkyne, only sparing amounts of precipitate were formed.

Different attempts were made to optimize the reaction, such as making fresh $CuSO_4$ and ascorbic acid solutions, varying the heating times, and changing the equivalents of the reagents, but nothing worked. Similar trials were attempted with 3-cyclopentyl-1-propyne and 1-ethynyl-4-methylbenzene. But even after extensive heating in the MW reactor, these too harbored no traces of precipitated product.

The question then became why didn't these reactions work? First, the literature sources ran all reactions at room temperature, while ours were performed under microwave irradiation. Heating in the microwave reactor could have possibly caused degradation of the alkynes rendering them un-reactive under the conditions of the experiment. Second, the solvent system could stand re-examination. Instead of water, a more traditional high-boiling organic solvent could be tested in the microwave. Finally, Cassidy and co-workers reported using a ligand to aid in the orientation of the copper in the reaction. Perhaps this ligand can be synthesized in order to be employed in this microwave-assisted reaction. Alternatively, since we are attempting to use a "green" technique like heating in the MW reactor, perhaps running the reaction with no solvent at all, or a more green solvent that can possibly act in a ligand-like fashion such as polyethylene glycol could be employed,.

Towards the Synthesis of Artificial Cartilage

The last section of this research dealt with the attempt to synthesize a monomer that could potentially be used as a full-deficit replacement for damaged articular cartilage in the human knee. Upon polymerization with a common dental co-polymer in the presence of a peroxide, this new monomer could mimic the properties of human cartilage. The research proposed the use of bisphenol A diglycidyl ether (BADGE) as the starting material for this reaction, the structure of which is shown in Figure 8. BADGE is readily available from commercial sources and is fairly easy to handle as a highly viscous liquid. However, it is prone to crystallization at room temperature and other molecules in the same family have recently been reported to have toxic effects in their normal uses as coatings for food containers.

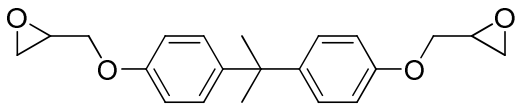

Figure 8: Structure of BADGE.

From a synthetic chemist's point of view, BADGE is a target-rich starting material. The molecule can be thought of possessing two convenient chemical "handles" in the form of the terminal epoxides, which can be readily manipulated and functionalized. It is also soluble in many organic solvents, and is not difficult to monitor during the reaction by simple methods such as TLC.

The first completed step in the synthesis was the opening up of the epoxide with sodium azide utilizing Poly(ethylene glycol) (PEG) 400 as the solvent. It is crucial that this reaction be done in a regioselective manner so the azide is on the terminal carbon,

and the newly formed hydroxyl is attached on the adjacent carbon. Many sources were found that discussed the topic of opening epoxides and aziridines in a similar manner, but not all afforded us the desired regiochemistry. One paper, however, provided us with the reaction conditions illustrated in Equation 18.[43]

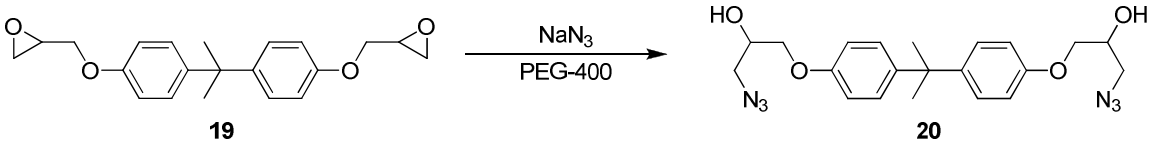

19 **20**

Equation 18: 3-3'-(4-4'-(propane-2,2-diyl)bis(4,1-phenylene))bis(oxy)bis-(azidopropan-2-ol) (**20**) from BADGE (**19**).

Das and co-workers showed that under these conditions, at room temperature, when sodium azide was reacted with a terminal epoxide, the terminal azide **20** was always formed. The author's substrates were similar in structure but none reached the size or number of epoxides as found in BADGE; the reagents were doubled and the reaction stirred overnight to afford **20** as confirmed by IR spectroscopy, in relatively high yields. IR provided the most information during the reaction as one could observe the azide and broad alcohol absorbance forming, showing that the epoxide had been successfully opened. The IR spectrum showed a broad absorbance at 3474 cm^{-1}, indicating presence of the hydroxyl, and also an absorbance at 2102 cm^{-1}, providing confirmation of the azide. Neither of these two key absorbances were present in the starting material. NMR spectroscopy was performed; however, the data analysis required for the confirmation of the synthesis of these products was beyond the scope of this research.

The next step in the reaction was the ether synthesis on the newly formed hydroxyl. The procedure was obtained and modified from Penny Miner's YSU master's thesis.[44] The reaction itself is a Williamson ether synthesis, which results in conjugating a terminal alkyne to the molecule through an ether linkage, as shown in Equation 19.

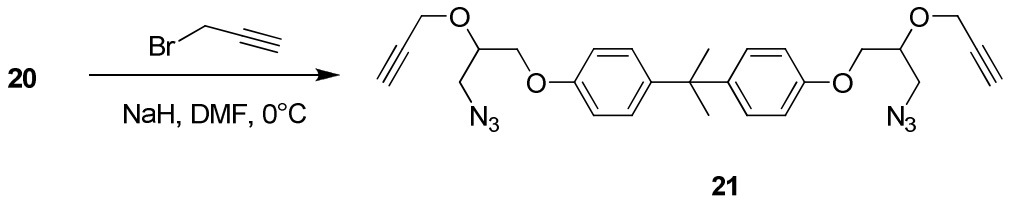

21

Equation 19: Synthesis of 4,4-(propane-2,2-diyl)bis((3-azido-2-(prop-2-ynyloxy)propoxy)benzene (**21**) from **20**.

.

The reagents were again doubled from the original source, and the reaction was run at 0 °C at least overnight. Care was taken to try to keeping the reaction as water-free as possible while maintaining an inert atmosphere over the solution of **20**, as well as the NaH before reacting together. Again, monitoring by IR showed the alcohol absorbance disappearing, while maintaining the azide absorbance at 2102 cm^{-1}, and the appearance of a strong, narrow 3285 cm^{-1} absorbance characteristic of the alkyne proton stretching. There was some concern that as soon as the alkyne was attached, it would undergo rapid cyclization with the azide to form the five-membered triazole ring. However, this was found not to be the case, even when the product was left to sit at room temperature for an extended period of time from monitoring by IR before and after the time period.

The final reaction that was attempted, but not completed on this synthesis was the Staudinger reaction on the terminal azide, as adapted from Abdul-Basit Alhassan's YSU

master's thesis[45], illustrated in Equation 20. The Staudinger conditions, with 1,2-bis(diphenylphosphino)ethane (DPPE) and DMF, should link together the terminal azide and methacryloyl chloride in an amide bond that would be easily recognizeable by ^{1}H NMR from the appearance of a peak at ~8 ppm. However, this reaction proved difficult, mainly due to solvent choice. It was thought that DMF would act as an adequate polar, aprotic solvent for the reaction. But, when attempts were made to put DPPE into solution, it would not dissolve. It is believed that this problem could be solved by substituting tetrahydrofuran (THF) for the DMF, and other researchers have found that DPPE is soluble in THF, thereby aiding the reaction. This reaction was necessary as the functional groups that the reaction would place on the molecule are key to the polymerization by formation of a methacrylate bond; when ^{1}H NMR spectroscopy was performed on the crude and column purified product, no signal at ~8 ppm was observed.

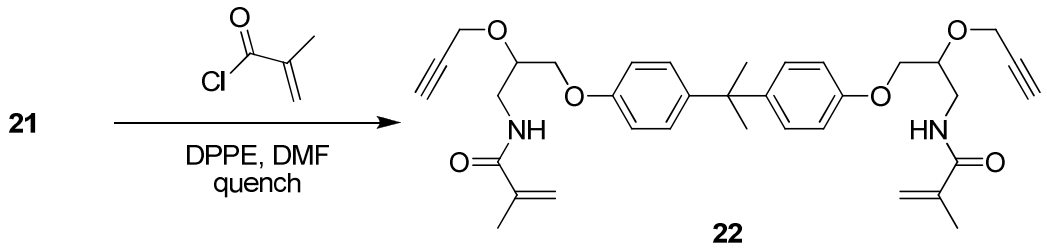

Equation 20: Attempted Staudinger reaction on **21**.

Conclusions

The methodology for the synthesis of azides from alcohols in the microwave reactor using sulfonyl azides showed unexpected results. While the reaction worked and produced azides as confirmed by IR, NMR and MS, there were unexpected side-products that formed during heating. Another unintended class of products were the aldehydes and ketones formed from primary and secondary alcohols repectively. More refinement of the procedure is needed before it can be said with certainty that it is reliable for azide synthesis under the conditions in the microwave.

The synthesis of *N*-Sulfonylamides in the microwave also needs further refinement. As none of the reactions worked in the microwave, new conditions such as solvent, heating time, or use of ligand must be addressed.

Finally, the synthesis of a potential monomer for the use as an artificial cartilage showed great promise. The Staudinger reaction in the third step of the synthetic route must be re-examined, possibly using a new solvent such as THF, to aid in the dissolution of DPPE and complete reaction of the reagents. Also, mechanical tests on the monomer, once it is synthesized, must be performed to accurately assess the wear values of the new polymer.

Experimental

General Experimental Procedure for Synthesis

Unless otherwise noted, all reactions were performed in the CEM Discover Microwave Reactor, fitted with the BenchMate pressure control system, in 10.0 mL thick-walled Pyrex reaction tubes fitted with pressure sensitive septa caps. All reactions performed in the microwave reactor were carried out at 50W power and heated to the specified temperature in the experimental procedure. Infrared spectra were taken on a Thermo Electron Corporation IR 200 spectrophotometer and analyzed using EZ-OMNIC software. The ^{1}H and ^{13}C NMR were recorded on a Bruker Avance II 400 MHz NMR spectrometer with indirect detection probe. Chemical shifts were reported in parts per million (ppm) from a standard of tetramethylsilane in $CDCl_3$ (0.1% w/v TMS) or D6-DMSO (d_6, 99.9 atom% D). NMR spectra multiplicities are defined as follows: s (singlet), d (doublet), t (triplet), m (multiplet), dd (doublet of doublets), and all coupling constants, (*J*), are labeled in Hertz. The mass spectra were obtained on a Bruker Esquire-HP LC/MS spectrometer in ESI+ detection mode. Thin layer chromatography was performed on Whatman aluminum-backed plates with varying eluent systems. Flash column chromatography was performed using 32-60 Å silica gel with varying eluent systems. COSY and HMQC spectra were included for completeness as they aided in the assignments of the peaks in the ^{1}H and ^{13}C NMR spectra.

Formation of *para*-nitrobenzenesulfonyl azide (4) from *para*-nitrobenzenesulfonyl chloride (3).

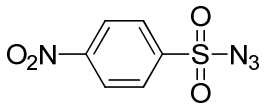

4

To a flame-dried, 100 mL round bottomed flask, fitted with magnetic stir-bar, 5.00 g (22.56 mmol) of 4-nitrobenzene sulfonyl chloride was added and then dissolved in 40.0 mL anhydrous methanol. When partially dissolved, 2.93 g (45.12 mmol, 2.0 eq.) of sodium azide was added. The reaction mixture was then allowed to stir at room temperature for 24 hours. The methanol was then removed with the rotary evaporator with the temperature kept below 40 °C. The resulting slurry was then partitioned between CH_2Cl_2/H_2O (40.0 mL), and separated. The organic layer was then dried over $MgSO_4$, filtered, and the solvent removed *in vacuo* resulting in 3.65 g of an off-white solid in 70.6% yield.

^{1}H NMR: δ 8.17-8.19 (d, 2H, Ar-H, J = 9.08 Hz), 8.46-8.49 (d, 2H, J = 4.66 Hz).

^{13}C NMR: δ 151.2, 143.7, 128.9 (double intensity), 124.9 (double intensity).

IR spectrum: 3546, 2930, 2141 cm^{-1}.

Melting Point: 95-98 °C

Synthesis of Azides from Alcohols

General procedure for the conversion of alcohols to azides

In a clean, dry microwave tube fitted with magnetic stir-bar, 5.0 equivalents of sodium hydride (NaH) was dissolved in 2.0 mL *N,N*-dimethyl formamide (DMF). To this mixture 1.0 equivalent of the alcohol was added along with 2.0 mL additional DMF. This reaction mixture was allowed to stir at room temperature for 30 minutes. After 30 minutes, 1.5 equivalents of *p*-nitrobenzene sulfonyl azide (*p*-NBSA) was added to the reaction mixture, changing color from a yellow to a deep red and then to a brown, along with 2.0 mL of DMF, for a total solvent volume of 5.0 mL DMF. The reaction mixture was then placed in the microwave reactor for 10 minutes at 100 °C. Once complete by TLC, with staining by *p*-anisaldehyde, the reaction was poured into 100 mL cyclohexane in a separatory funnel to separate the DMF which is immiscible in cyclohexane. The layers were separated and the cyclohexane was poured off through filter paper to filter any small amounts of DMF that remained in the cyclohexane. The cyclohexane was then removed *in vacuo*, and the crude reaction mixture was purified by flash column chromatography, unless otherwise noted.

Formation of biphenyl-4-carbaldehyde (2) from 4-biphenylmethanol (1).

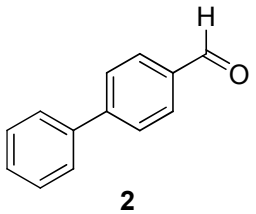

2

Following the general procedure for azide synthesis, 0.109 g (2.71 mmol, 5.0 eq.) NaH was added to DMF and reacted with 0.100 g (0.534 mmol) 4-biphenylmethanol at room temperature for 30 minutes. After 30 minutes, 0.249 g (1.086 mmol, 1.5 eq.) *p*-NBSA was added to the reaction mixture which was then placed in the microwave reactor for 20 minutes at 100 °C. The reaction was determined to be complete by TLC (7:1 hexanes/ethyl acetate) R_f = 0.61, 0.71. The crude mixture was worked up with cyclohexane and separated on a silica gel flash column (75 mL silica, 7:1 hexanes/ethyl acetate), yielding 0.09 g product for a 78.9% final yield.

^{1}H NMR: δ 7.45-7.54 (m, 4H, Ar-H), 7.8 (d, 2H, Ar-H, *J* = 7.7 Hz), 7.9 (d, 2H, Ar-H, *J* = 7.9 Hz), 8.0 (d, Ar-H, *J* = 8.0 Hz), 10.0 (s, 1H, CHO).

^{13}C NMR: δ 115.8, 127.6, 127.8, 129.0, 129.6, 130.6, 139.3, 146.3, 193.2.

m/z calculated: 182.07

m/z found: 181.0.

Formation of 1-(azidomethyl)-2,3-dimethoxybenzene (6) from 2,3-dimethoxybenzyl alcohol (5).

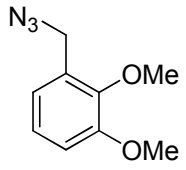

6

Following the general procedure for azide synthesis, 0.119 g (2.97 mmol, 5.0 eq.) NaH was added to DMF and reacted with 0.100 g (0.595 mmol) 2,3-dimethoxybenzyl alcohol at room temperature for 30 minutes. After 30 minutes, 0.214 g (0.892 mmol, 1.5 eq.) of *p*-NBSA was added to the reaction mixture which was then placed in the microwave reactor for 10 minutes at 100 °C. The reaction was determined to be complete by TLC (1:1 hexanes/ethyl acetate) $R_f = 0.45$. The mixture was then worked up with cyclohexane and purified on a silica gel flash column (40 mL silica, 7:1 hexanes/ethyl acetate), yielding 0.115 g product for a 60.9% final yield.

^{1}H NMR: δ 3.7 (s, 3H, OCH_3), 3.8 (s, 3H, OCH_3), 4.3 (s, 2H, CH_2), 6.91-6.93 (m, 1H, Ar-H), 7.07-7.09 (m, 2H, Ar-H).

^{13}C NMR: δ 49.5, 56.2, 60.9, 114.0, 122.3, 124.5, 129.2, 147.5, 152.9.

m/z calculated: 193.09

m/*z* found: 151.8 (mass – N_3)

IR spectrum: 2016 cm^{-1}

Formation of 5-(azidomethyl)benzo[*d*][1,3]dioxole (8) from piperonyl alcohol (7).

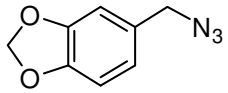

8

Following the general procedure for azide synthesis, 0.131 g of (3.29 mmol, 5.0 eq.) NaH was suspended in DMF and reacted with 0.100 g (0.657 mmol) of piperonyl alcohol at room temperature for 30 minutes, the reaction mixture turned dark brown-black after 10 minutes of stirring at room temperature. After 30 minutes, 0.226 g (0.986 mmol, 1.5 eq.) of *p*-NBSA was added to the reaction mixture which was then placed in the microwave reactor for 20 minutes at 100 °C, monitoring every 10 minutes by TLC. The reaction was determined to be complete by TLC (7:1 hexanes/ethyl acetate), R_f = 0.60. The mixture was then worked up with cyclohexane and purified on a silica gel flash column (75 mL silica, 1:1 hexanes/ethyl acetate), yielding 0.037 g product, as brown clear oil, for a 31.9% final yield.

m/*z* (calculated): 177.05

m/*z* (found): 135.1 (mass – N_3)

IR spectrum: 2100 cm^{-1}

Formation of 1,4-bis(azidomethyl)benzene (10) from 1,4-benzenedimethanol (9).

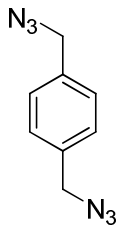

10

Following the general procedure for azide synthesis, 0.144 g (3.67 mmol, 5.0 eq.) NaH was added to 2.0 mL of DMF and reacted with 0.100 g (0.724 mmol) 1,4-benzenedimethanol for 30 minutes at room temperature. To this was added 0.495 g (2.17 mmol, 3.0 eq.) *p*-NBSA. The reaction was then placed in the microwave reactor for 20 minutes at 100 °C. The TLC of the reaction showed complete conversion of the starting material, 7:1; hexanes/ethyl acetate, R_f = 0.60, for 37.9% yield of the product after the cyclohexane workup procedure.

^{1}H NMR: δ 4.7 (s, 4H, CH_2), 7.4 (s, 4H, Ar-H).

^{13}C NMR: δ 53.7, 128.3, 129.2.

m/*z* (calculated): 188.08

m/*z* (found):185.9

IR spectrum: 2102 cm^{-1}

Formation of 1-azido-2,3-dihydro-1*H*-indene (12) from 1-indanol (11).

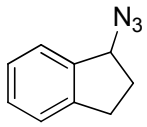

12

Following the general procedure for azide synthesis, 0.149 g (3.73 mmol, 5.0 eq.) NaH was suspended in DMF and reacted with 0.100 g (0.745 mmol) of 1-indanol at room temperature for 30 minutes. After 30 minutes, 0.256 g (1.12 mmol, 1.5 eq.) of *p*-NBSA was added to the reaction mixture, which was then placed in the microwave reactor for 40 minutes at 100 °C, and monitored by TLC every 20 minutes. The reaction was determined to be complete by TLC (7:1 hexanes/ethyl acetate) R_f = 0.64, 0.48. The crude reaction mixture was then worked up with cyclohexane and purified on a silica gel flash column (75 mL silica, 7:1 hexanes/ethyl acetate), yielding 0.042 g product for a 35.4% final yield.

^{1}H NMR: δ 1.95-2.03 (m, 1H, CH_2), 2.35-2.44 (m, 1H, CH_2), 2.8 (dddd, 1H, CH_2, J = 16.1, 5.4, 8.1), 2.80-2.87 (m, 1H, CH_2), 5.0 (dd, 1H, CH, J = 7.1, 4.2), 7.22-7.40 (m, 4H, Ar-H).

^{13}C NMR: 30.4, 65.7, 124.9, 125.5, 127.1, 129.2, 140.9, 144.0.

m/*z* calculated: 159.08

m/*z* found: 158.9

IR spectrum: 2094 cm^{-1}

Formation of 2-azido-2,3-dihydro-1*H*-indene (14) from 2-indanol (13).

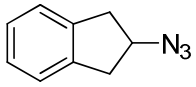

14

Following the general procedure for azide synthesis, 0.149 g (3.73 mmol, 5.0 eq.) NaH was added to DMF and reacted with 0.100 g (0.745 mmol) of 2-indanol at room temperature for 30 minutes. After 30 minutes, 0.256 g (1.12 mmol, 1.5 eq.) *p*-NBSA was added to the reaction mixture which was then placed in the microwave reactor for 20 minutes at 100°C. The reaction was determined to be complete by TLC (7:1 hexanes/ethyl acetate) R_f = 0.80, 0.50. The crude reaction mixture was then worked up with cyclohexane, and purified on a silica gel flash column (75 mL silica, 7:1 hexanes/ethyl acetate), yielding 0.063g product as a yellowish syrup for a 53.1% final yield.

^{1}H NMR: 2.9 (dd, 2H, CH_2, J = 16.3, 3.5), 3.2 (dd, 2H, CH_2, J = 16.4, 6.5), 4.5 (tt, 1H, J = 6.8, 3.4), 7.1-7.3 (m, 4H, Ar-H).

^{13}C NMR: 61.9, 79.4, 125.0, 127.2, 140.7.

m/z (calculated): 159.08

m/z (found):158.9

IR spectrum: 2101 cm^{-1}

Formation of (±) 2-(1-azidoethyl)naphthalene (16) from (±) α-methyl-2-napthalene methanol (15).

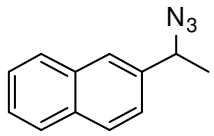

16

Following the general procedure for azide synthesis, 0.116 g (2.90 mmol, 5.0 eq.) NaH was suspended in DMF and reacted with 0.100 g (0.581 mmol) (±) α-methyl-2-napthalenemethanol at room temperature for 30 minutes. After 30 minutes, 0.200 g (0.871 mmol, 1.5 eq.) *p*-NBSA was added to the reaction mixture which was then placed in the microwave reactor for 20 minutes at 100 °C, monitoring every 10 minutes by TLC. The reaction was determined to be complete by TLC (7:1 hexanes/ethyl acetate). The crude reaction mixture was then worked up with cyclohexane and purified on a silica flash column (75 mL silica, 7:1 hexanes/ethyl acetate), yielding 0.02 g product, as a reddish oil, for a 17.5% final yield.

^{1}H NMR: δ 1.6 (d, 3H, CH_3, J = 6.84 Hz), 4.75 (q, 1H, CH, J = 6.82 Hz), 7.43-7.50 (m, 3H, Ar-H), 7.76-7.87 (m, 4H, Ar-H).

^{13}C NMR: δ 21.6, 61.3, 124.2, 125.3, 126.3, 126.4, 127.7, 128.0, 128.8, 133.1, 133.2, 138.2.

m/*z* (calculated): 197.10

m/*z* (found): 154.0 (mass – N_3), 167.0 (mass – N_2)

IR spectrum: 2106 cm^{-1}

Synthesis of 9-fluorenone (18) from 9-hydroxyfluorene (17).

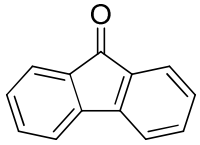

18

Following the general procedure for azide synthesis, 0.110 g (2.74 mmol, 5.0 eq.) NaH was added to DMF and reacted with 0.100 g (0.549 mmol) 9-hydroxyfluorene at room temperature for 30 minutes. After 30 minutes, 0.189 g (0.823 mmol, 1.5 eq.) of *p*-NBSA was added to the reaction mixture which was then placed in the microwave reactor for 10 minutes at 100 °C. The reaction was determined to be complete by TLC (7:1 hexanes/ethyl acetate) R_f = 0.48. The crude reaction mixture was then worked up with cyclohexane and purified on a silica gel flash column (75 mL silica, 7:1 hexanes/ethyl acetate), yielding 0.06 g product as a bright yellow solid for a 52.6% final yield.

^{1}H NMR: 7.2-7.7 (m, 4H, Ar-H)

^{13}C NMR: 120.3, 124.3, 129.1 (double intensity), 134.7, 144.4, 194.0.

m/*z* (calculated): 180.06

m/*z* (found): 181.1

Towards the synthesis of artificial cartilage

Synthesis 3-3'-(4-4'-(propane-2,2-diyl)bis(4,1-phenylene))bis(oxy)bis(1-azidopropan-2-ol) from bis-phenol A diglycidyl ether.

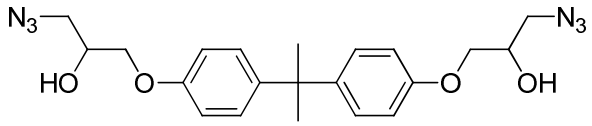

20

Following the procedure from the literature, 0.369 g (1.08 mmol), BADGE placed in a clean, flame-dried 100 mL round-bottomed flask. To this was added 2.02 g of PEG 400 as the solvent and the mixture was stirred to combine. Once mixed completely, 0.170 g (2.40 mmol) of sodium azide was added. This did not completely dissolve for the course of the reaction. After 2.0 hours of stirring at room temperature, the crude reaction mixture was poured onto 10 mL water, separated, and extracted with ethyl acetate (2 x 10 mL), dried over $MgSO_4$, filtered and the solvent removed *in vacuo* resulting in 0.306 g of crude product for a 66.1% crude yield. The crude product was then purified by column chromatography (2:1 Hexanes/Ethyl Acetate) for a final yield of 0.063 g or 13.7%.

IR spectrum: 3474 (broad), 2101 cm^{-1}.

Synthesis of 4,4-(propane-2,2-diyl)bis((3-azido-2-(prop-2-ynyloxy)propoxy)benzene from 20.

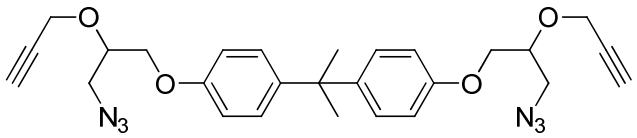

21

In a clean, dry, 100 mL round-bottomed flask, 0.88 g of **20** was dissolved in 5.0 mL of anhydrous DMF under inert atmosphere. Once dissolved, 0.205 g (5.159 mmol, 2.5 eq) of sodium hydride was added to the solution in portions at room temperature. The reaction turned yellow after 5 minutes at room temperature, at which time it was placed in an ice-water bath. The mixture was stirred at 0 °C for 15 minutes before adding 0.56 mL (5.16 mmol, 2.5 eq.) of propargyl bromide to the solution. The reaction was stirred at 0 °C overnight, and the solvent was removed *in vacuo*. The crude reaction mixture was then partitioned between methylene chloride and H_2O (20 mL) and separated. The aqueous layer was washed with methylene chloride (3 x 10 mL), and the organic extracts were combined, dried over $MgSO_4$, filtered, and the solvent removed *in vacuo*. The product was purified on a silica gel flash chromatography column (100 mL silica, ethyl acetate), providing 0.535 g pure product for a 55.6% final yield.

IR spectrum: 2102, 3285 (narrow) cm^{-1}

References

1. Scriven, E. F. V.; Turnbull, K. "Azides: Their Preparation and Synthetic Uses," *Chem. Rev.* **1988**, *88*, 298-368.
2. Bräse, S.; Gil, C.; Knepper, K.; Zimmermann, V., "Organic Azides: An Exploding Diversity of a Unique Class of Compounds," *Angew. Chem. Int. Ed.* **2005**, *44*, 5188-5240.
3. Papeo, G.; Posteri, H.; Vianello, P.; Varasi, M., "Nicotinoyl Azide (NCA)-Mediated Mitsunobu Reaction: An Expedient One-Pot Transformation of Alcohols into Azides," *Synthesis* **2004**, *17*, 2886-2892.
4. Viaud, M. C.; Rollin, P. "Zinc Azide Mediated Mitsunobu Substitution. An Expedient Method for the One-Pot Azidation of Alcohols," *Synthesis* **1989**, 130-132.
5. Thompson, A. S.; Humphrey, G. R.; DeMarco, A. M.; Mathre, D. J.; Grabowski, E. J. J. "Direct Conversion of Activated Alcohols to Azides Using Diphenyl Phosphorazidate. A Practical Alternative to Mitsunobu Conditions," *J. Org. Chem.* **1993**, *58*, 5886-5888.
6. Mizuno, M.; Shioiri, T. "Efficient Method for the One-Pot Azidation of Alcohols Using Bis(*p*-nitrophenyl)phosphorazidate," *Chem. Commun.* **1997**, 2165-2166.
7. Yu, C.; Liu, B.; Hu, L. "A Simple One-Pot Procedure for the Direct Conversion of Alcohols to Azides *via* Phosphate Activation," *Org. Lett.* **2000**, *2*, 1959-1961.
8. Sacui, I. "Synthesis and Decomposition of Novel Diazosugars," Youngstown State University MS Thesis, 2006.

9. Rad, M.; Behrouz, S.; Khalafi-Nezhad, A. "A Simple One-Pot Procedure for the Direct Conversion of Alcohols into Azides using TsIm," *Tetrahedron Lett.* **2007**, *48*, 3445-3449.

10. Jayanthi, A.; Gumaste, V. K.; Deshmukh, A. R. A. S. "A Simple One-Pot Method for the Preparation of Allyl Azides from Allyl Alcohols Using Triphosgene: Synthesis of *N*1-Cinnamyl Azetidin-2-ones," *Synlett* **2004**, *6*, 979-982.

11. Loupy, A. *Microwaves in Organic Synthesis*, Wiley VCH: New York, 2002.

12. Gabriel, C.; Gabriel, S.; Grant, E. H.; Halstead, B. S. J.; Mingos, D. M. P. "Dielectric Parameters Relevant to Microwave Dielectric Heating," *Chem. Soc. Rev.* **1998**, *27*, 213-223.

13. de la Hoz, A.; Diaz-Ortiz, A.; Moreno, A. "Microwaves in Organic Synthesis. Thermal and Non-Thermal Microwave Effects," *Chem. Soc. Rev.* **2005**, *34*, 164-178.

14. Kappe, C. O. "Controlled Microwave Heating in Modern Organic Synthesis," *Angew. Chem. Int. Ed.* **2004**, *43*, 6250-6284.

15. Varma, R. S. "Solvent-Free Organic Syntheses," *Green Chem.* **1999**, 43-55.

16. Cho, S. H.; Yoo, E. J.; Bae, I.; Chang, S. "Copper-Catalyzed Hydrative Amide Synthesis with Terminal Alkyne, Sulfonyl Azide, and Water," *J. Am. Chem. Soc.* **2005**, *127*, 16046-16047.

17. Cassidy, M. P.; Raushel, J.; Fokin, V. V. "Practical Synthesis of Amides from In Situ Generated Copper (I) Acetylides and Sulfonyl Azides," *Angew. Chem. Int. Ed.* **2006**, *45*, 3154-3157.

18. Rostovtsev, V. V.; Green, L. G.; Fokin, V. V.; Sharpless, K. B. "A Stepwise Huisgen Cycloaddition Process: Copper (I)-Catalyzed Regioselective 'Ligation' of Azides and Terminal Alkynes," *Angew. Chem. Int. Ed.* **2002**, *41*, 2596-2599.
19. Kolb, H. C.; Sharpless, K. B. "The Growing Impact of Click Chemistry on Drug Discovery," *DDT* **2003**, *8*, 1128-1137.
20. Ikada, Y. Biological Materials. In *Integrated Biomaterials Science*, Barbucci, R., Ed. Kluwer Academic Publishers/Plenum Publishers: New York, 2002; pp 1-12 and 14-22.
21. Marconi, W.; Piozzi, A. Structure and Properties of Polymeric Materials. In *Integrated Biomaterials Science*, Barbucci, R., Ed. Kluwer Academic Publishers/Plenum Publishers: New York, 2002; pp 25-66.
22. Gatti, A. M.; Knowles, J. C. Biocompatibility and Biological Tests. In *Integrated Biomaterials Science*, Barbucci, R., Ed. Kluwer Academic Publishers/Plenum Publishers: New York, 2002; pp 793-813.
23. Flik, K. R.; Verma, N.; Cole, B. J.; Bach, B. R. Jr. Articular Cartilage: Structure Biology and Function. In *Cartilage Repair Strategies*, Williams, R. J. Ed. Humana Press: Totowa, New Jersey, 2007; pp 1-11.
24. Meyer, U.; Wiesmann, H. P. *Bone and Cartilage Engineering*; Springer-Verlag: New York, 2006; pp 25-35 and 163-177.
25. Hall, A. C. Physiology of Cartilage. In *Sciences Basics to Orthopaedics*, Hughes, S. P. F.; McCarthy, I. D. Eds. W. B. Saunders Company Ltd: London, 1998; pp 45-69.

26. Abbot, A. E.; Levine, W. N.; Mow, V. C. Biomechanics of the Articular Cartilage and Menisci of the Adult Knee. In *The Adult Knee, Volume 1*, Callaghan, J. J.; Rosenberg, A. G.; Rubash, H. E.; Simonian, P. T. Eds. Lippincott, Williams & Williams: Philadelphia, 2003 pp 81-99.

27. Abatangelo, G.; Brun, P.; Radice, M.; Cortivo, R.; Auth, M. K. H. Tissue Engineering. In *Integrated Biomaterials Science*, Barbucci, R., Ed. Kluwer Academic Publishers/Plenum Publishers: New York, 2002; pp 907-916.

28. Katta, J. K.; Marcolongo, M.; Lowman, A.; Mansmann, K. A. "Friction and Wear Behavior of Poly(vinyl alcohol)/Poly(vinyl pyrrolidone) Hydrogels for Articular Cartilage Replacement," *J. Biomed. Mater. Res. Part A* **2007**, *83A*, 471-479.

29. Kobayashi, M.; Toguchida, J.; Oka, M. "Preliminary Study of Polyvinyl Acohol-Hydrogel (PVA-H) Artificial Meniscus," *Biomaterials* **2003**, *24*, 639-647.

30. Kobayashi, M.; Chang, Y. S.; Oka, M. "A Two Year *In Vivo* Study of Polyvinyl Alcohol-Hydrogel (PVA-H) Artificial Meniscus," *Biomaterials* **2005**, *26*, 3243-3248.

31. Gong, J. P.; Katsuyama, Y.; Kurokawa, T.; Osada, Y. "Double-Network Hydrogels with Extremely High Mechanical Strength," *Adv. Mater.* **2003**, *15*, 1155-1158.

32. Azuma, C.; Yasuda, K.; Tanebe, Y.; Taniguro, H.; Kanaya, F.; Nakayama, A.; Chen, Y. M.; Gong, J. P.; Osada, Y. "Biodegredation of High-Toughness Double Network Hydrogels as Potential Materials for Artificial Cartilage," *J. Biomed. Mater. Res. Part A* **2007**, *81A*, 373-380.

33. Hutcheon, G. A.; Messiou, C.; Wyre, R. M.; Davies, M. C.; Downes, S. "Water Absorption and Surface Properties of Novel Poly(ethylmethacrylate) Polymer Systems for Use in Bone and Cartilage Repair," *Biomaterials* **2001**, *22*, 667-676.

34. Hutcheon, G. A.; Downes, S.; Davies, M. C. "Interaction of Chondrocytes with Methacrylate Copolymers," *J. Mater. Sci.: Mater. Med.* **1998**, *9*, 815-818.

35. Wyre, R. M.; Downes, S. "An *In Vitro* Investigation of the PEMA/THFMA Polymer System as a Biomaterial for Cartilage Repair," *Biomaterials* **2000**, *21*, 335-343.

36. Sanchis, M. J.; Díaz-Calleja, R.; García-Bernabé, A.; Alegría, L.; Gargallo, L.; Radic, D. "Water Sorption by Poly(tetrahyrofurfuril methacrylate)'s," *J. Polym. Sci., Part A: Polym. Phys.* **2008**, *46*, 109-120.

37. Barry, J. J. A.; Silva, M. M. C. G.; Popov, V. K.; Shakessheff, K. M.; "Supercritical Carbon Dioxide: Putting the Fizz Into Biomaterials," *Phil. Trans. R. Soc. A* **2006**, *364*, 249-261.

38. Kramer, F.; Klemm, D.; Schumann, D.; Heßler, N.; Wesarg, F.; Fried, W.; Staderman, D. "Nanocellulose Polymer Composites as Innovative Pool for (Bio)Material Development," *Macromol. Symp.* **2006**, *244*, 136-148.

39. Crews, P.; Rodriguez, J.; Jaspars, M. *Organic Structure Analysis*, Oxford University Press: New York, 1998; p. 334.

40. Imperio, D.; Pirali, T.; Galli, U.; Pagliai, F.; Cafici, L.; Canonico, P. L.; Sorba, G.; Genazzani, A. A.; Tron, G. C. "Replacement of the Lactone Moiety on the Podophyllotoxin and Steganacin Analogues with a 1,5-Disubstituted 1,2,3-

Triazole via Ruthenium Catalyzed Click Chemistry," *Bioorg. Med. Chem*. **2007**, *21*, 6748-6757.

41. O'Neil, E. J.; DiVittorio, K. M.; Smith, B. D. "Phosphatidylcholine-Derived Bolaamphiphiles via Click Chemistry," *Org. Lett.* **2007**, *9,* 199-202.
42. Smith, M. B.; March, J. *March's Advanced Organic Chemistry 3rd Edition*, John Wiley: New York, 2001; pp. 850-854.
43. Das, B.; Reddy, V. S.; Tehseen, F.; Krishnaiah, M. "Catalyst-Free Highly Regio- and Stereoselective Ring-Opening of Epoxides and Aziridines with Sodium Azide using Poly(ethylene glycol) as an Efficient Reaction Medium," *Synthesis* **2007**, *5*, 666-668.
44. Miner, P. "Synthesis of Diverse Compounds using Mannofuranose as a Chiral Scaffold," Youngstown State University MS Thesis, 2004 p. 64.
45. Alhassan, A. B. "Formation of *N*-Acetyl-L-fucosamine (L-FucNAc) and Analogs as Potential Inhibitors of *Staphylococcus aureus* Capsular Polysaccharide Biosynthesis," Youngstown State University MS Thesis, 2006 pp. 46-48.

Appendix A

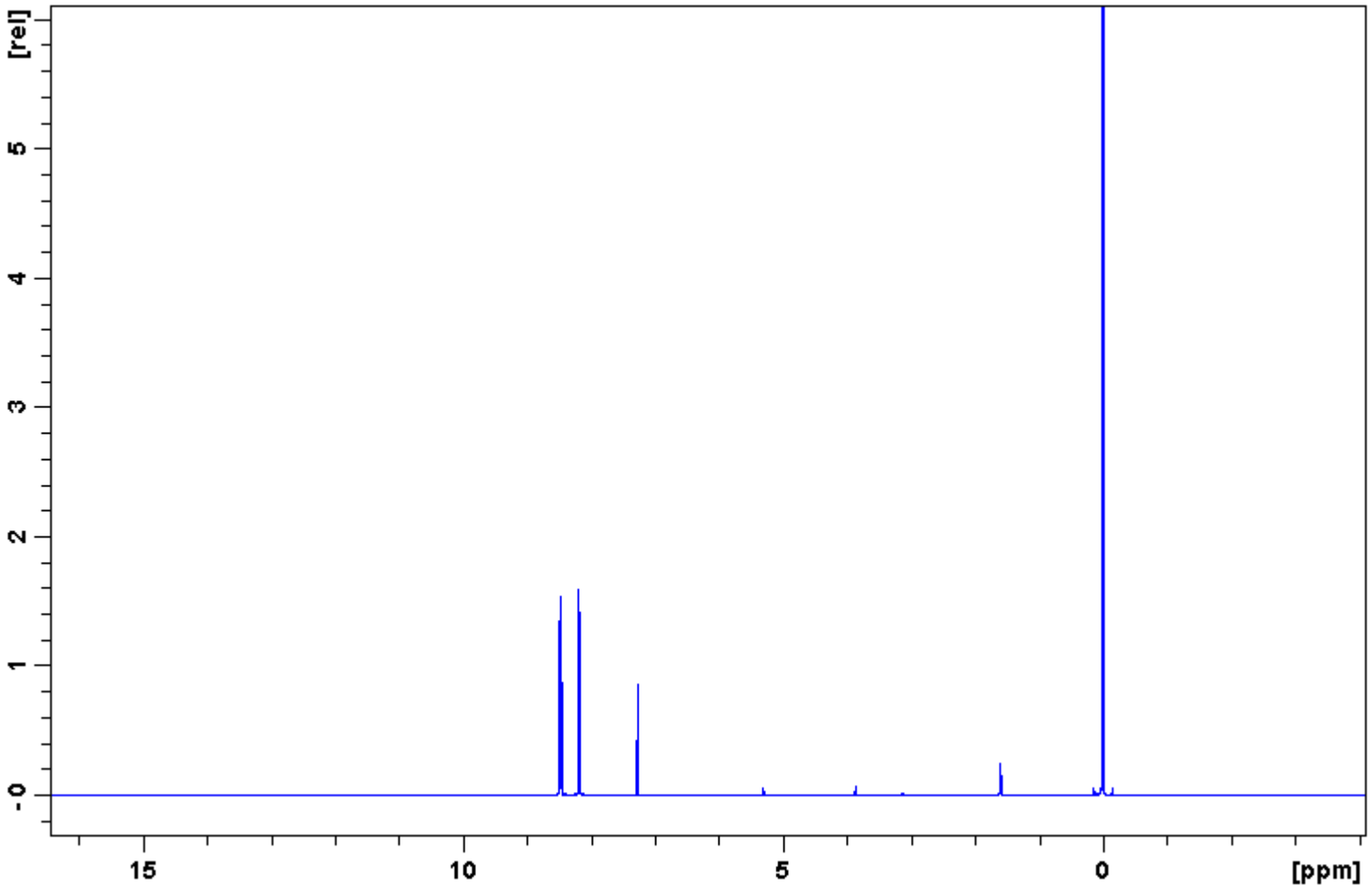

Figure 9: 400 MHz ^{1}H NMR spectrum of **4**.

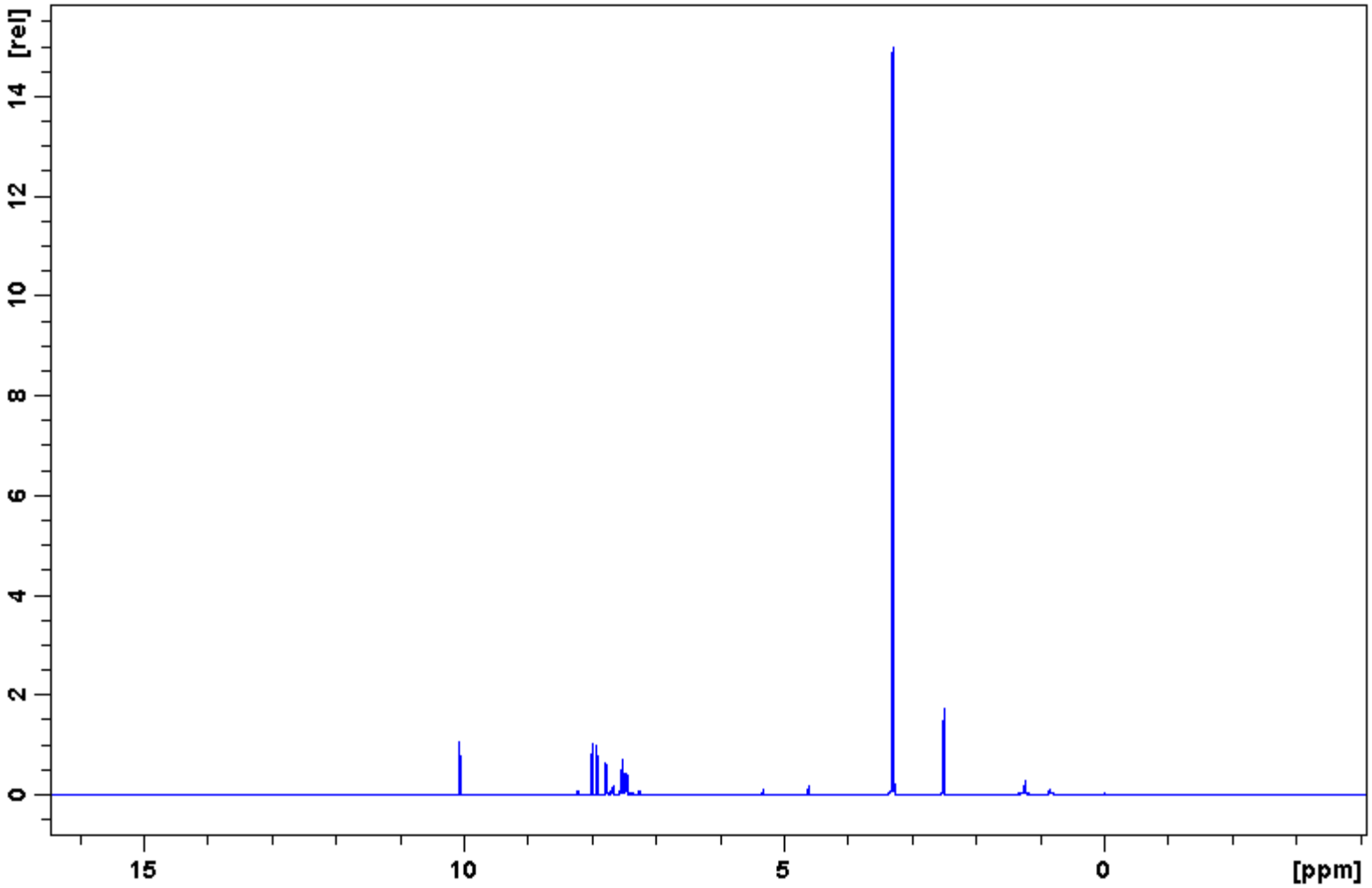

Figure 10: 400 MHz ^{1}H spectrum of **2**.

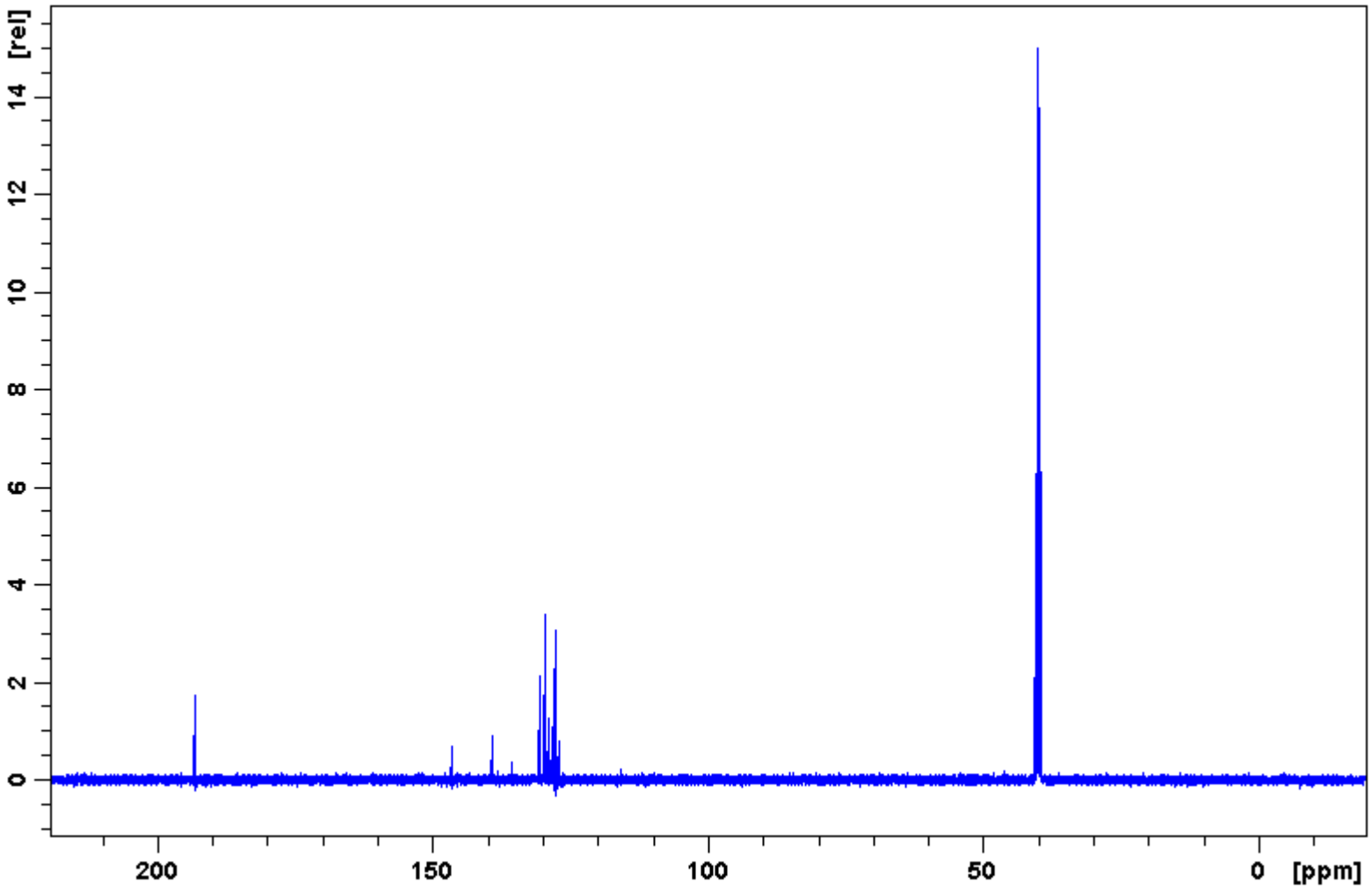

Figure 11: 100 MHz ^{13}C spectrum of **2**.

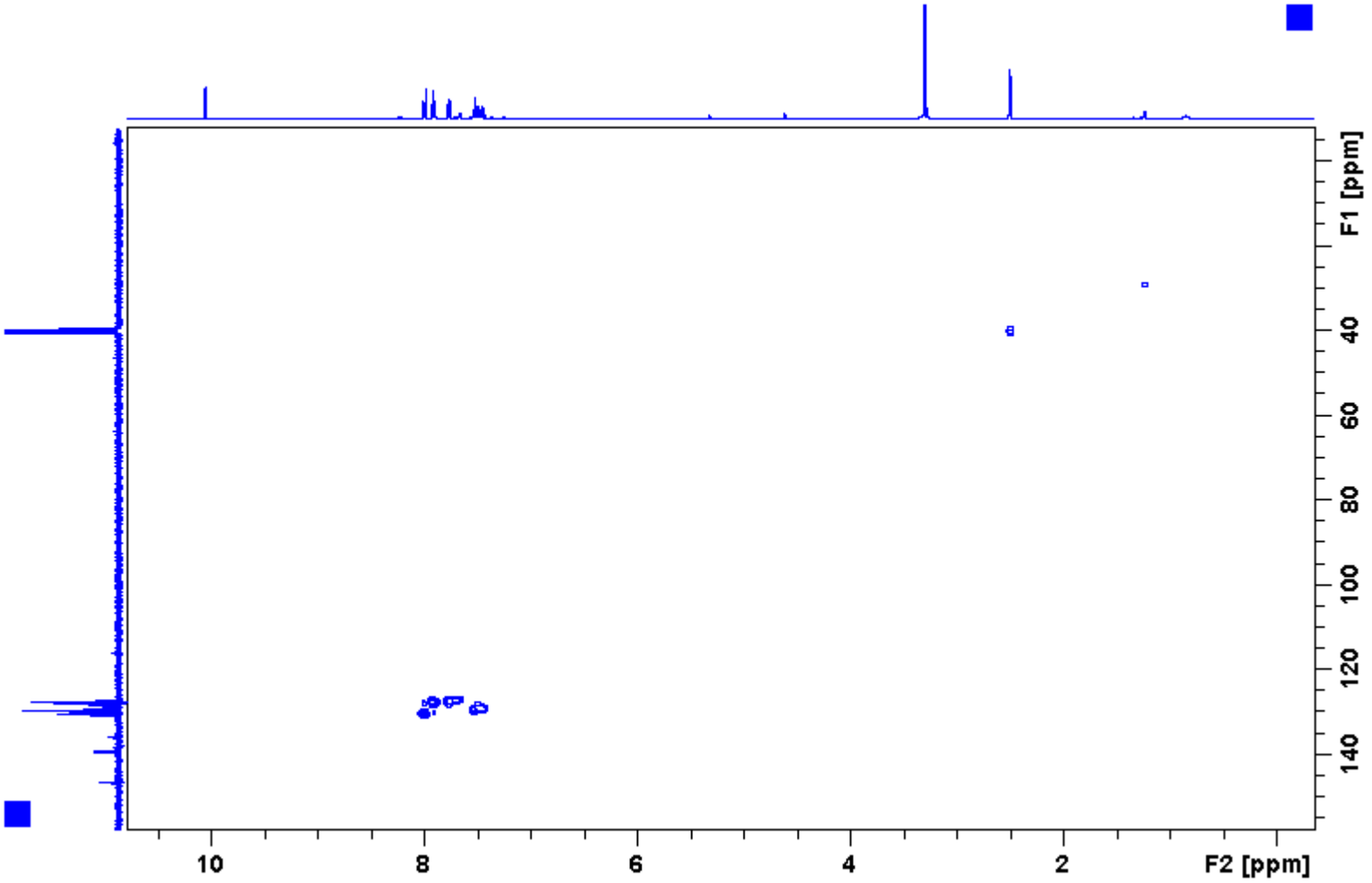

Figure 12: ^{1}H-^{1}H COSY spectrum of **2**.

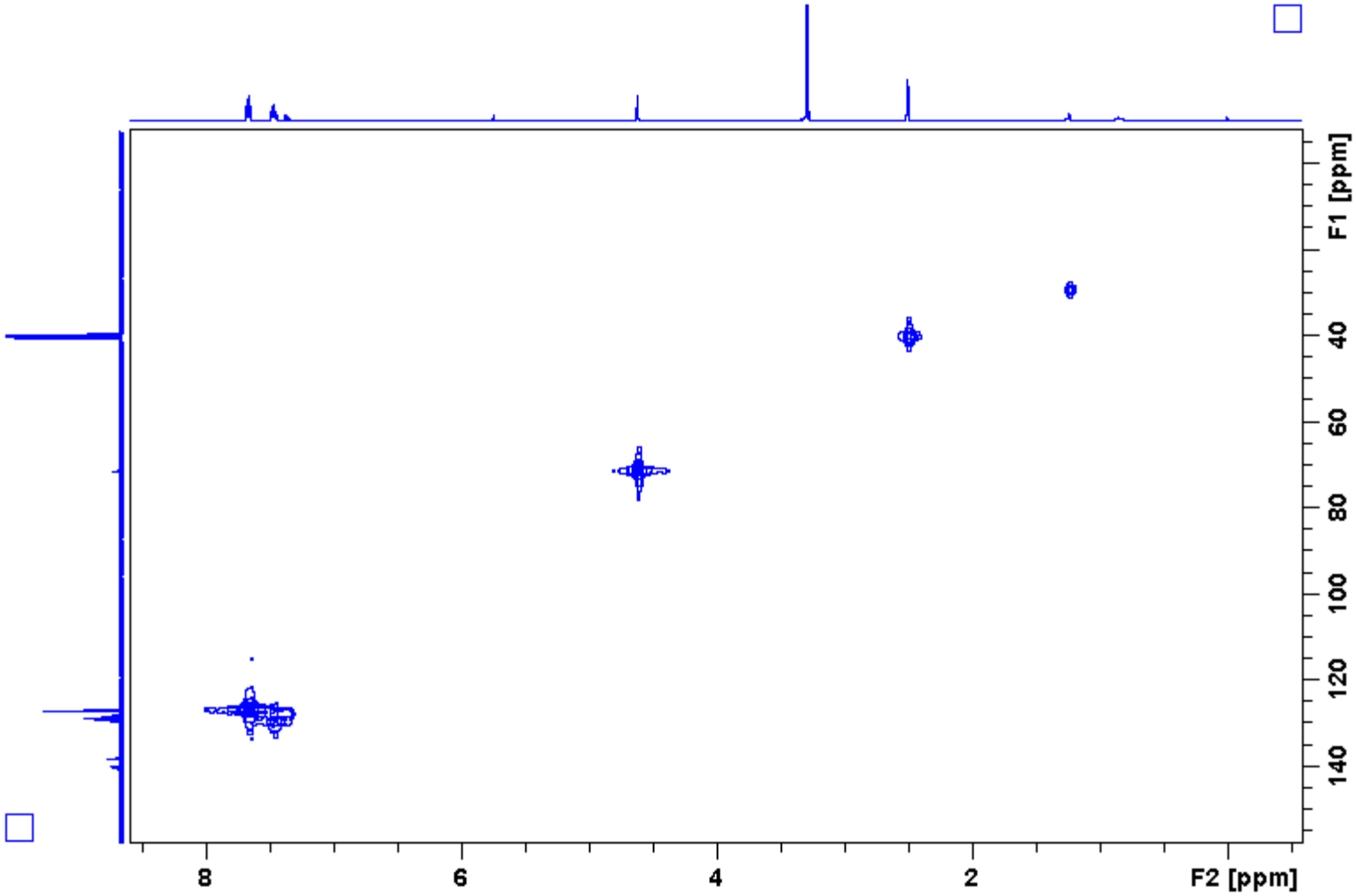

Figure 13: ^{1}H-^{13}C HMQC spectrum of **2**.

Mass Spectrum List Report

Analysis Info

Analysis Name	3-059204.d	Acquisition Date	07/29/08 20:00:07
Method	XQ Default.ms	Operator	Administrator
Sample Name	SK-III-005	Instrument	Esquire-LC_00135
Comment	BD-3-059		

Acquisition Parameter

Ion Source Type	ESI	Ion Polarity	Positive	Alternating Ion Polarity	n/a
Mass Range Mode	Std/Normal	Scan Begin	100.00 m/z	Scan End	400.00 m/z
Capillary Exit	116.5 Volt	Skim 1	45.4 Volt	Trap Drive	20.0
Accumulation Time	50000 µs	Averages	10 Spectra	Auto MS/MS	Off

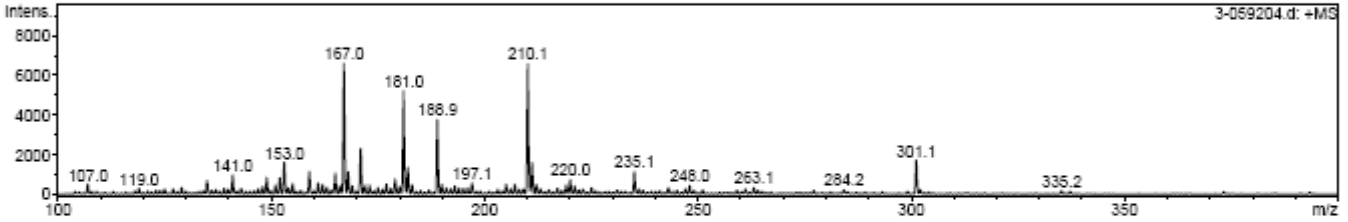

#	m/z	I	FWHM	S/N
1	153.0	1604	0.4	37.2
2	158.9	1137	0.3	26.4
3	167.0	6602	0.4	153.0
4	171.0	2295	0.4	53.2
5	181.0	5201	0.4	120.5
6	182.0	1345	0.3	31.2
7	188.9	3760	0.3	87.1
8	210.1	6574	0.4	152.4
9	211.1	1600	0.3	37.1
10	301.1	1711	0.4	39.7

Figure 14: Mass spectrum of **2**.

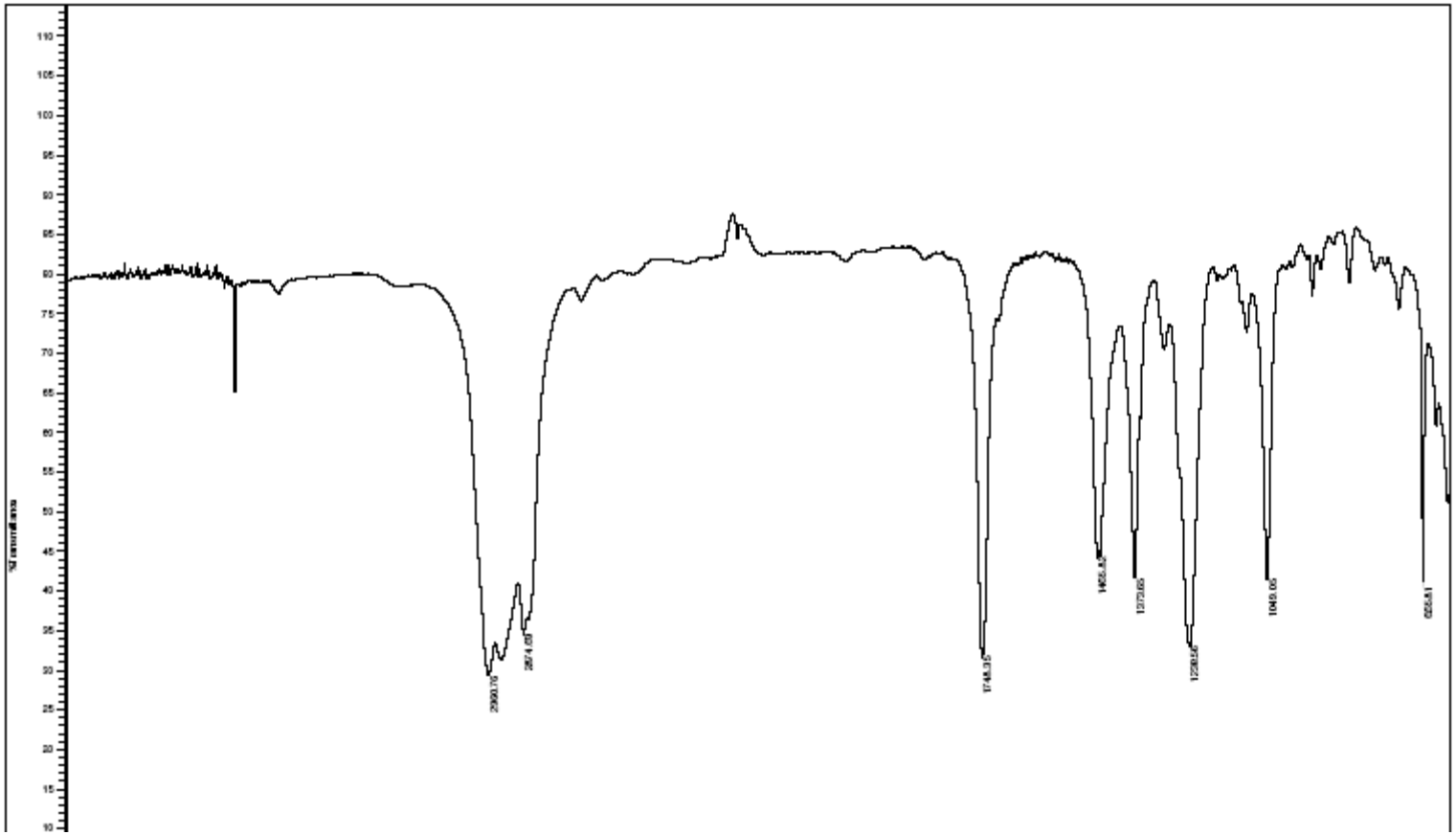

Figure 15: IR spectrum of **2**.

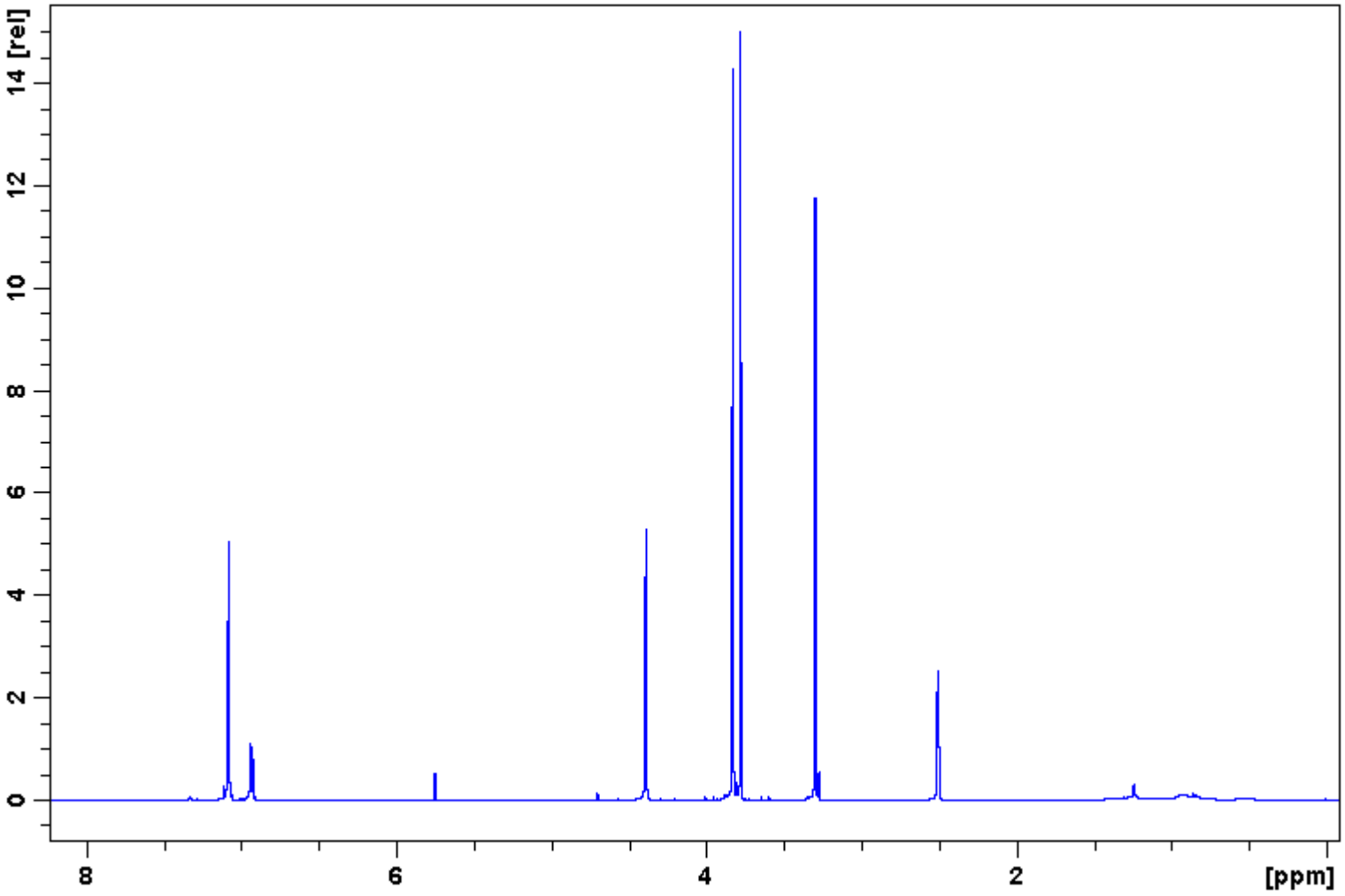

Figure 16: 400 MHz ^{1}H spectrum of **6**.

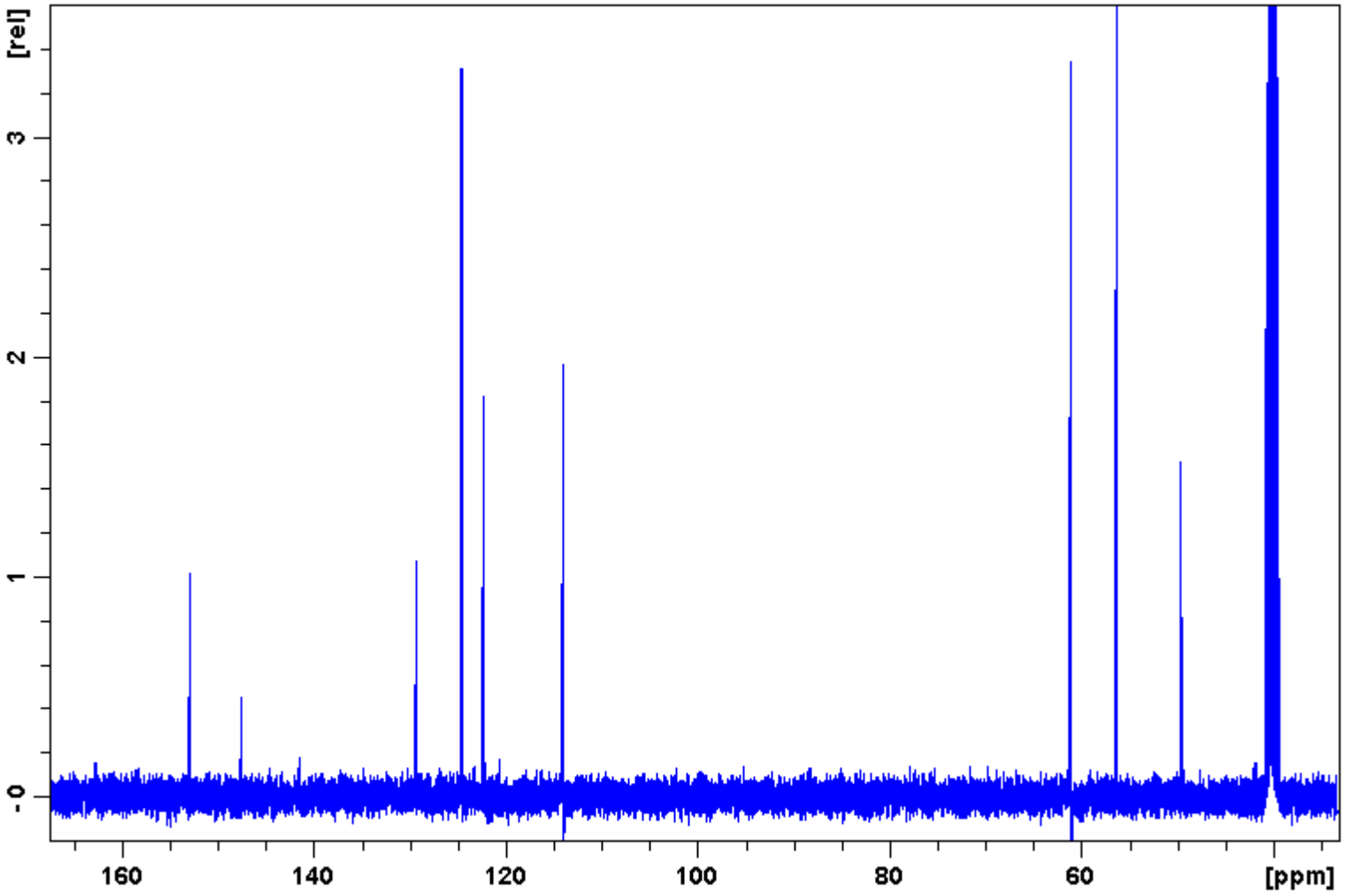

Figure 17: 100 MHz ^{13}C spectrum of **6**.

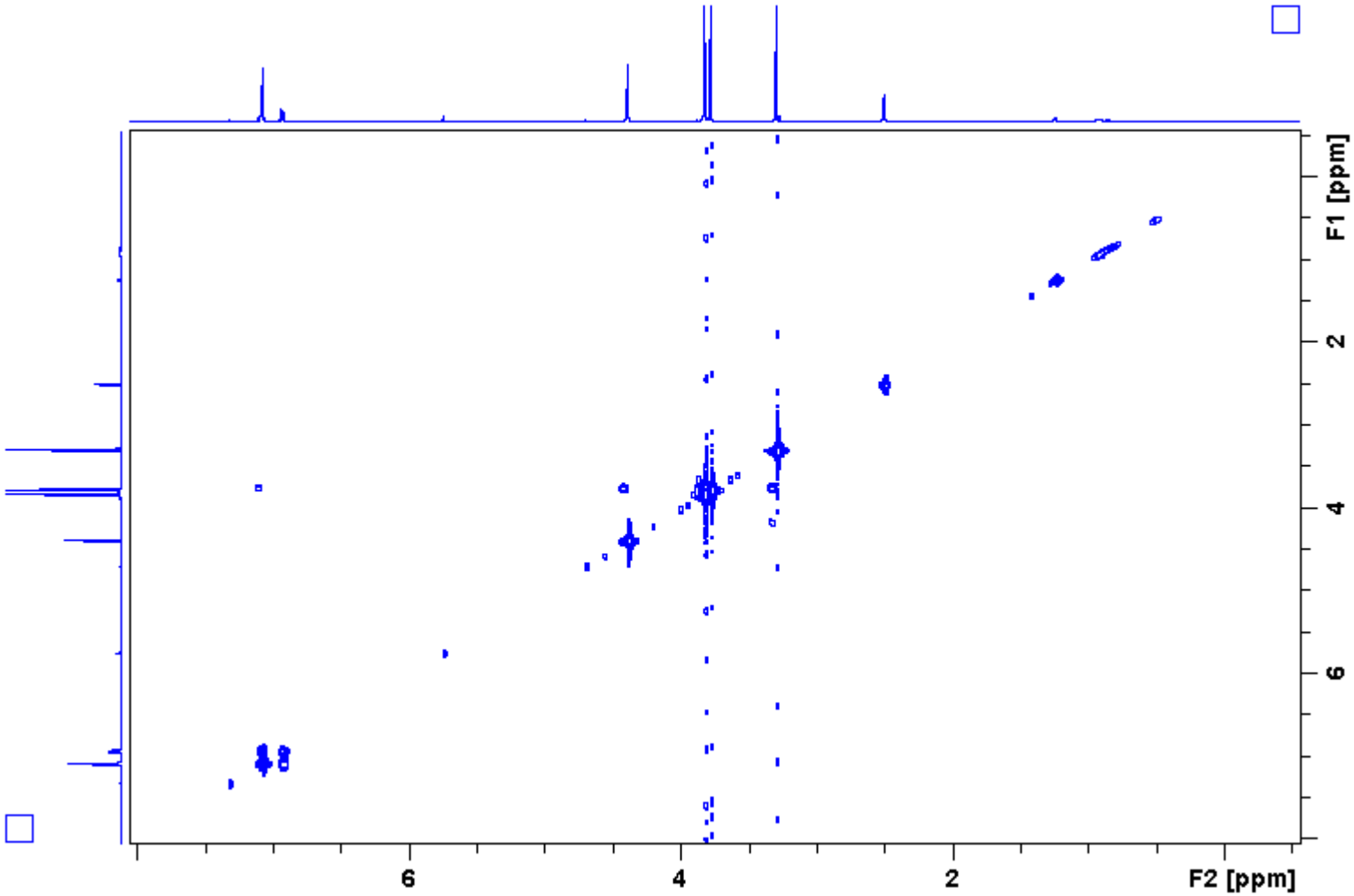

Figure 18: ^{1}H-^{1}H COSY spectrum of **6**.

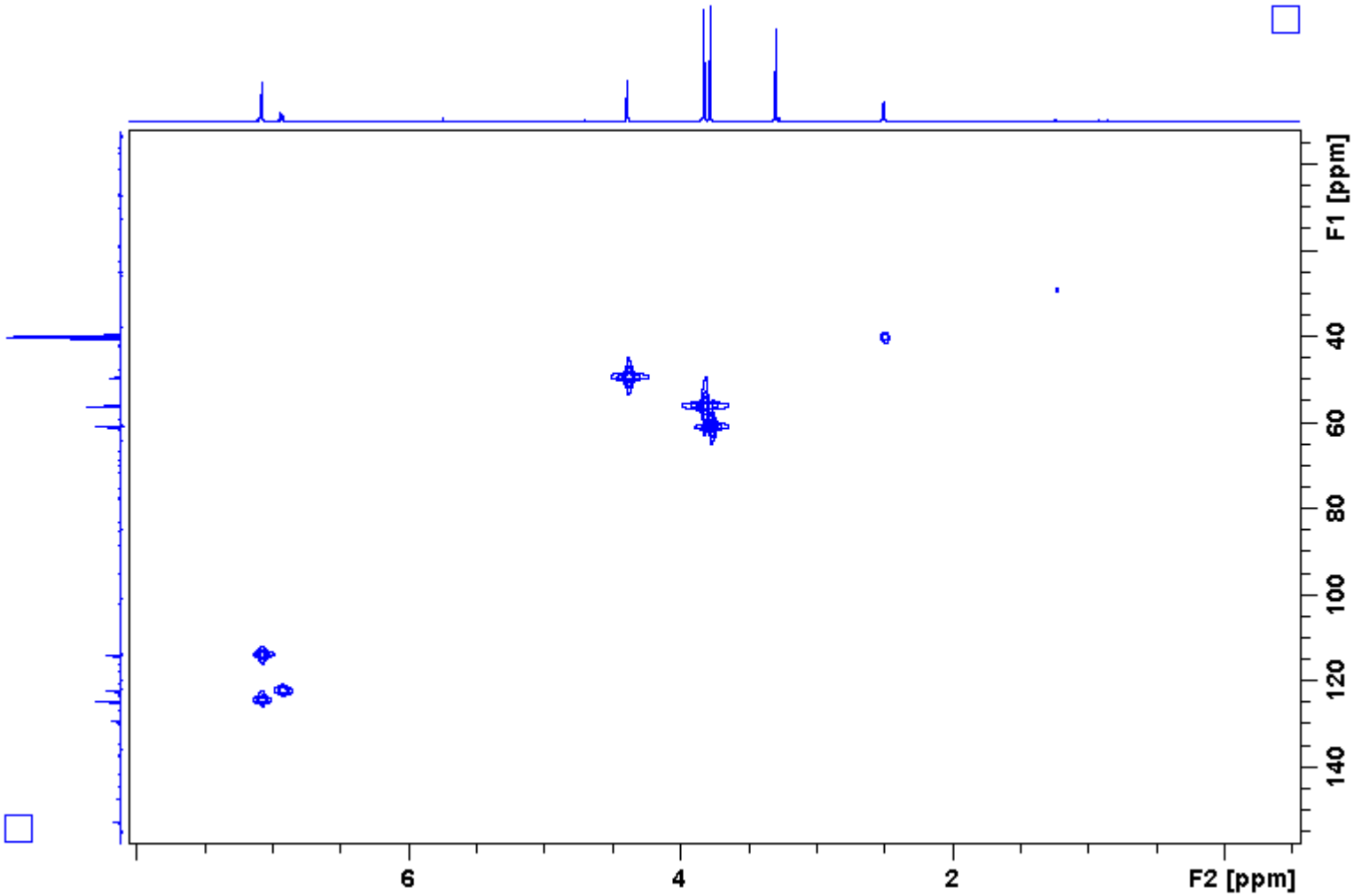

Figure 19: ^{1}H-^{13}C HMQC spectrum of **6**.

Mass Spectrum List Report

Analysis Info

Analysis Name	20330000.d	Acquisition Date	07/29/08 21:59:03
Method	XQ Default.ms	Operator	Administrator
Sample Name	bg6298	Instrument	Esquire-LC_00135
Comment	background 7/29/08		

Acquisition Parameter

Ion Source Type	ESI	Ion Polarity	Positive	Alternating Ion Polarity	n/a
Mass Range Mode	Std/Normal	Scan Begin	75.00 m/z	Scan End	225.00 m/z
Capillary Exit	104.1 Volt	Skim 1	32.1 Volt	Trap Drive	42.3
Accumulation Time	50000 µs	Averages	10 Spectra	Auto MS/MS	Off

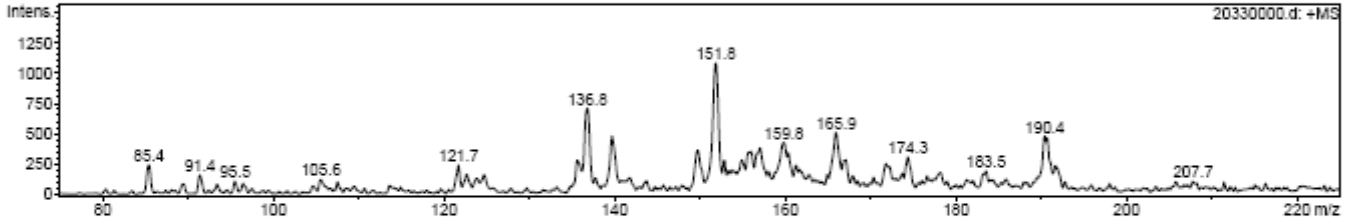

#	m/z	I	FWHM	S/N
1	136.8	709	0.6	30.6
2	139.7	480	0.6	20.7
3	149.7	361	0.7	15.6
4	151.8	1081	0.7	46.7
5	155.9	353	0.7	15.2
6	157.0	382	0.8	16.5
7	159.8	427	0.7	18.4
8	165.9	509	0.6	22.0
9	190.4	479	0.3	20.7
10	190.6	465	0.2	20.1

Figure 20: Mass spectrum of **6**.

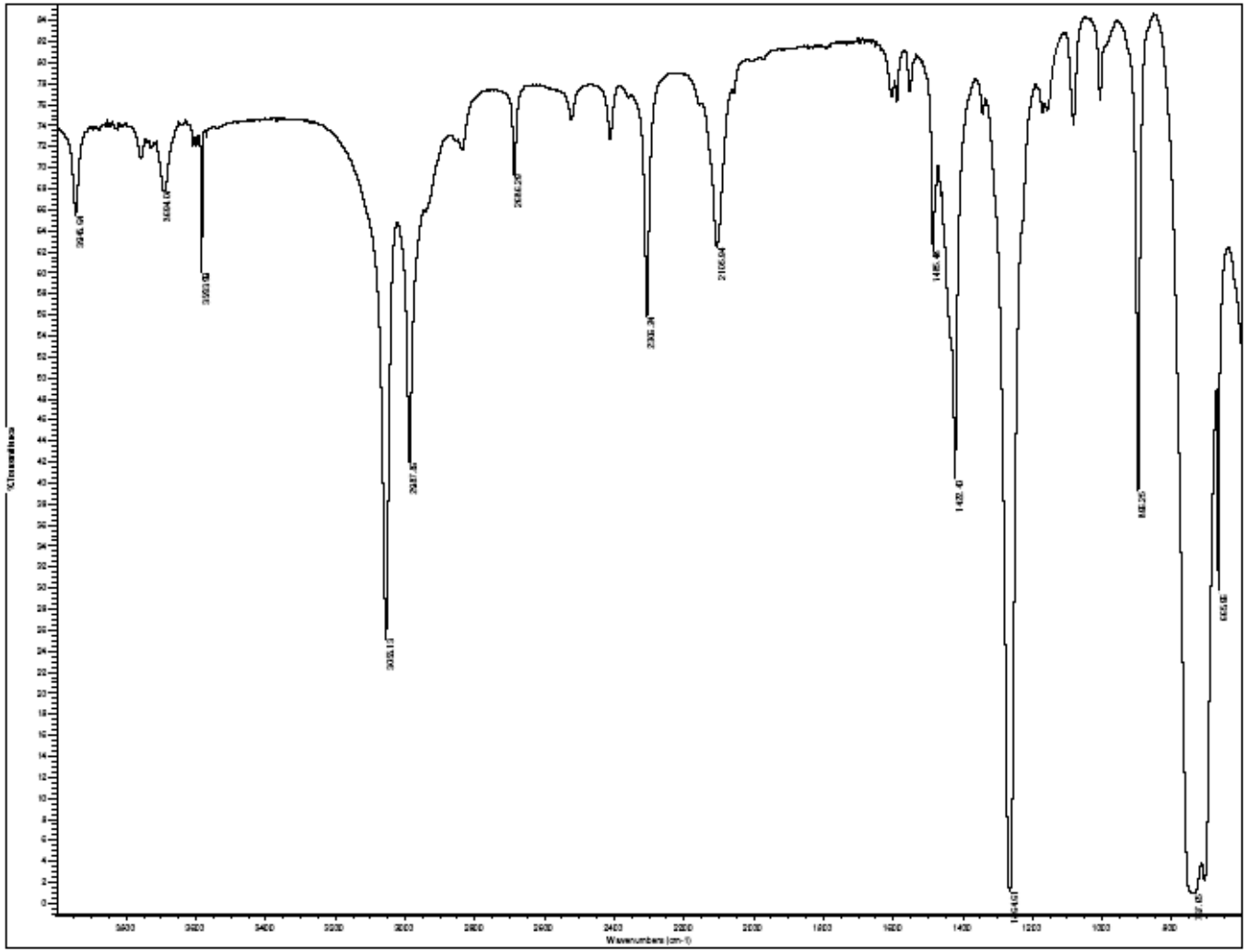

Figure 21: IR spectrum of **6**.

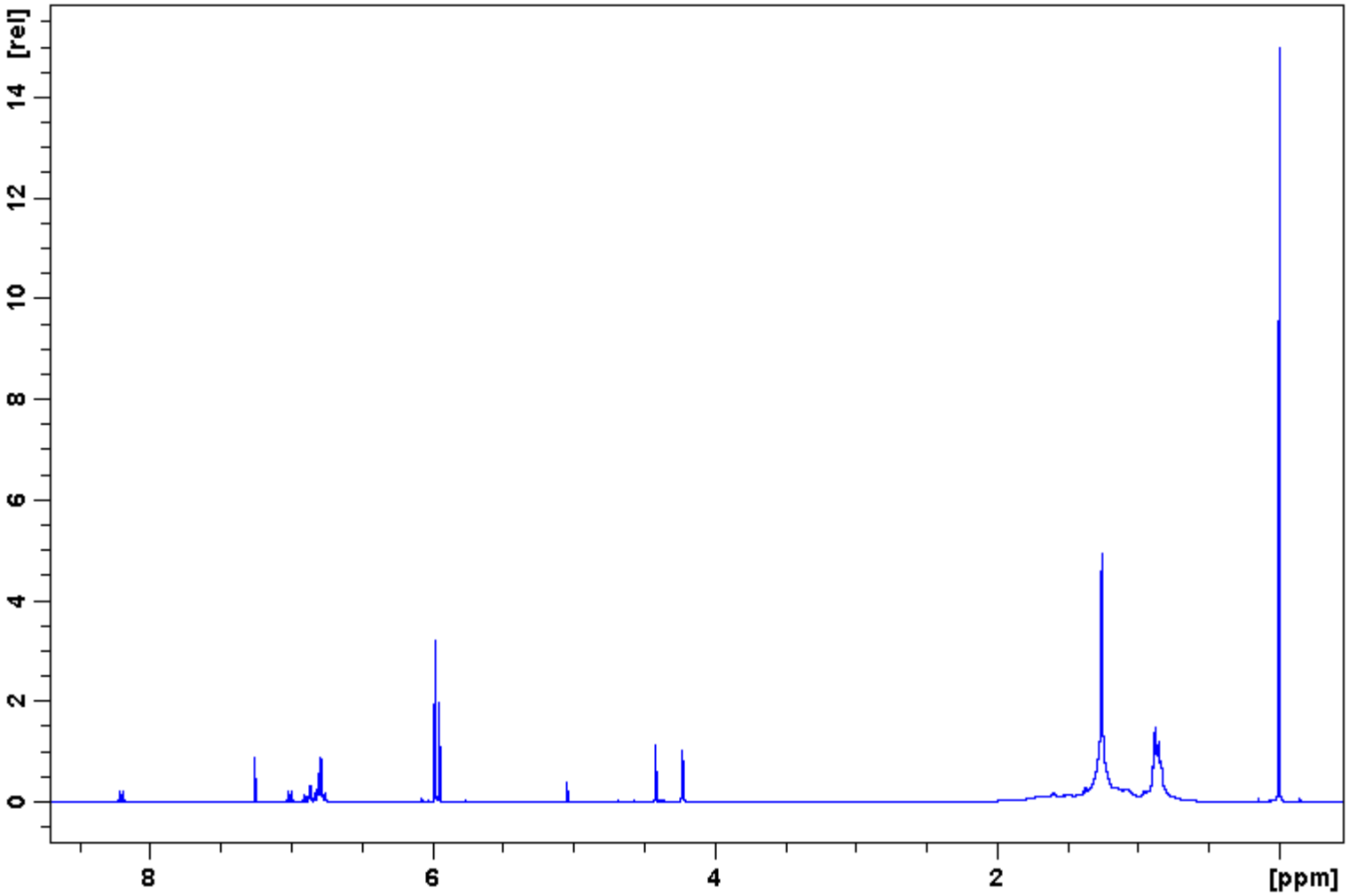

Figure 22: 400 MHz ^{1}H spectrum of **8**.

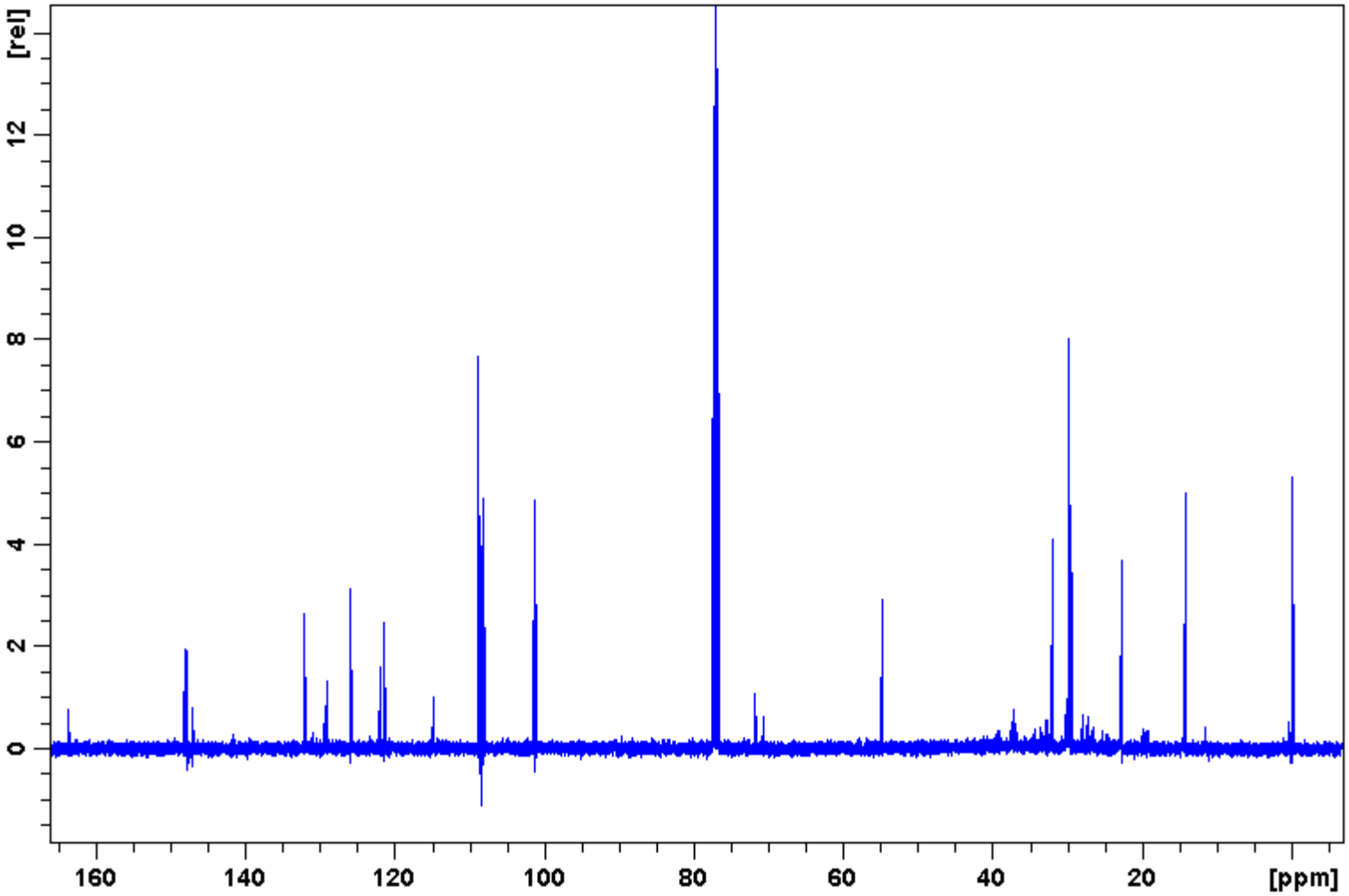

Figure 23: 100 MHz ^{13}C spectrum of **8**.

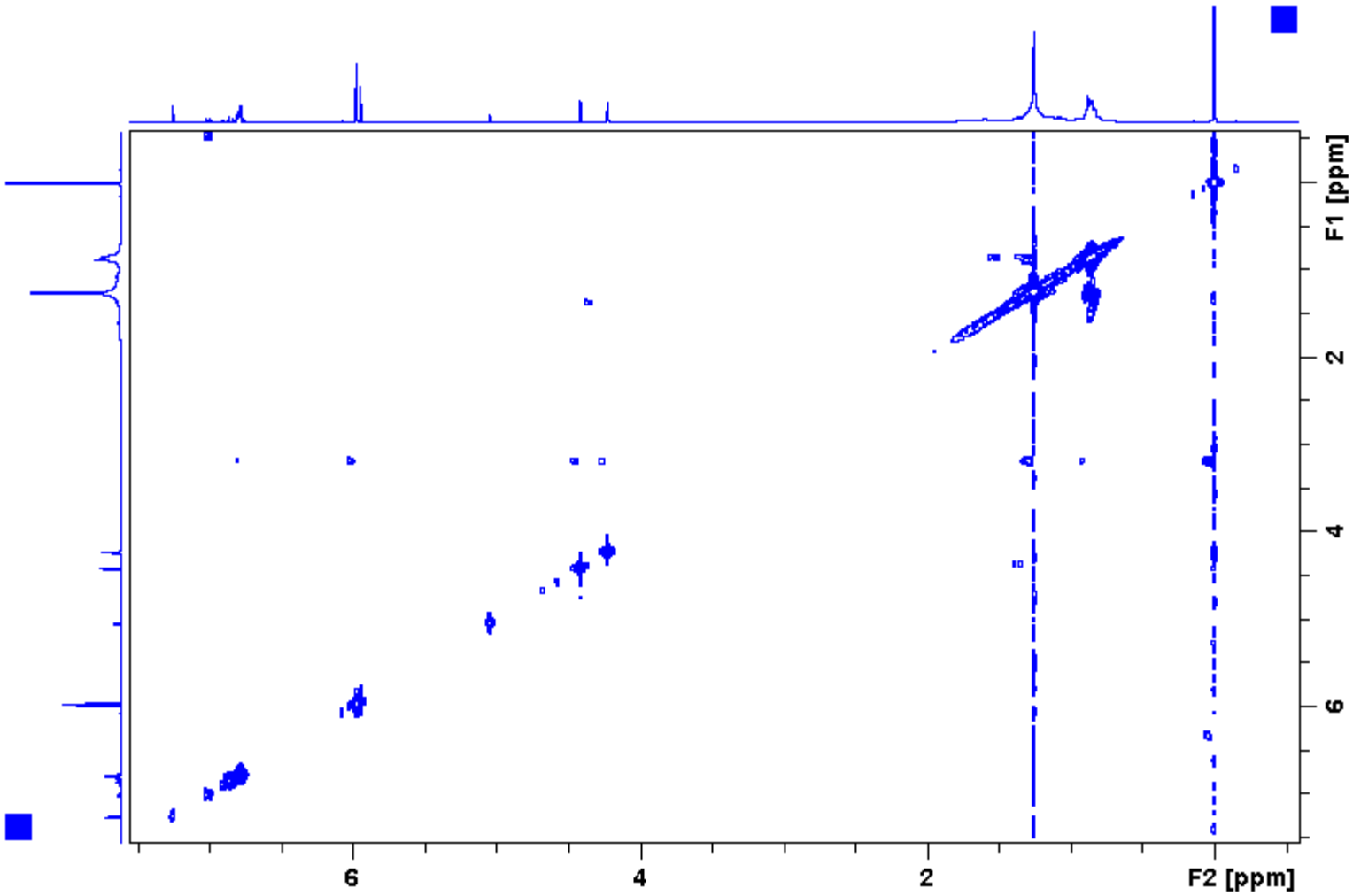

Figure 24: ^{1}H-^{1}H COSY spectrum of **8**.

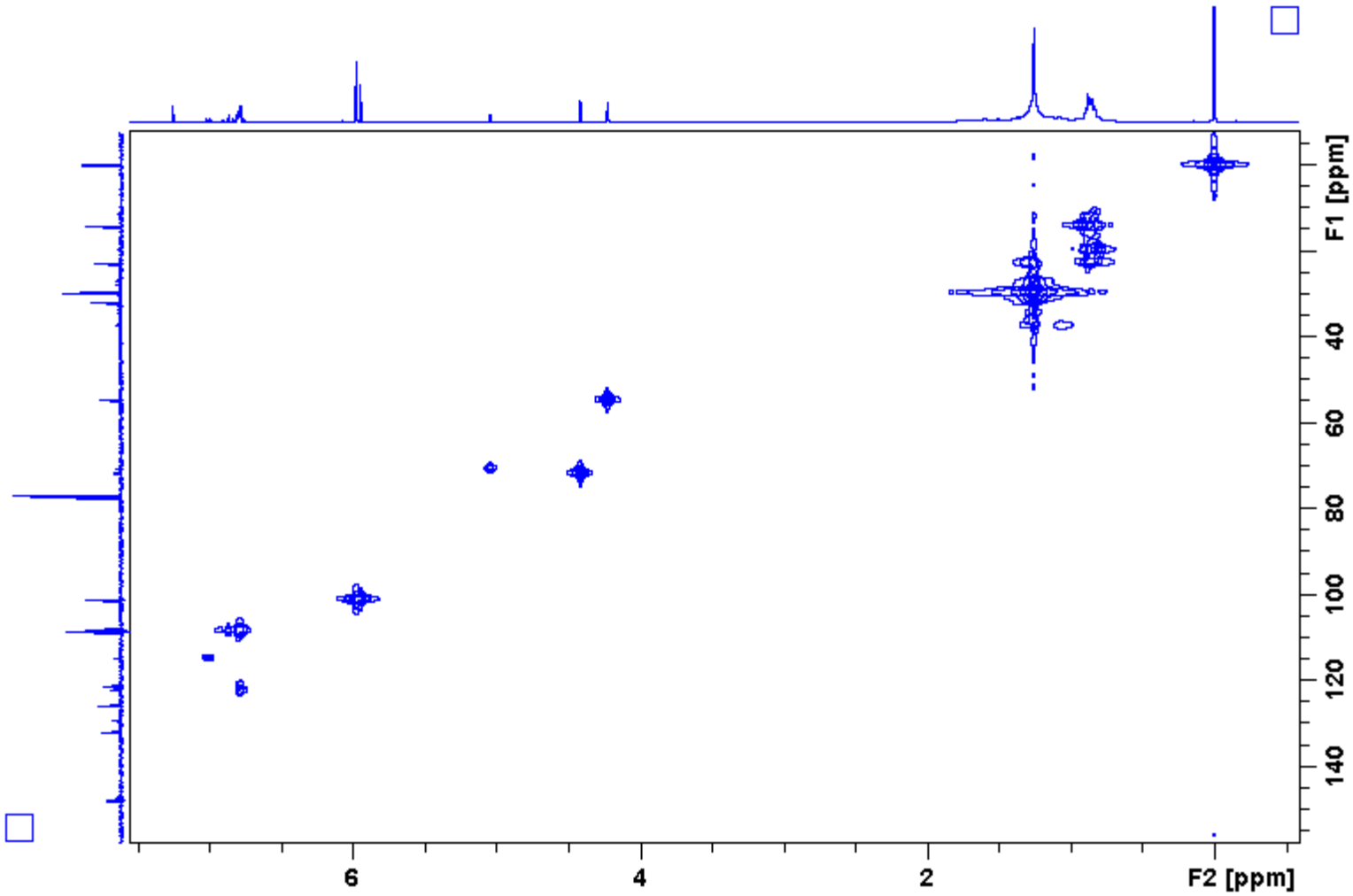

Figure 25: ^{1}H-^{13}C HMQC spectrum of **8**.

Mass Spectrum List Report

Analysis Info

Analysis Name	BJD-5001.d	Acquisition Date	07/21/08 13:28:34
Method	XQ Default.ms	Operator	Administrator
Sample Name	BD-2-103	Instrument	Esquire-LC_00135
Comment	BD-2-103		

Acquisition Parameter

Ion Source Type	ESI	Ion Polarity	Positive	Alternating Ion Polarity	n/a
Mass Range Mode	Std/Normal	Scan Begin	100.00 m/z	Scan End	300.00 m/z
Capillary Exit	98.6 Volt	Skim 1	28.2 Volt	Trap Drive	43.7
Accumulation Time	31124 µs	Averages	10 Spectra	Auto MS/MS	Off

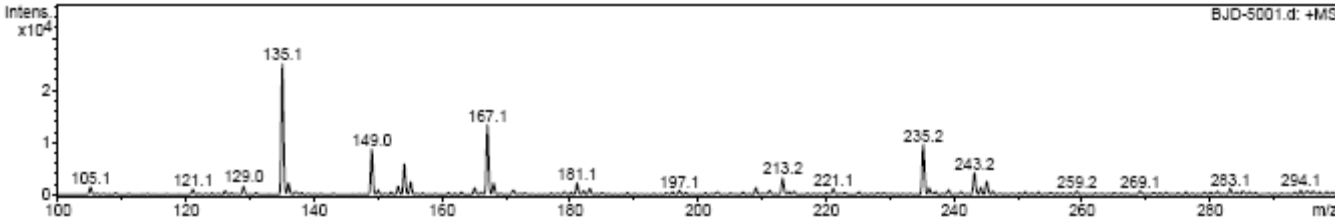

#	m/z	I	FWHM	S/N
1	135.1	25048	0.4	205.4
2	149.0	8676	0.4	71.2
3	154.1	5841	0.4	47.9
4	155.1	2423	0.4	19.9
5	167.1	13346	0.4	109.5
6	181.1	2210	0.4	18.1
7	213.2	3164	0.4	25.9
8	235.2	9563	0.4	78.4
9	243.2	4128	0.4	33.9
10	245.1	2540	0.4	20.8

Figure 26: Mass spectrum of **8**.

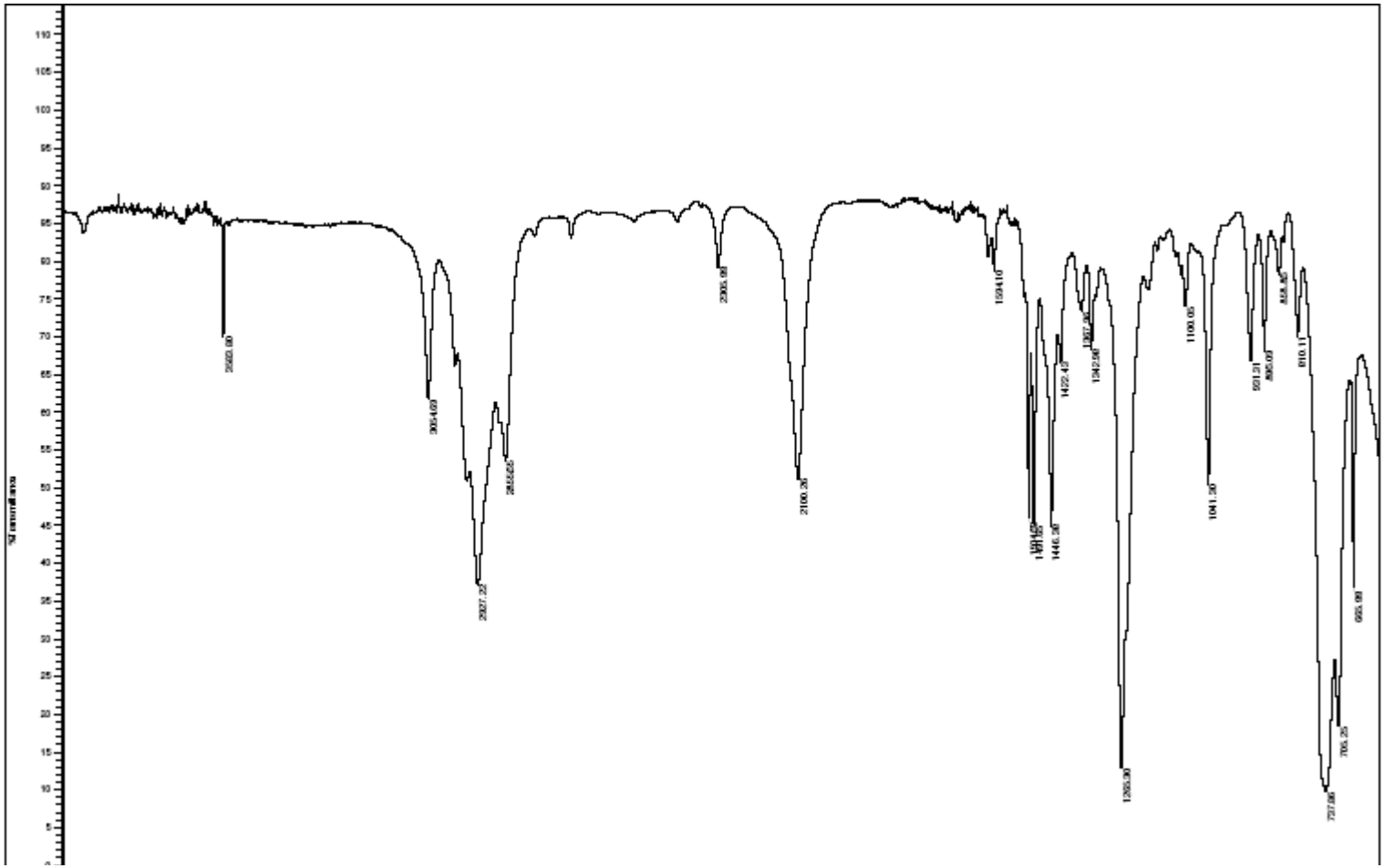

Figure 27: IR spectrum of **8**.

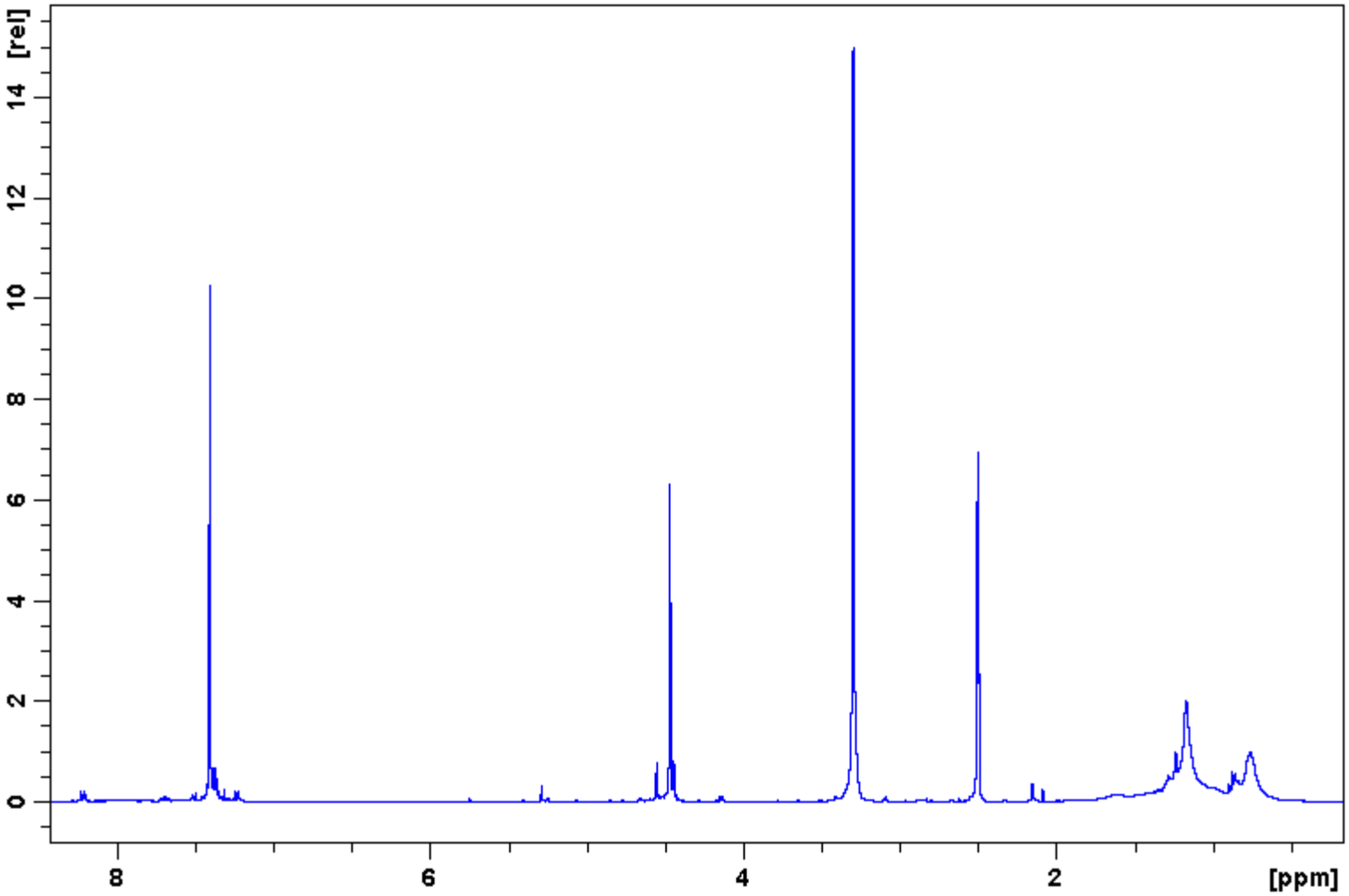

Figure 28: 400 MHz ^{1}H spectrum of **10**.

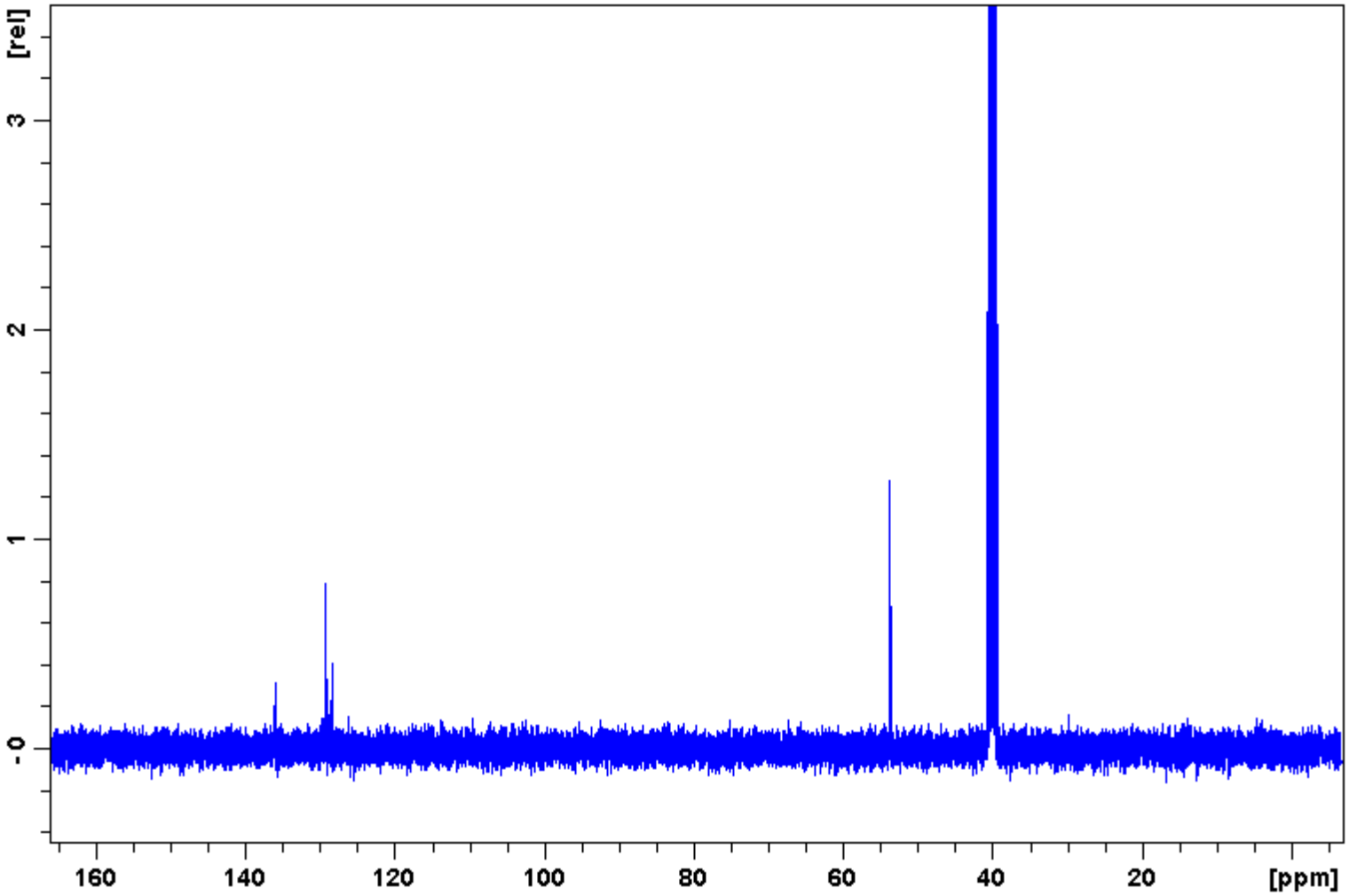

Figure 29:100 MHz ^{13}C spectrum of **10**.

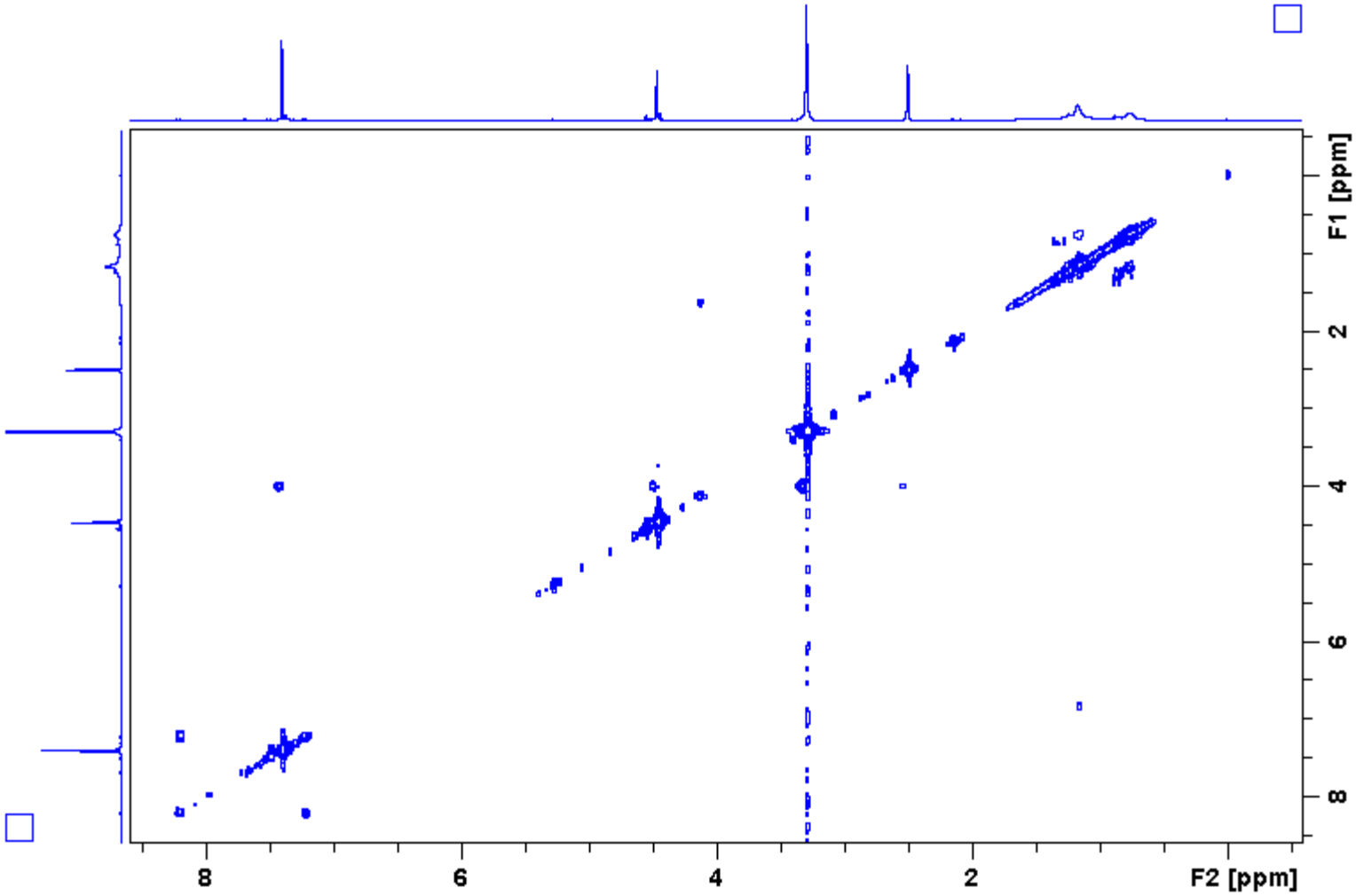

Figure 30: ^{1}H-^{1}H COSY spectrum of **10**.

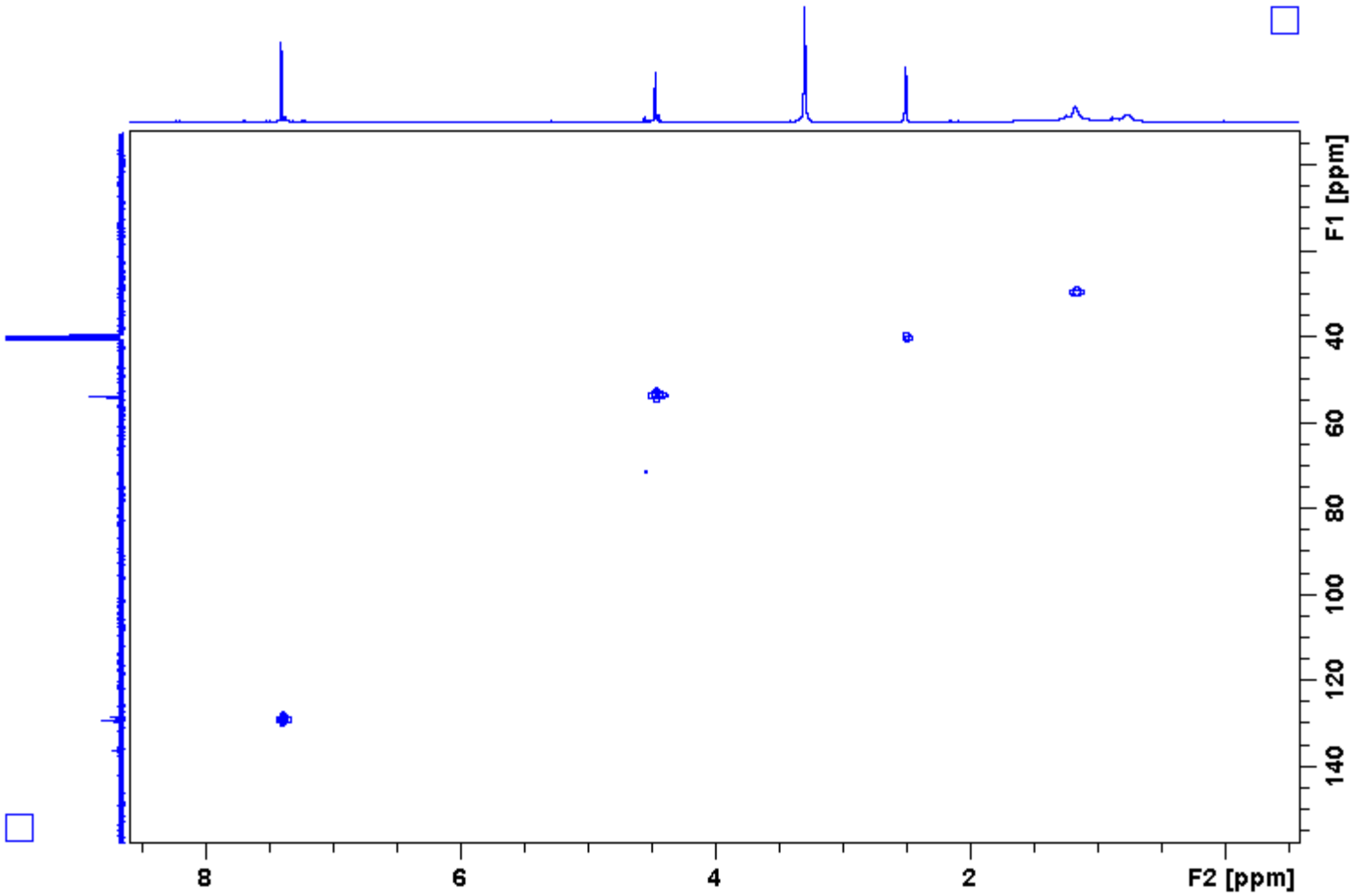

Figure 31: ^{1}H-^{13}C HMQC spectrum of **10**.

Mass Spectrum List Report

Analysis Info

Analysis Name	30310004.d	Acquisition Date	07/29/08 22:46:56
Method	XQ Default.ms	Operator	Administrator
Sample Name	bg6298	Instrument	Esquire-LC_00135
Comment	background 7/29/08		

Acquisition Parameter

Ion Source Type	ESI	Ion Polarity	Positive	Alternating Ion Polarity	n/a
Mass Range Mode	Std/Normal	Scan Begin	120.00 m/z	Scan End	250.00 m/z
Capillary Exit	103.5 Volt	Skim 1	31.6 Volt	Trap Drive	42.1
Accumulation Time	50000 µs	Averages	10 Spectra	Auto MS/MS	Off

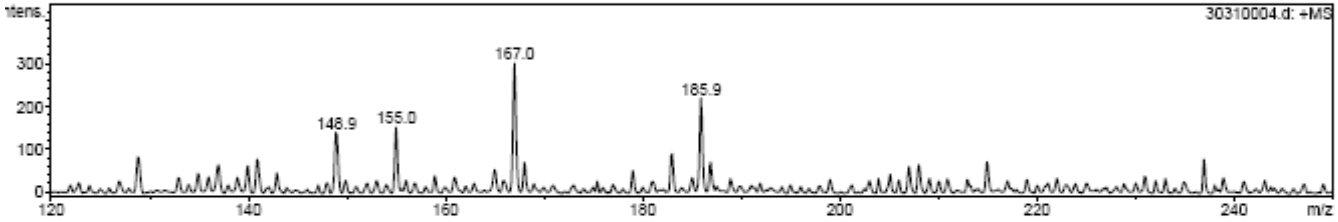

#	m/z	I	FWHM	S/N
1	148.9	139	0.4	15.4
2	155.0	151	0.3	16.7
3	167.0	300	0.3	33.3
4	185.9	219	0.3	24.3

Figure 32: Mass spectrum of **10**.

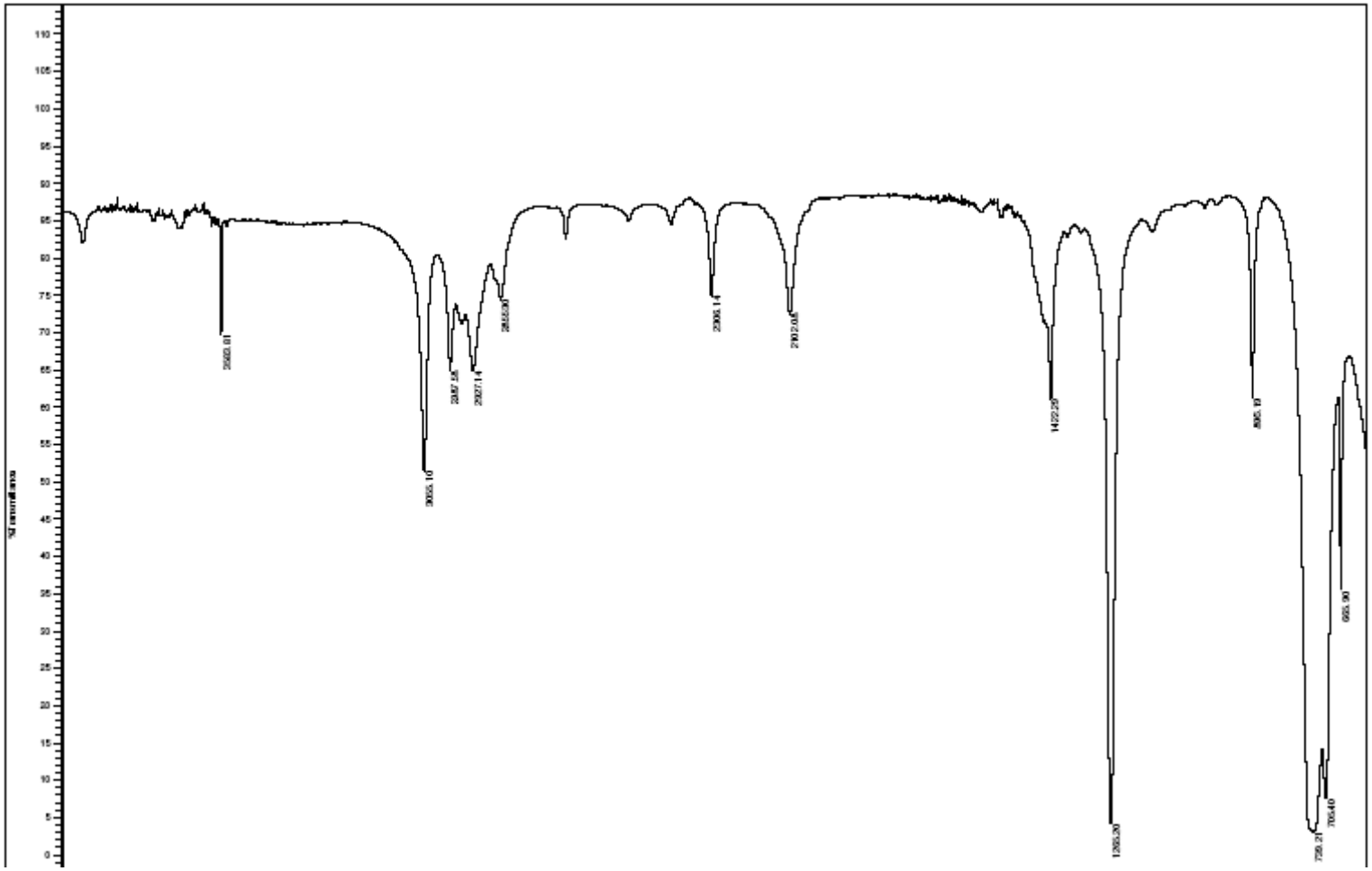

Figure 33: IR spectrum of **10**.

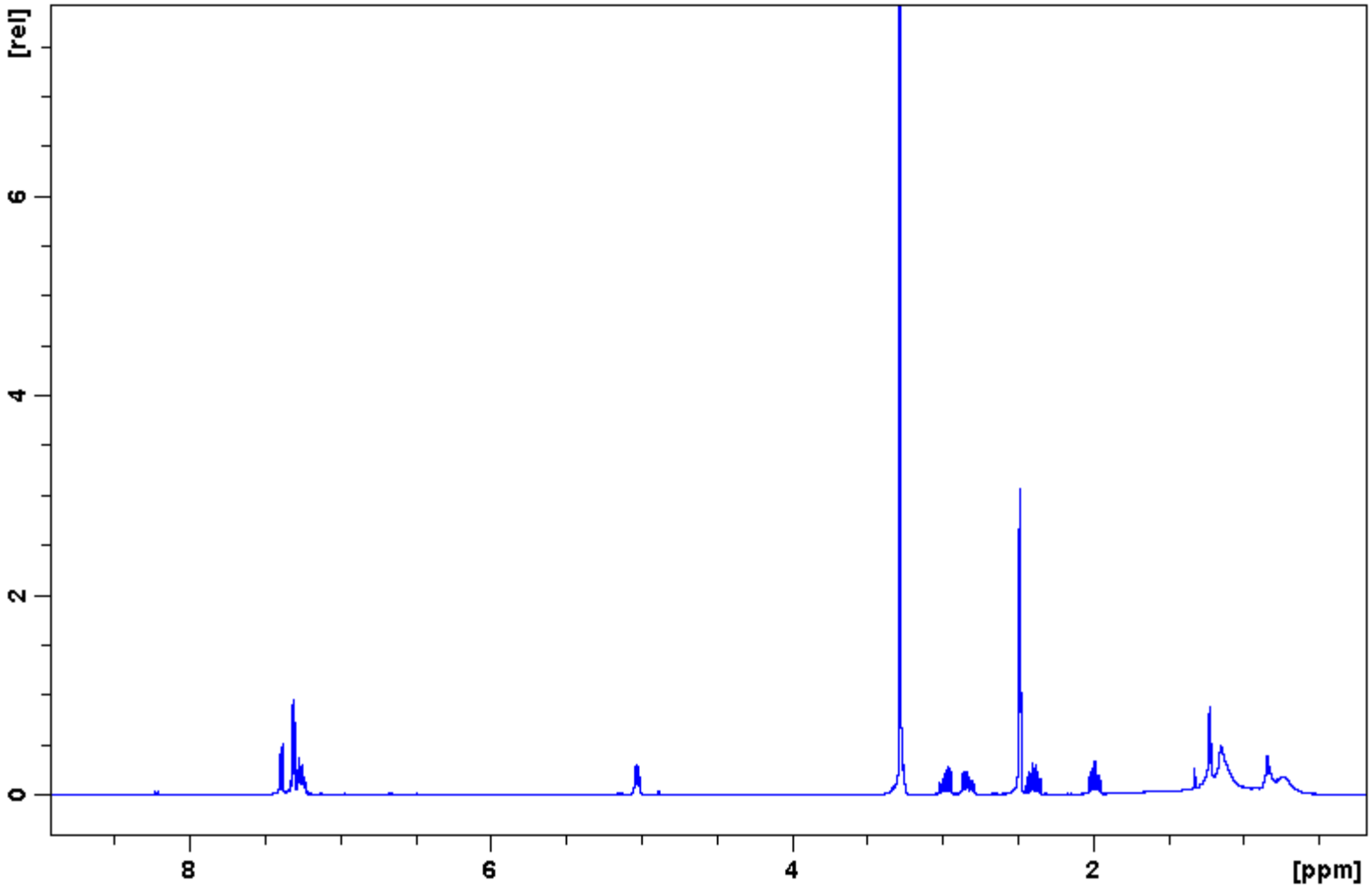

Figure 34: 400 MHz ^{1}H spectrum of **12**.

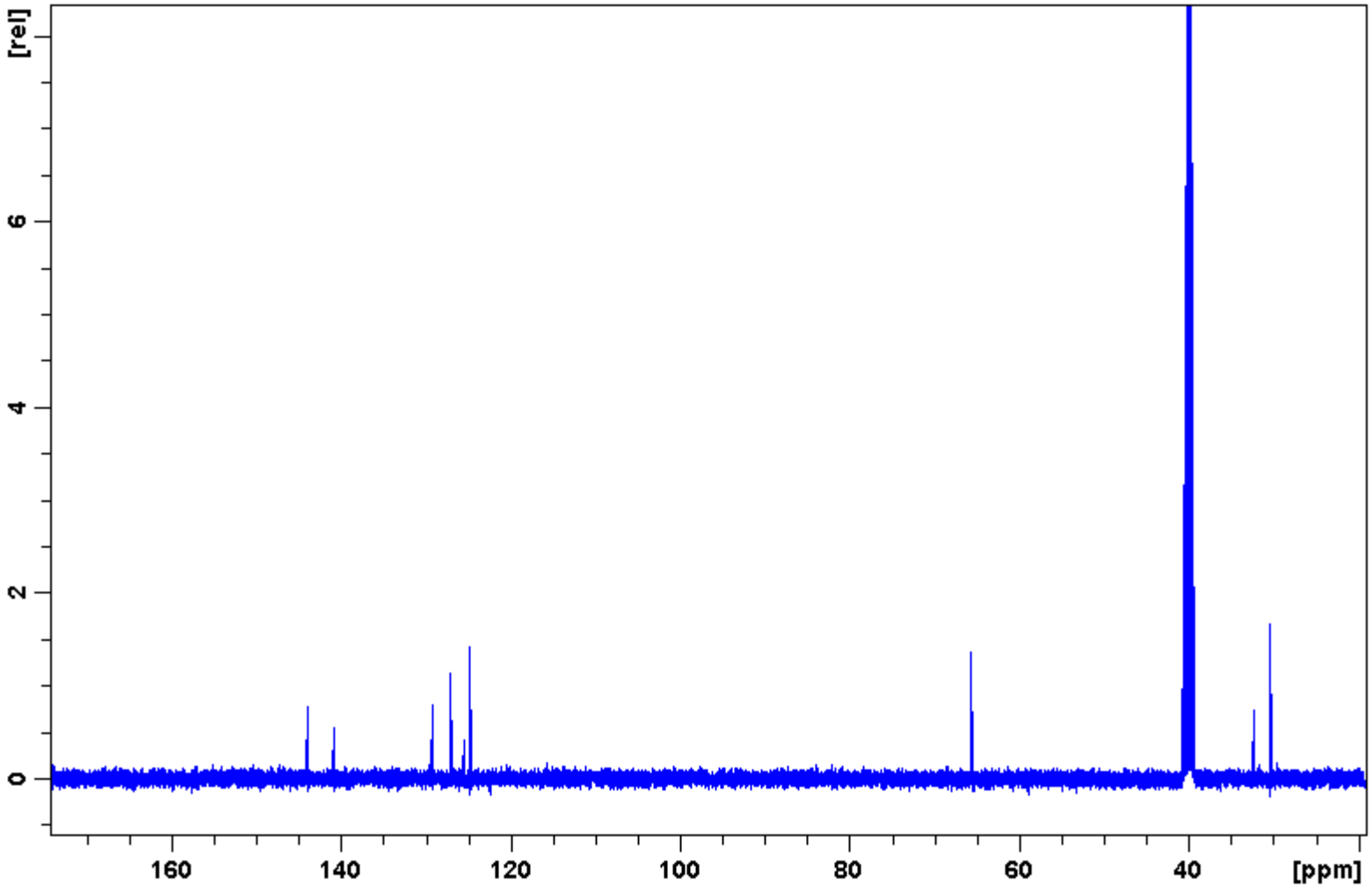

Figure 35: 100 MHz ^{13}C spectrum of **12**.

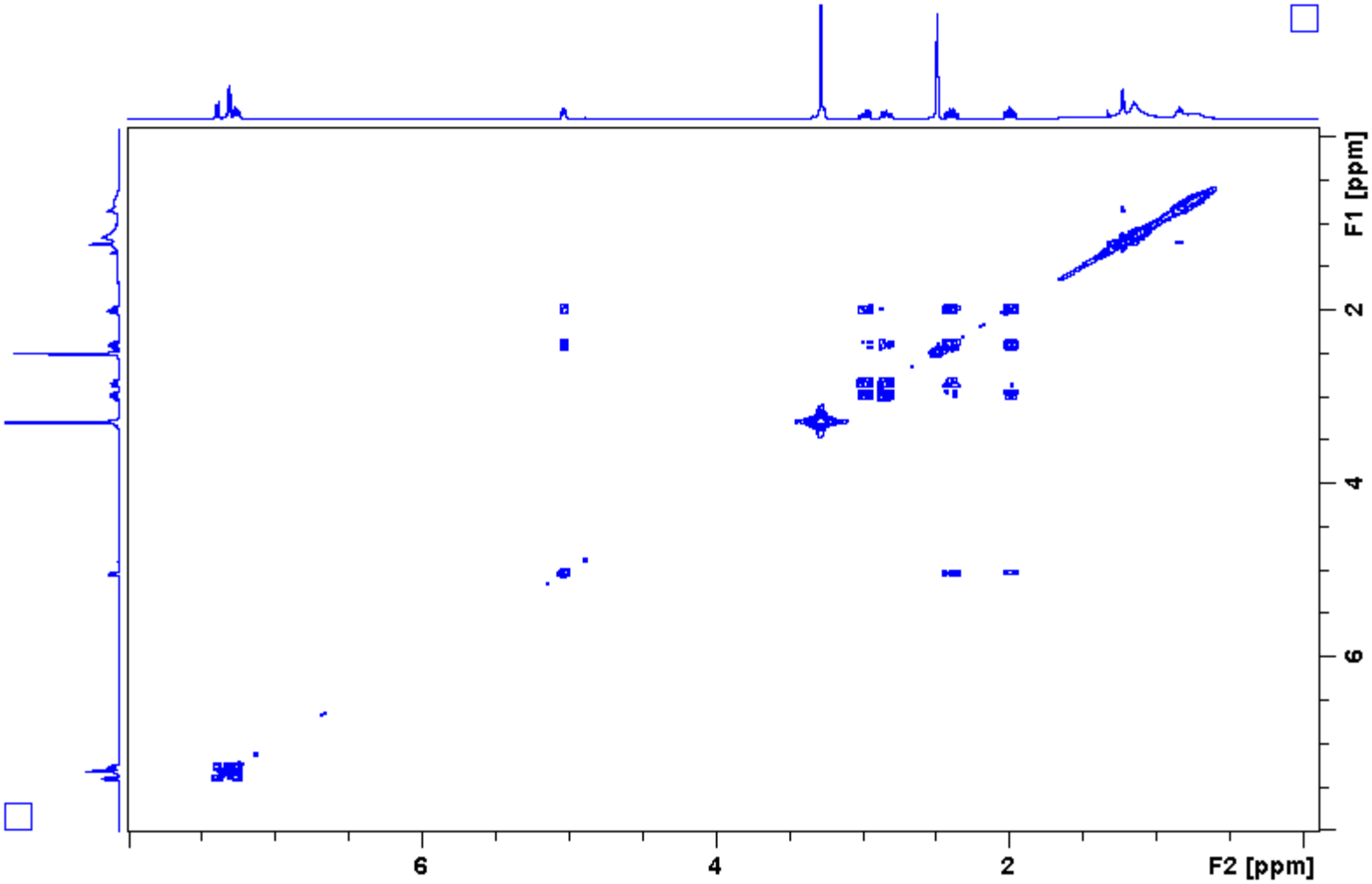

Figure 36: ^{1}H-^{1}H COSY spectrum of **12**.

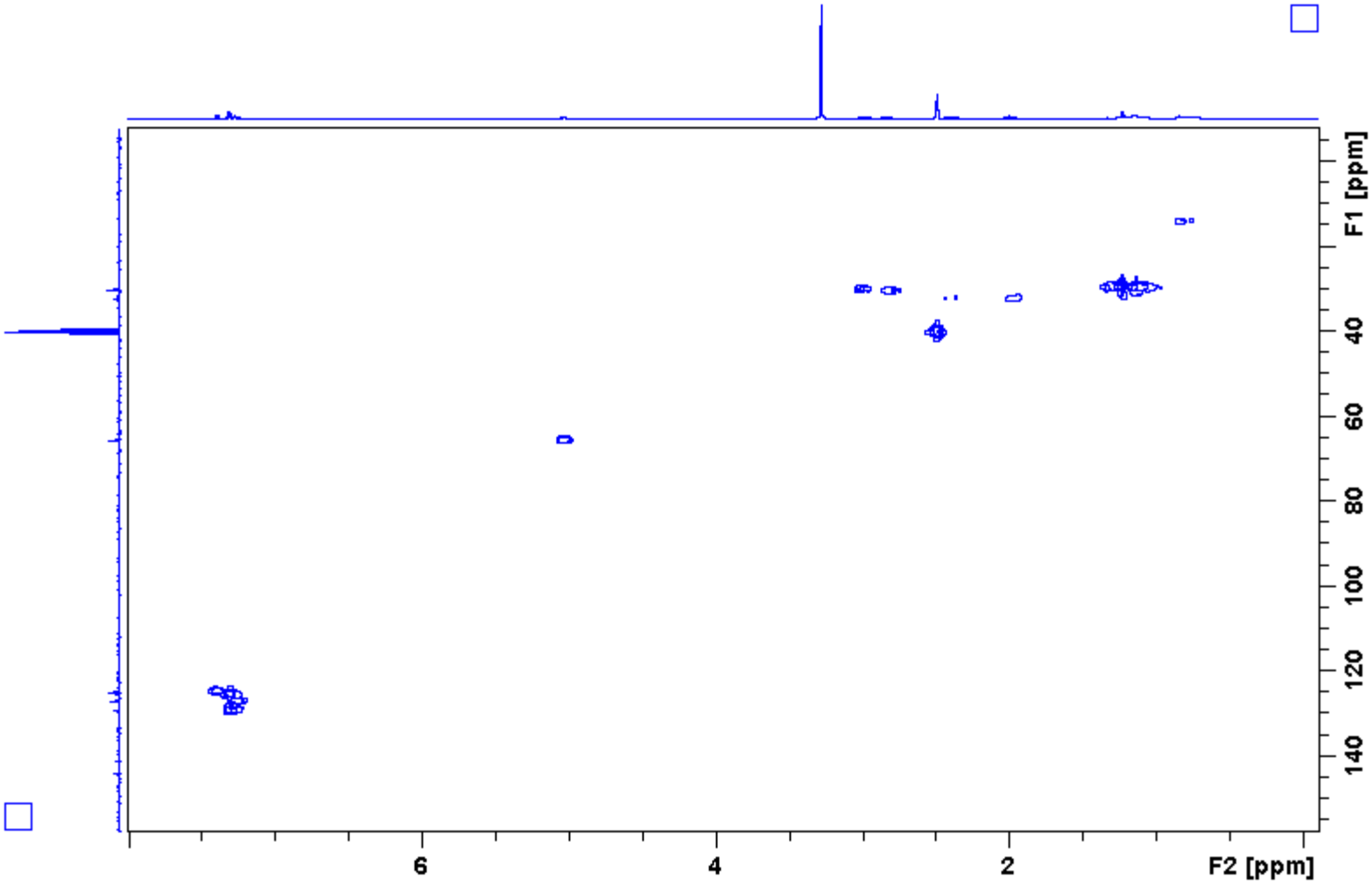

Figure 37: ^{1}H-^{13}C HMQC spectrum of **12**.

Mass Spectrum List Report

Analysis Info

Analysis Name	BD-3-049.d	Acquisition Date	07/29/08 18:38:10
Method	XQ Default.ms	Operator	Administrator
Sample Name	SK-III-005	Instrument	Esquire-LC_00135
Comment	BD-3-049		

Acquisition Parameter

Ion Source Type	ESI	Ion Polarity	Positive	Alternating Ion Polarity	n/a
Mass Range Mode	Std/Normal	Scan Begin	100.00 m/z	Scan End	550.00 m/z
Capillary Exit	108.5 Volt	Skim 1	37.4 Volt	Trap Drive	20.0
Accumulation Time	50000 µs	Averages	10 Spectra	Auto MS/MS	Off

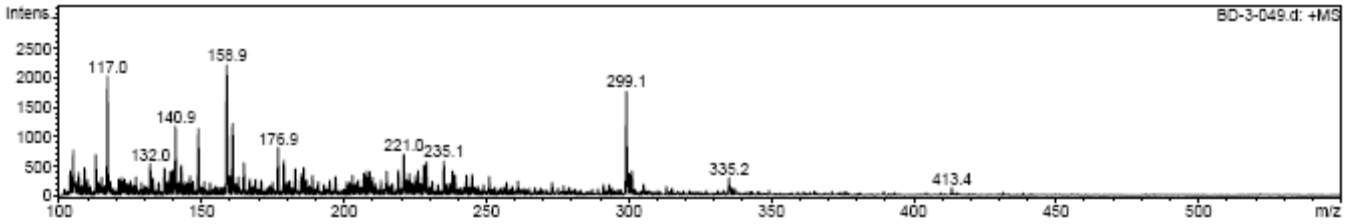

#	m/z	I	FWHM	S/N
1	105.0	763	0.3	32.5
2	113.0	688	0.3	29.3
3	117.0	2023	0.3	86.1
4	140.9	1167	0.4	49.6
5	148.9	1131	0.3	48.1
6	158.9	2214	0.4	94.2
7	160.9	1218	0.4	51.8
8	176.9	810	0.4	34.5
9	221.0	696	0.4	29.6
10	299.1	1766	0.4	75.1

Figure 38: Mass spectrum of **12**.

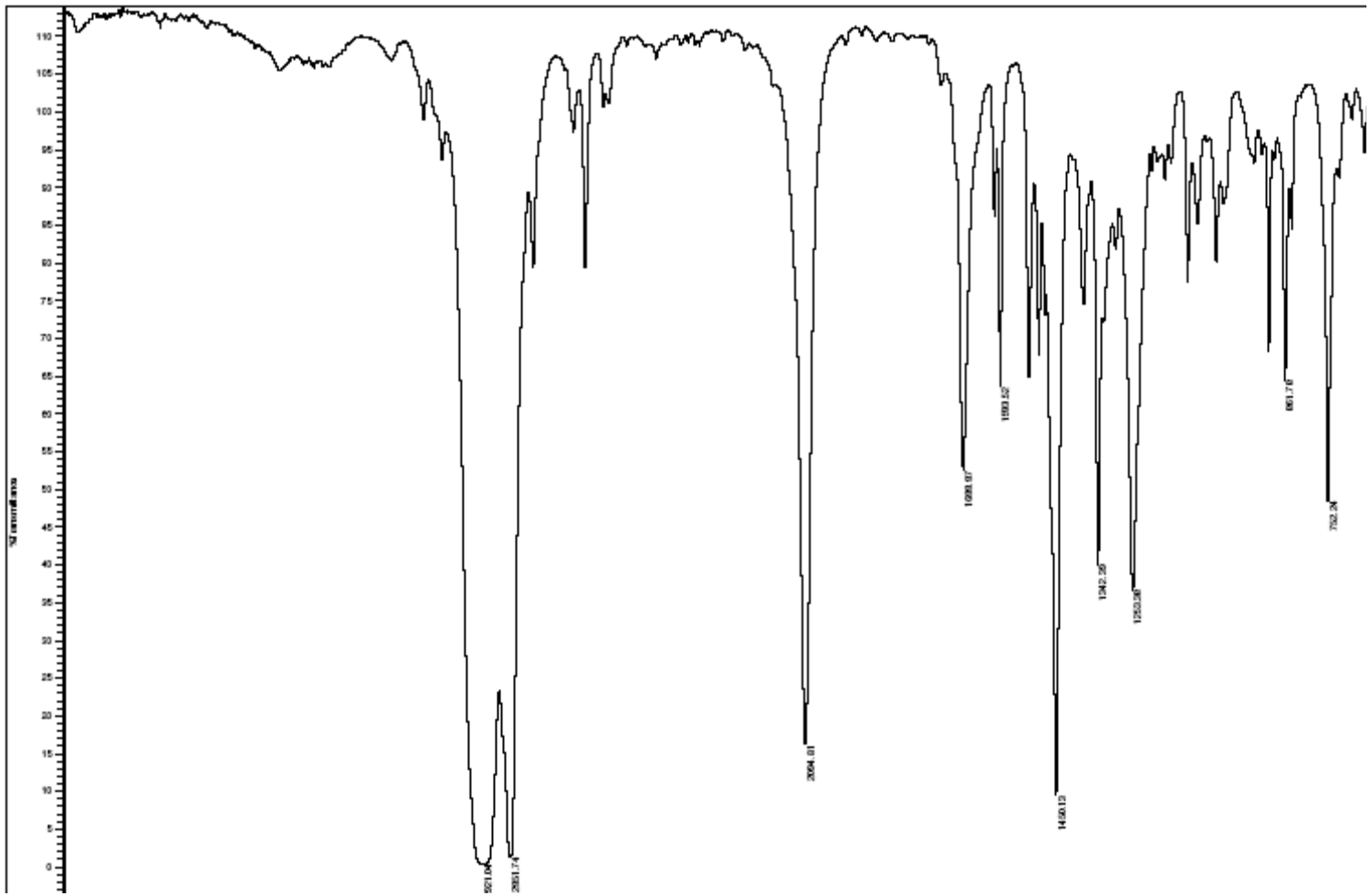

Figure 39: IR spectrum of **12**.

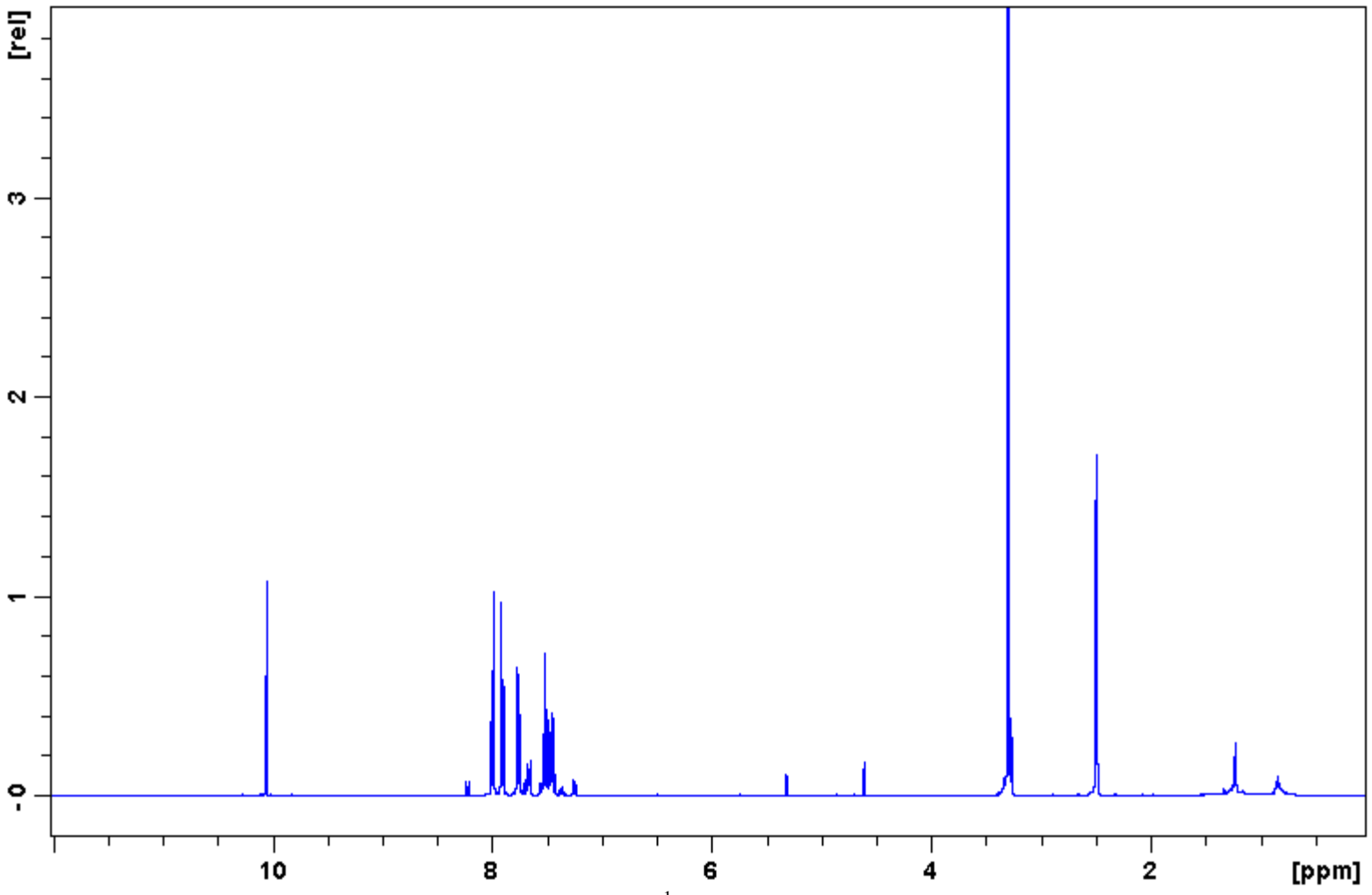

Figure 40: 400 MHz ^{1}H NMR spectrum of **14**.

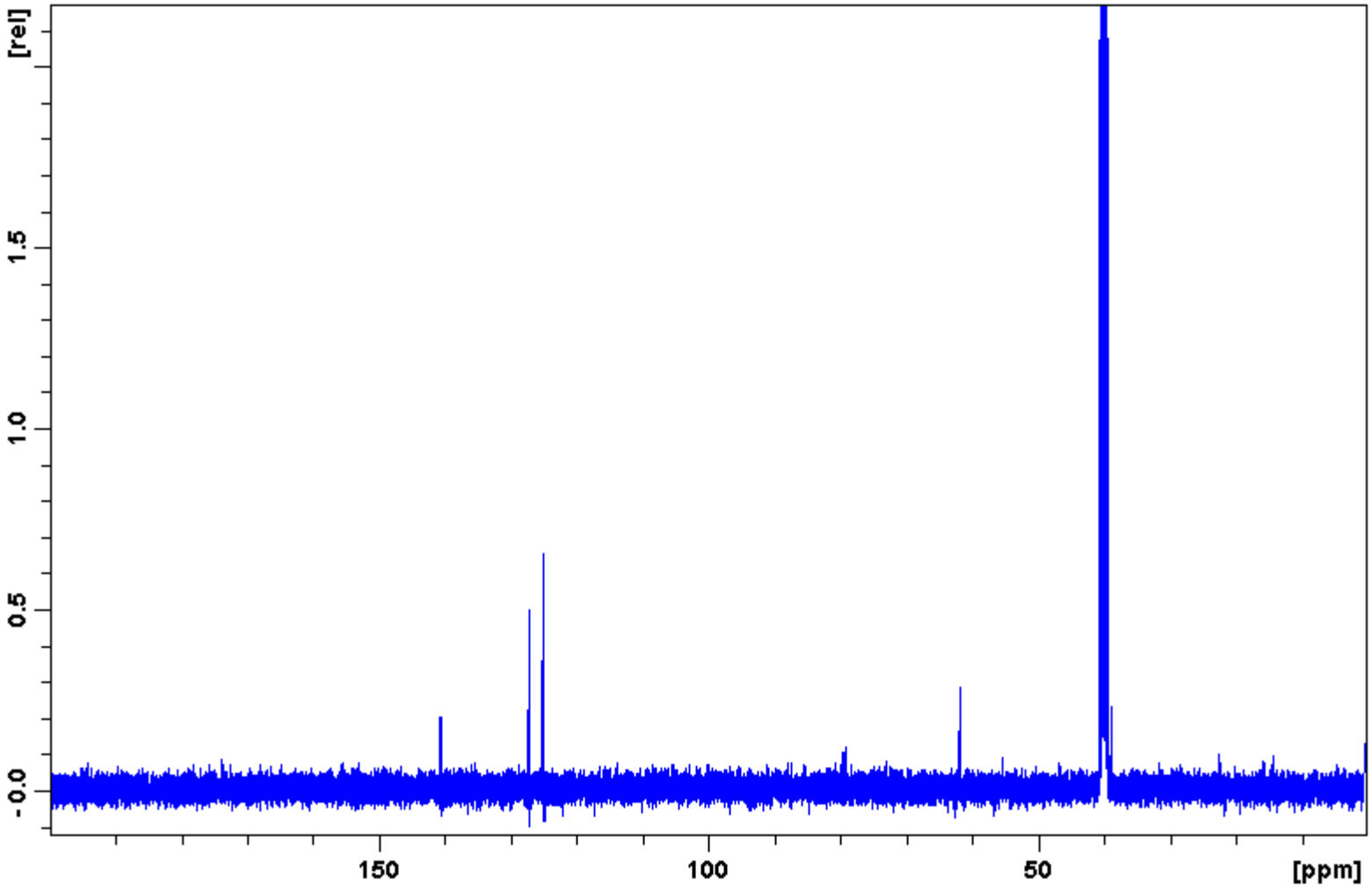

Figure 41: 100 MHz ^{13}C NMR spectrum of **14**.

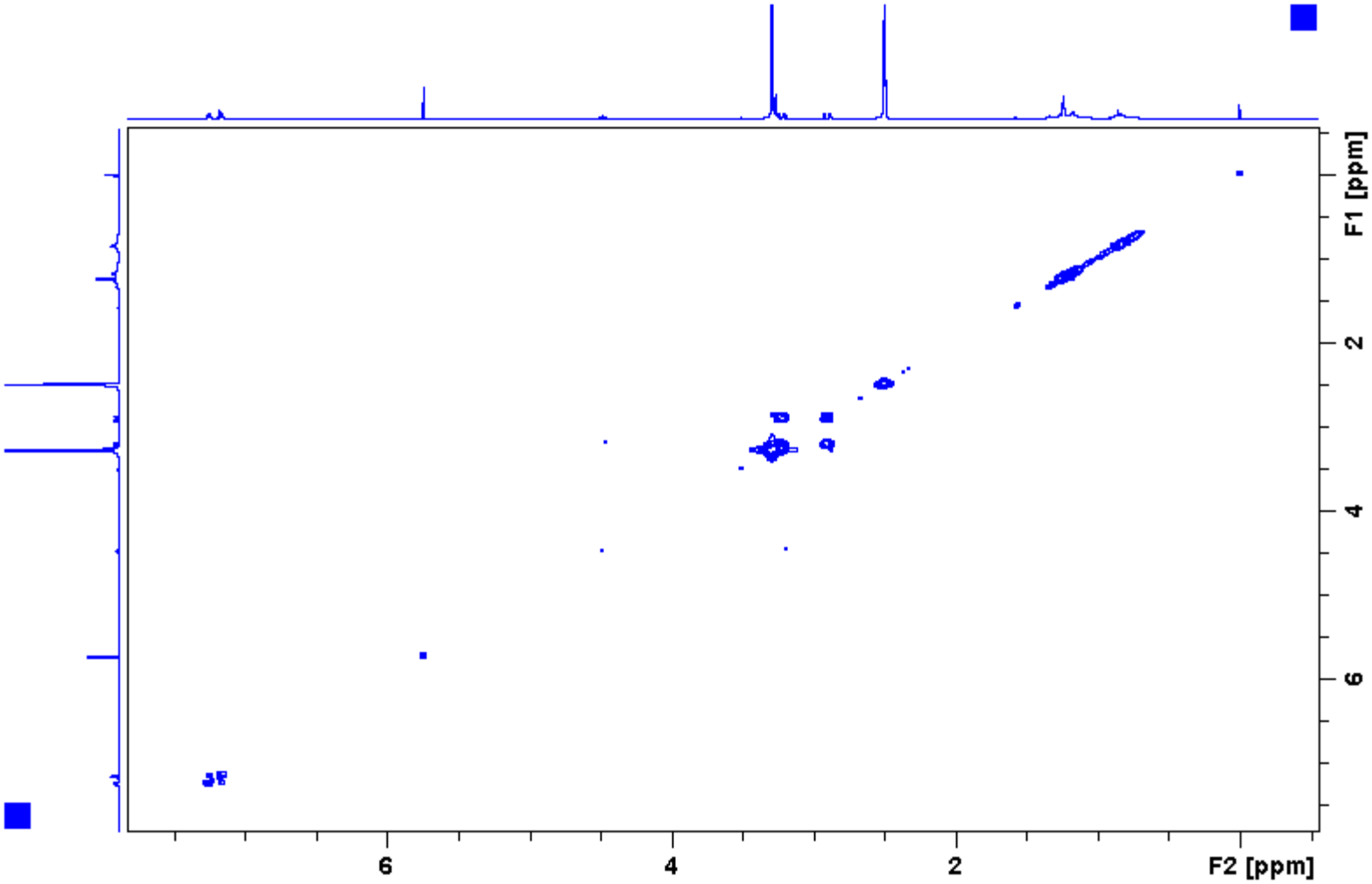

Figure 42: ^{1}H-^{1}H COSY spectrum of **14**.

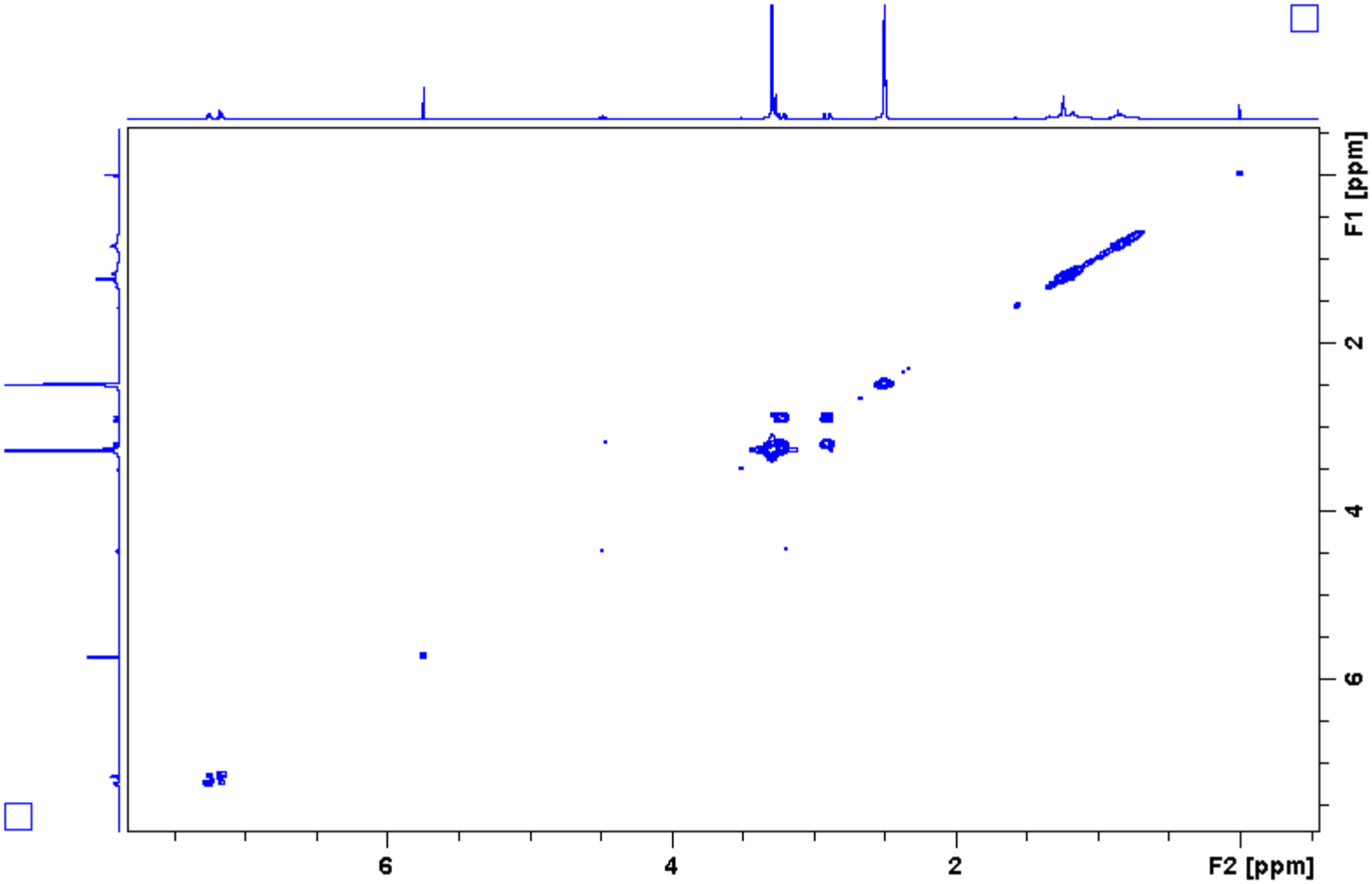

Figure 43: ^{1}H-^{13}C HMQC spectrum of **14**.

Mass Spectrum List Report

Analysis Info

Analysis Name	3-051003.d	Acquisition Date	07/29/08 20:40:13
Method	XQ Default.ms	Operator	Administrator
Sample Name	SK-III-005	Instrument	Esquire-LC_00135
Comment	BD-3-051		

Acquisition Parameter

Ion Source Type	ESI	Ion Polarity	Positive	Alternating Ion Polarity	n/a
Mass Range Mode	Std/Normal	Scan Begin	100.00 m/z	Scan End	400.00 m/z
Capillary Exit	104.2 Volt	Skim 1	33.1 Volt	Trap Drive	20.0
Accumulation Time	50000 µs	Averages	10 Spectra	Auto MS/MS	Off

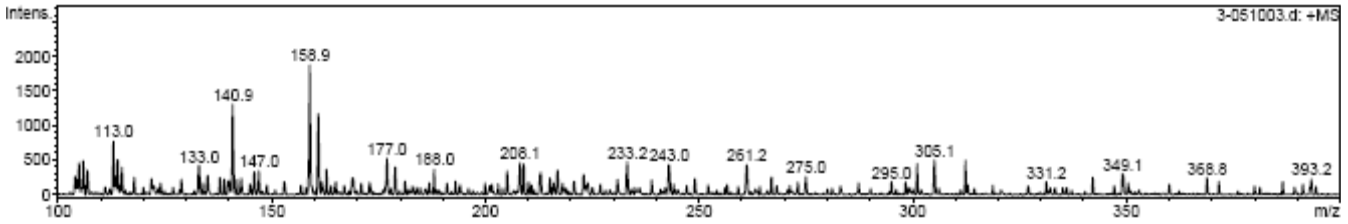

#	m/z	I	FWHM	S/N
1	105.9	485	0.3	12.2
2	113.0	764	0.3	19.2
3	114.0	500	0.3	12.5
4	140.9	1304	0.3	32.7
5	158.9	1872	0.3	47.0
6	160.9	1169	0.3	29.3
7	177.0	517	0.3	13.0
8	233.2	468	0.4	11.7
9	305.1	494	0.3	12.4
10	312.3	490	0.2	12.3

Figure 44: Mass spectrum of **14**.

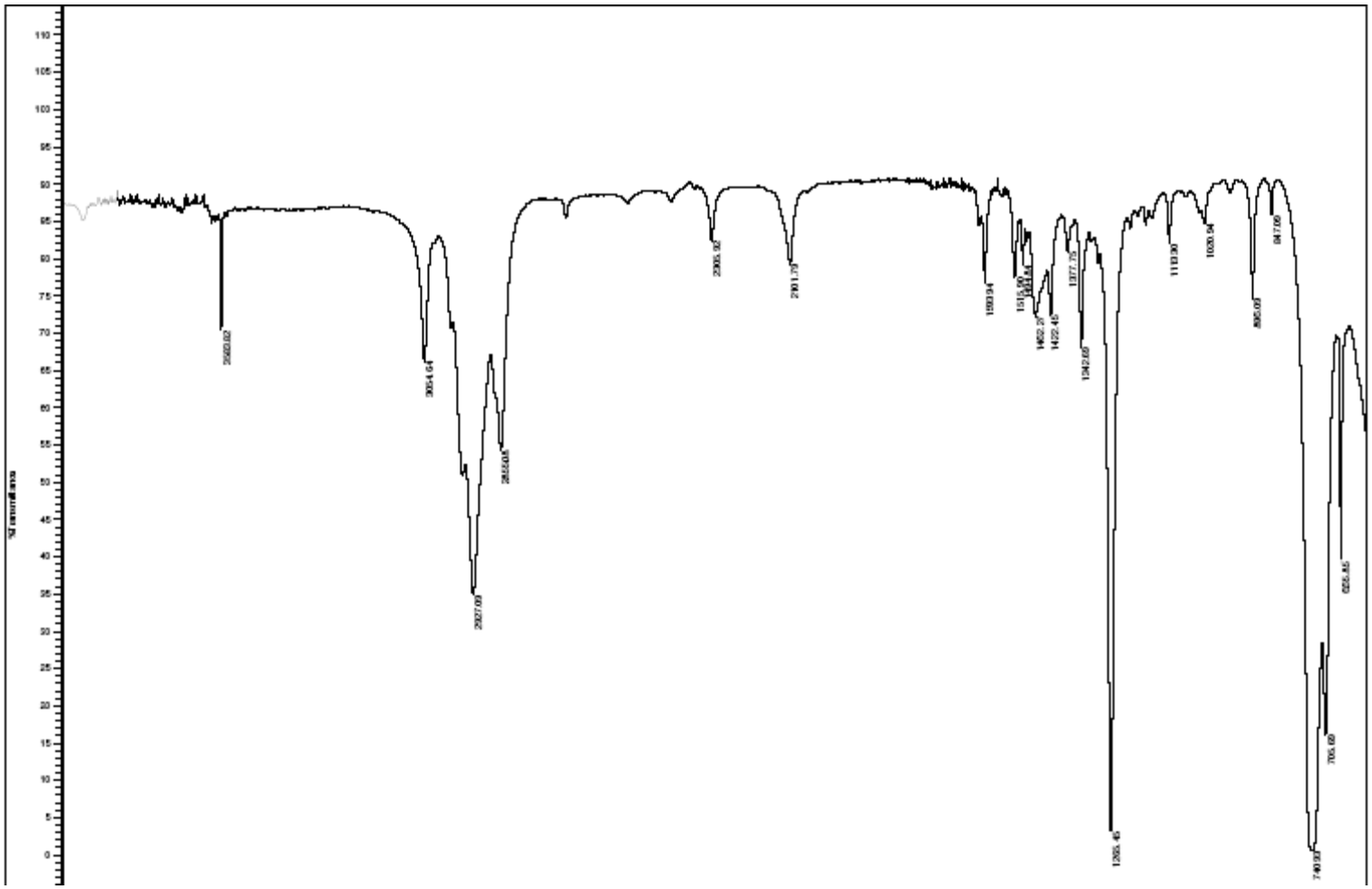

Figure 45: IR spectrum of **14**.

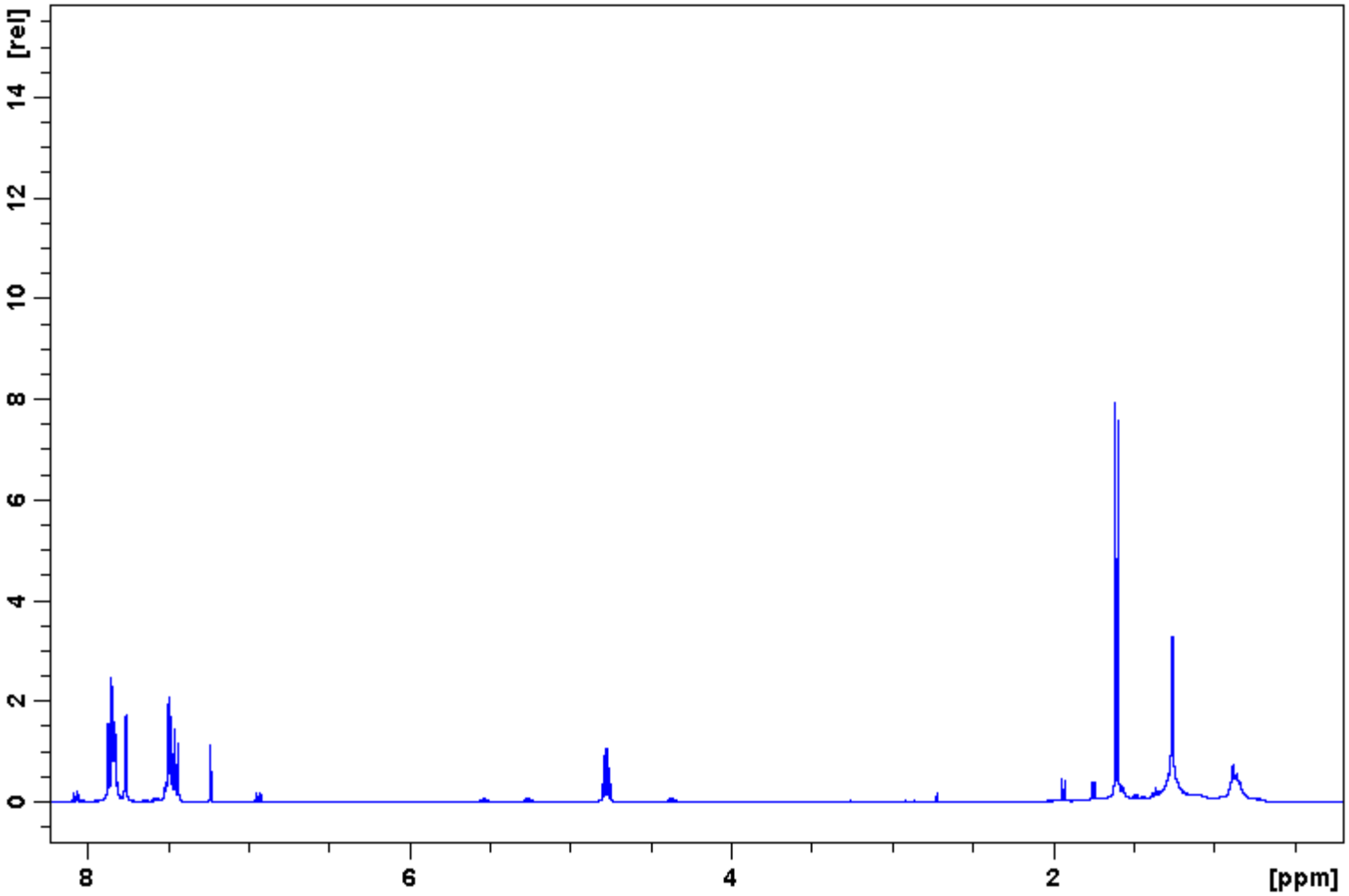

Figure 46: 400 MHz ^{1}H spectrum of **16**.

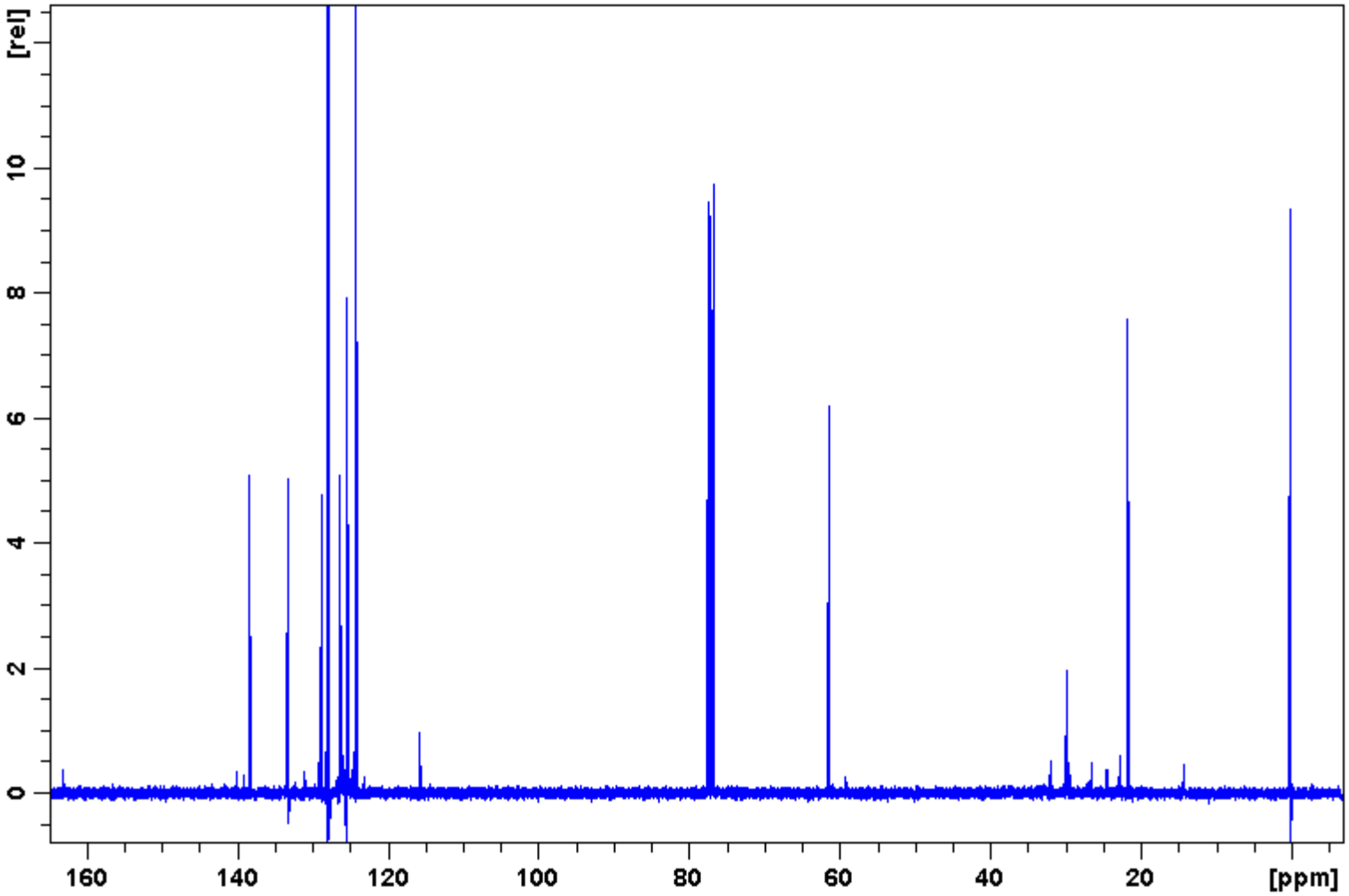

Figure 47: 100 MHz ^{13}C spectrum of **16**.

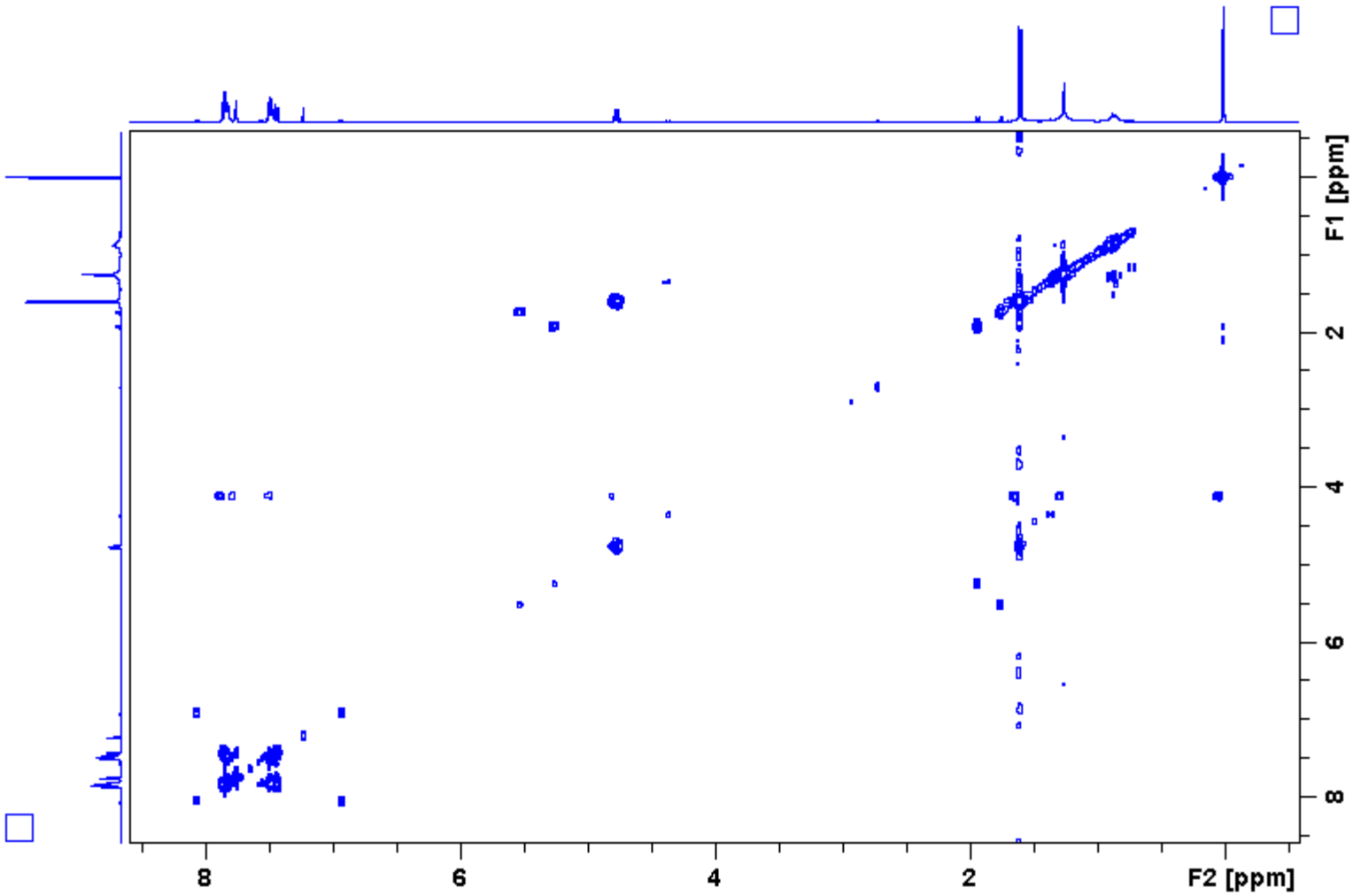

Figure 48: ^{1}H-^{1}H COSY spectrum of **16**.

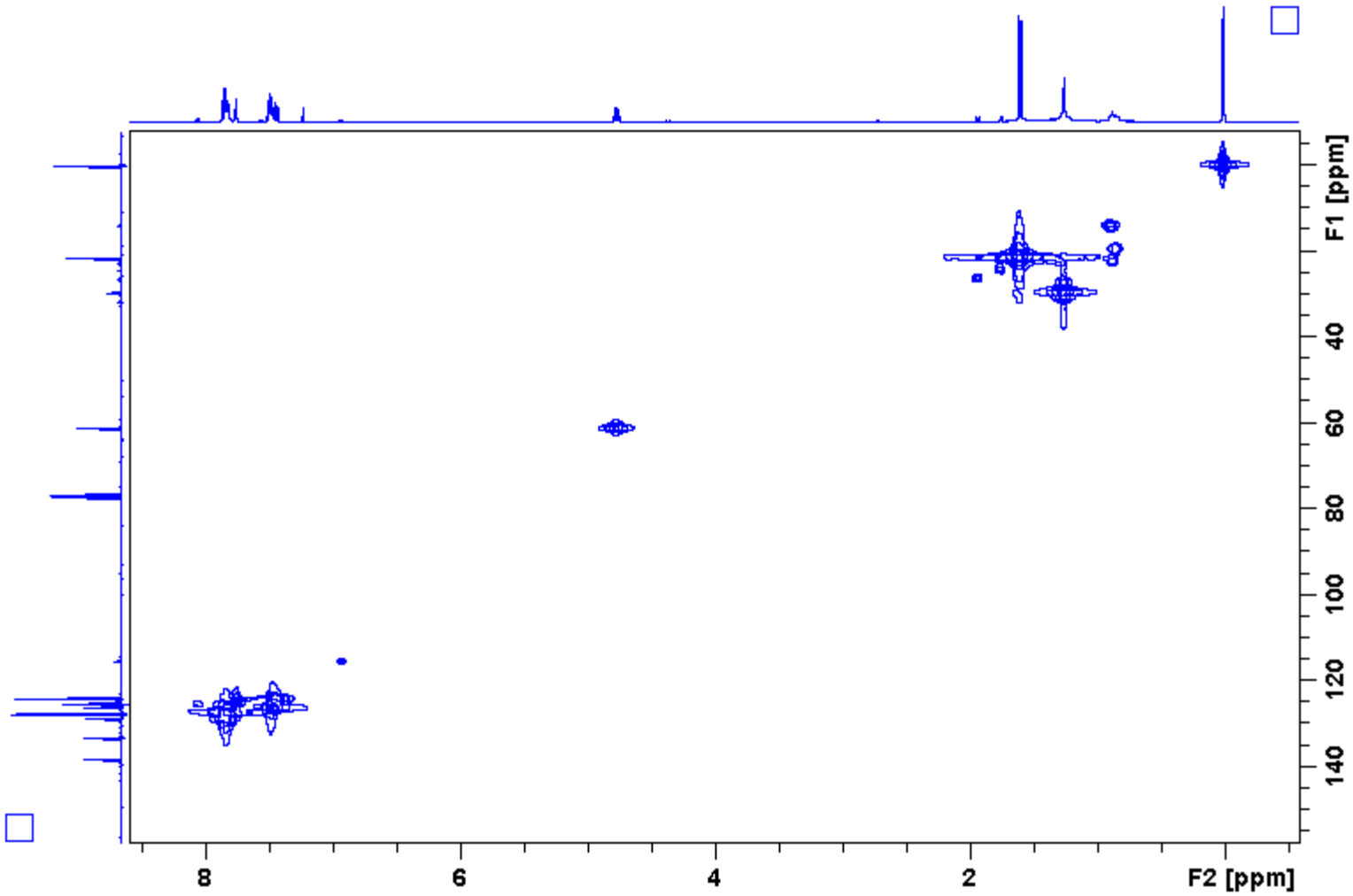

Figure 49: ^{1}H-^{13}C HMQC spectrum of **16**.

Mass Spectrum List Report

Analysis Info

Analysis Name	BJD-6000.d	Acquisition Date	07/21/08 14:14:22
Method	XQ Default.ms	Operator	Administrator
Sample Name	BD-2-099	Instrument	Esquire-LC_00135
Comment	BD-2-099		

Acquisition Parameter

Ion Source Type	ESI	Ion Polarity	Positive	Alternating Ion Polarity	n/a
Mass Range Mode	Std/Normal	Scan Begin	100.00 m/z	Scan End	300.00 m/z
Capillary Exit	98.6 Volt	Skim 1	28.2 Volt	Trap Drive	43.7
Accumulation Time	50000 µs	Averages	10 Spectra	Auto MS/MS	Off

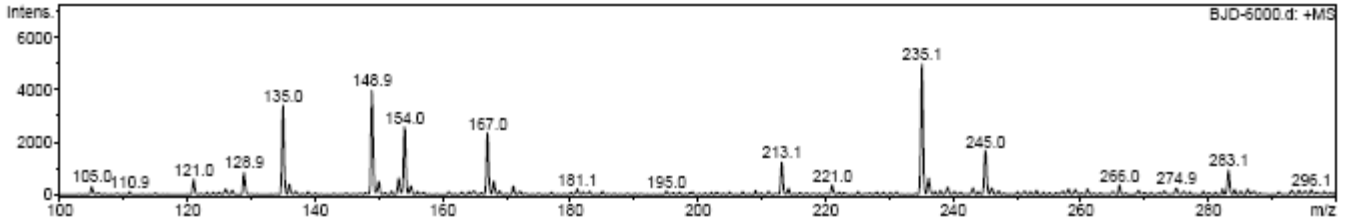

#	m/z	I	FWHM	S/N
1	128.9	847	0.3	26.4
2	135.0	3393	0.3	105.8
3	148.9	3968	0.3	123.7
4	153.1	625	0.3	19.5
5	154.0	2574	0.4	80.2
6	167.0	2351	0.3	73.3
7	213.1	1224	0.4	38.2
8	235.1	4982	0.4	155.3
9	245.0	1677	0.4	52.3
10	283.1	934	0.4	29.1

Figure 50: Mass spectrum of **16**.

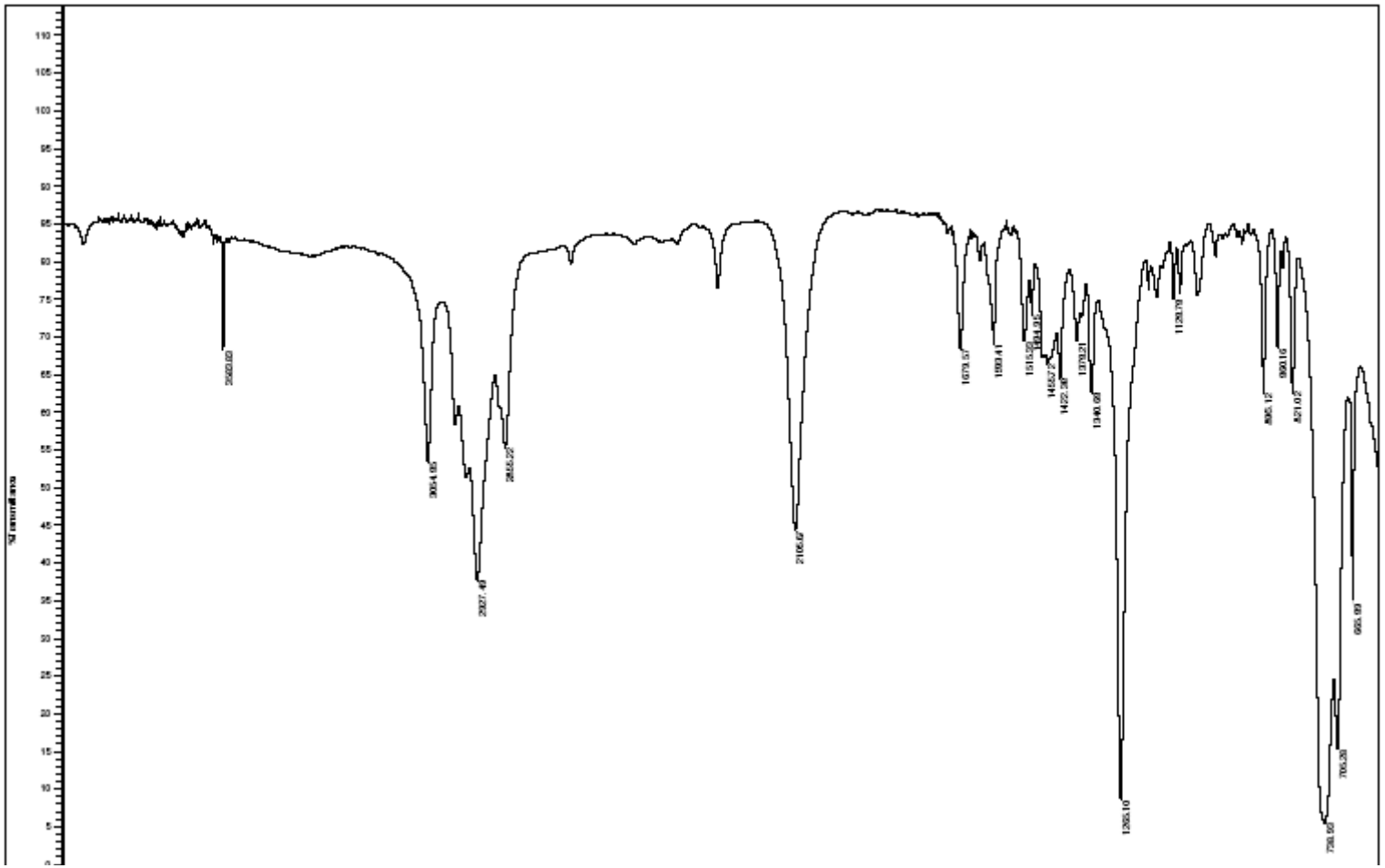

Figure 51: IR spectrum of **16**.

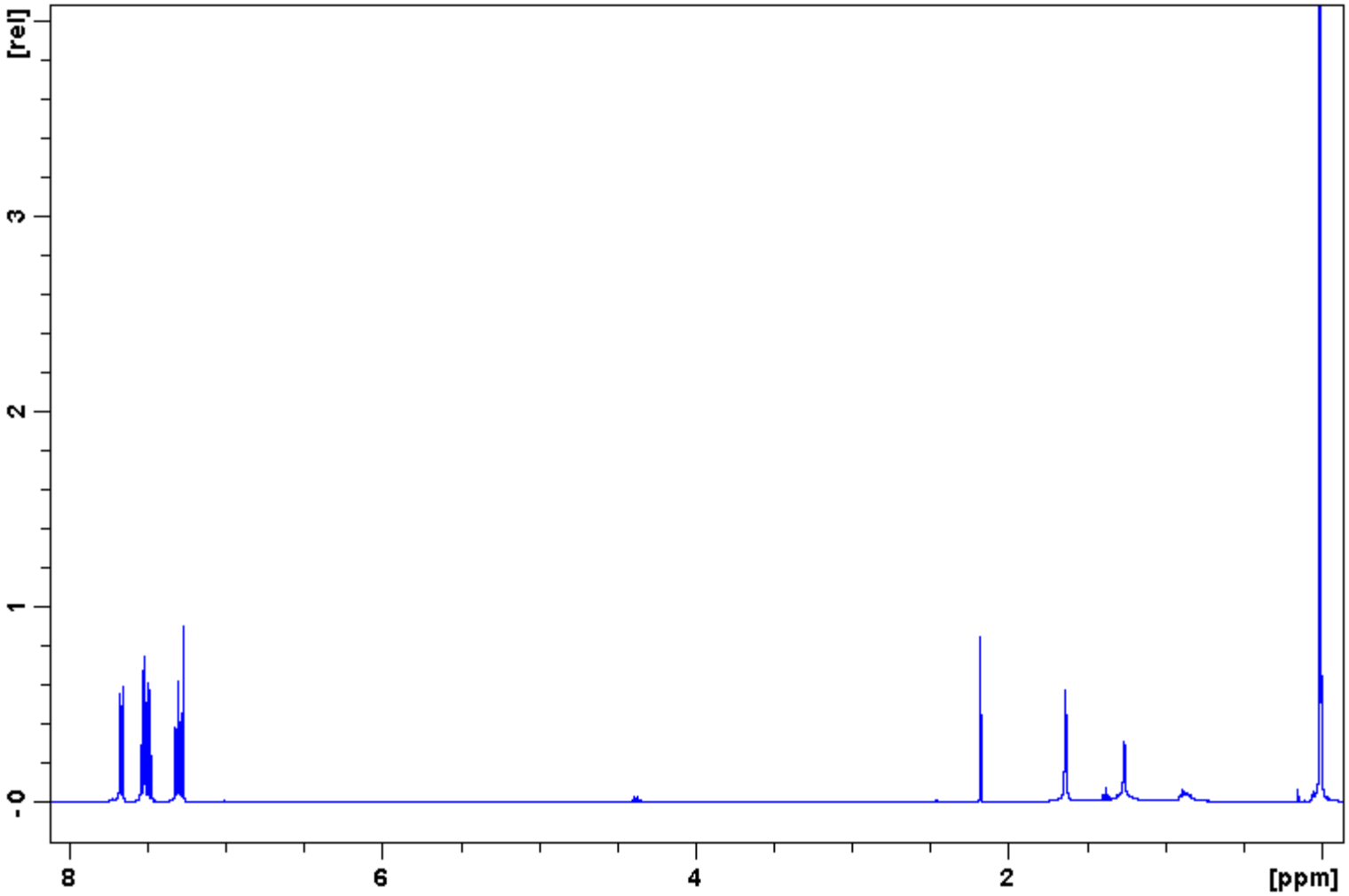

Figure 52: 400 MHz ^{1}H spectrum of **18**.

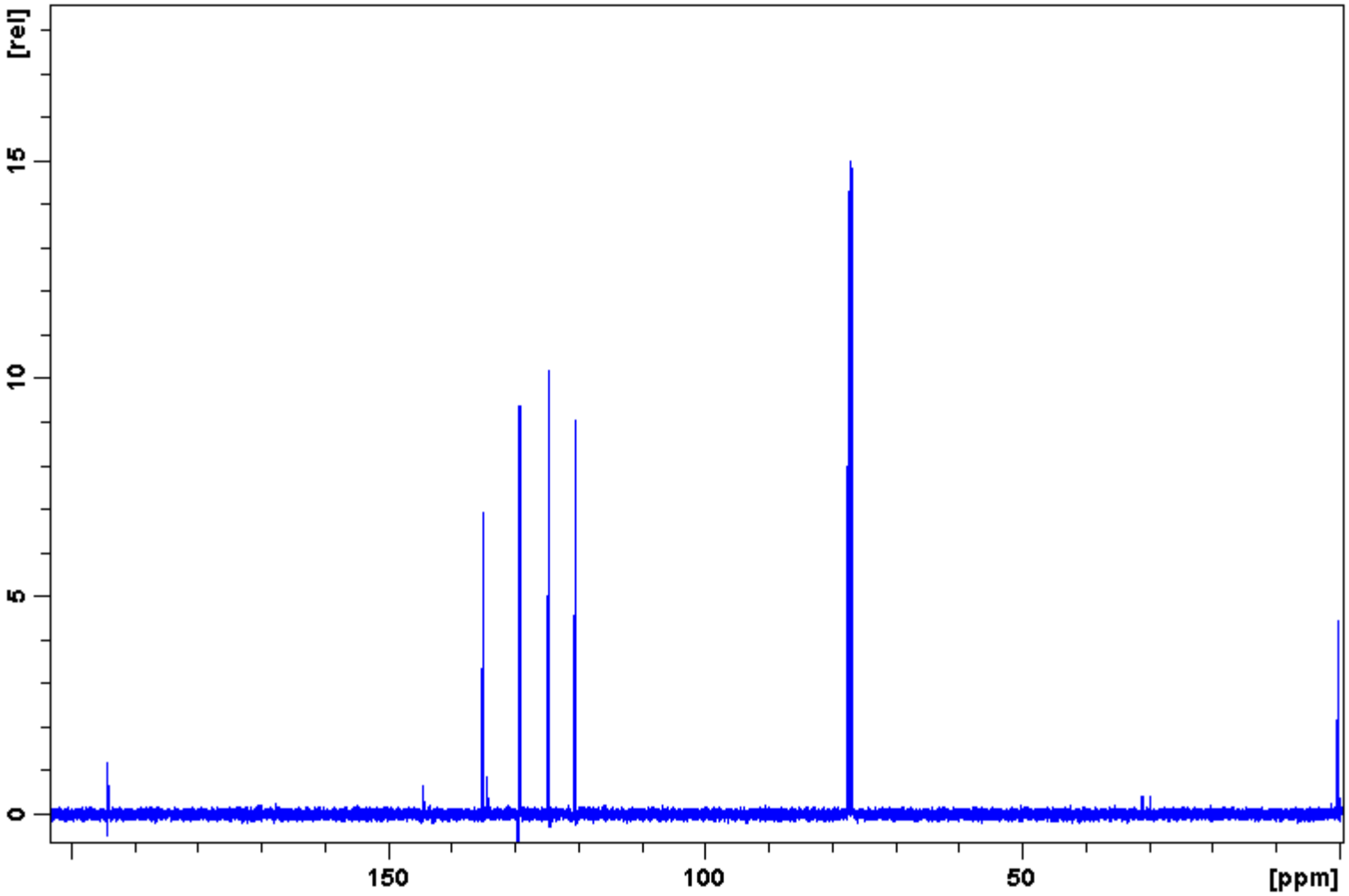

Figure 53: 100 MHz ^{13}C spectrum of **18**.

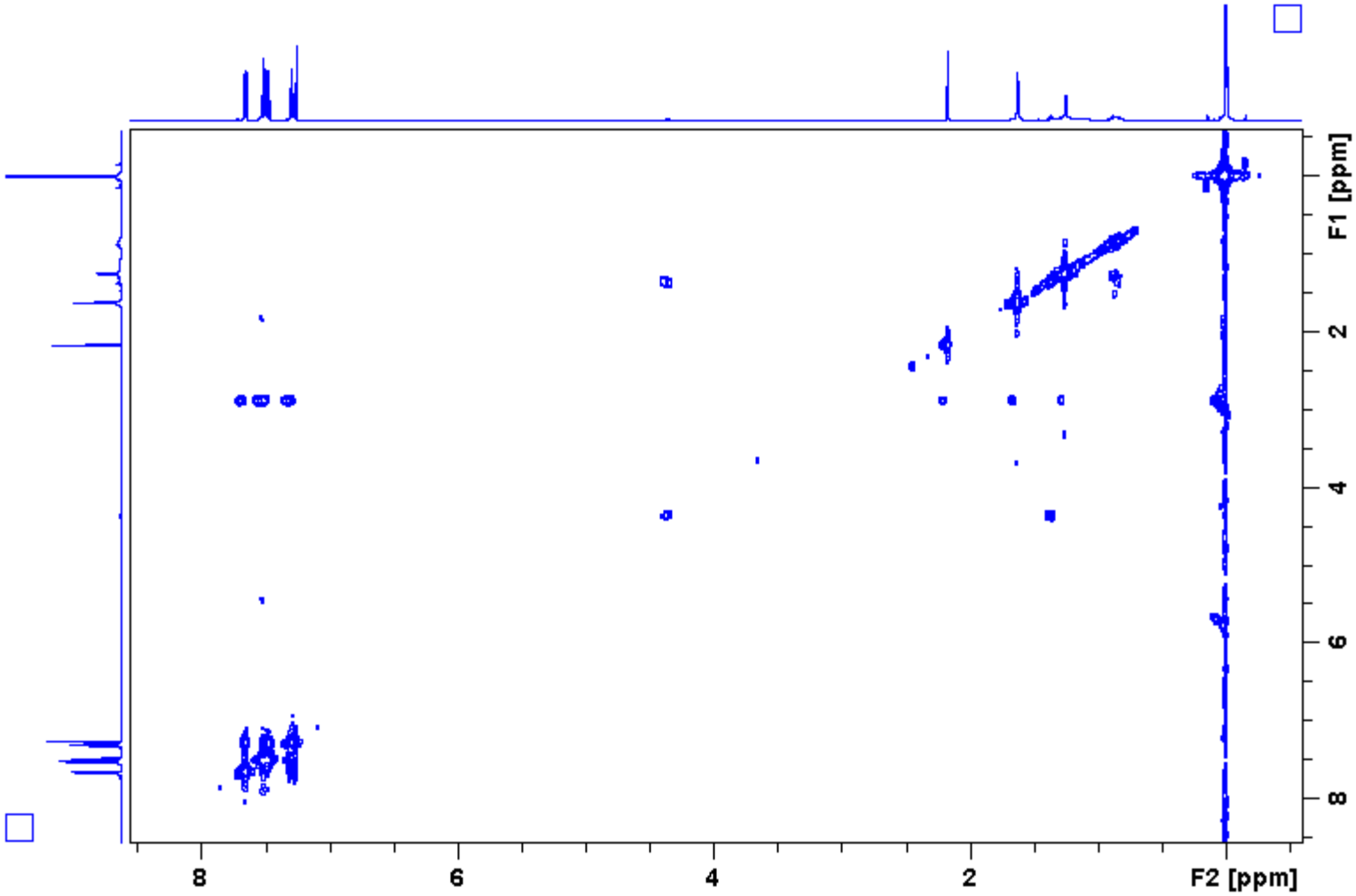

Figure 54: ^{1}H-^{1}H COSY spectrum of **18**.

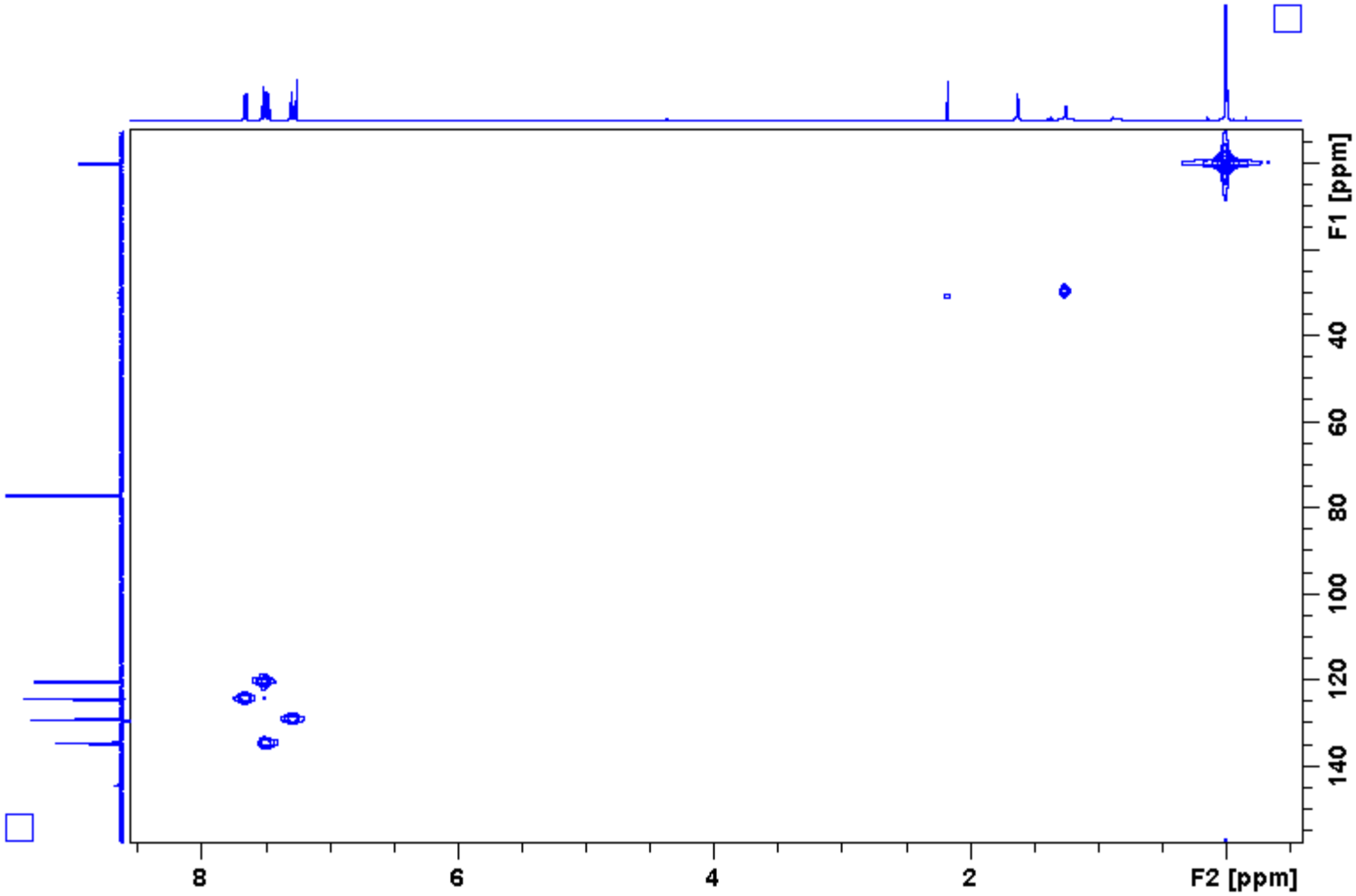

Figure 55: ^{1}H-^{13}C HMQC spectrum of **18**.

Mass Spectrum List Report

Analysis Info

Analysis Name	BJD-7008.d	Acquisition Date	07/21/08 14:56:42
Method	XQ Default.ms	Operator	Administrator
Sample Name	BD-2-087	Instrument	Esquire-LC_00135
Comment	BD-2-087		

Acquisition Parameter

Ion Source Type	ESI	Ion Polarity	Positive	Alternating Ion Polarity	n/a
Mass Range Mode	Std/Normal	Scan Begin	100.00 m/z	Scan End	300.00 m/z
Capillary Exit	98.6 Volt	Skim 1	28.2 Volt	Trap Drive	43.7
Accumulation Time	39123 µs	Averages	10 Spectra	Auto MS/MS	Off

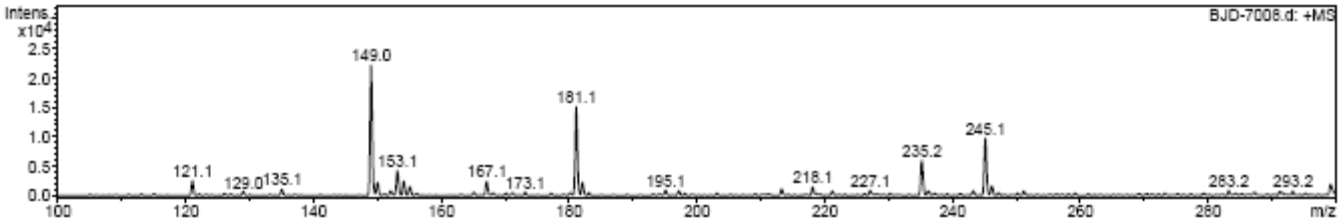

#	m/z	I	FWHM	S/N
1	121.1	2493	0.4	29.5
2	149.0	22128	0.4	261.8
3	150.0	2262	0.3	26.8
4	153.1	4242	0.4	50.2
5	154.1	2447	0.4	29.0
6	167.1	2434	0.4	28.8
7	181.1	15065	0.4	178.2
8	182.1	2243	0.3	26.5
9	235.2	5981	0.4	70.8
10	245.1	9725	0.4	115.1

Figure 56: Mass spectrum of **18**.

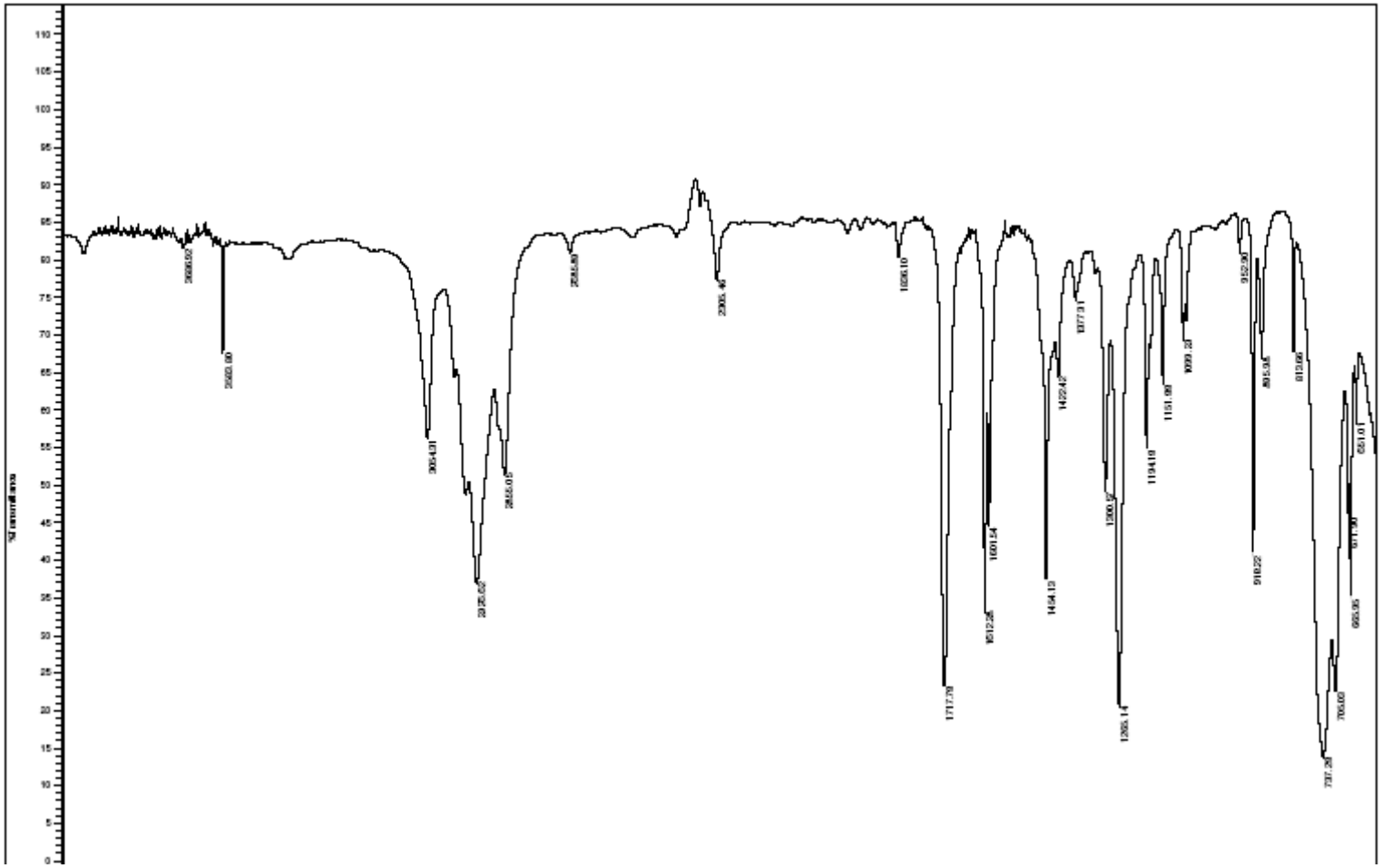

Figure 57: IR spectrum of **18**.

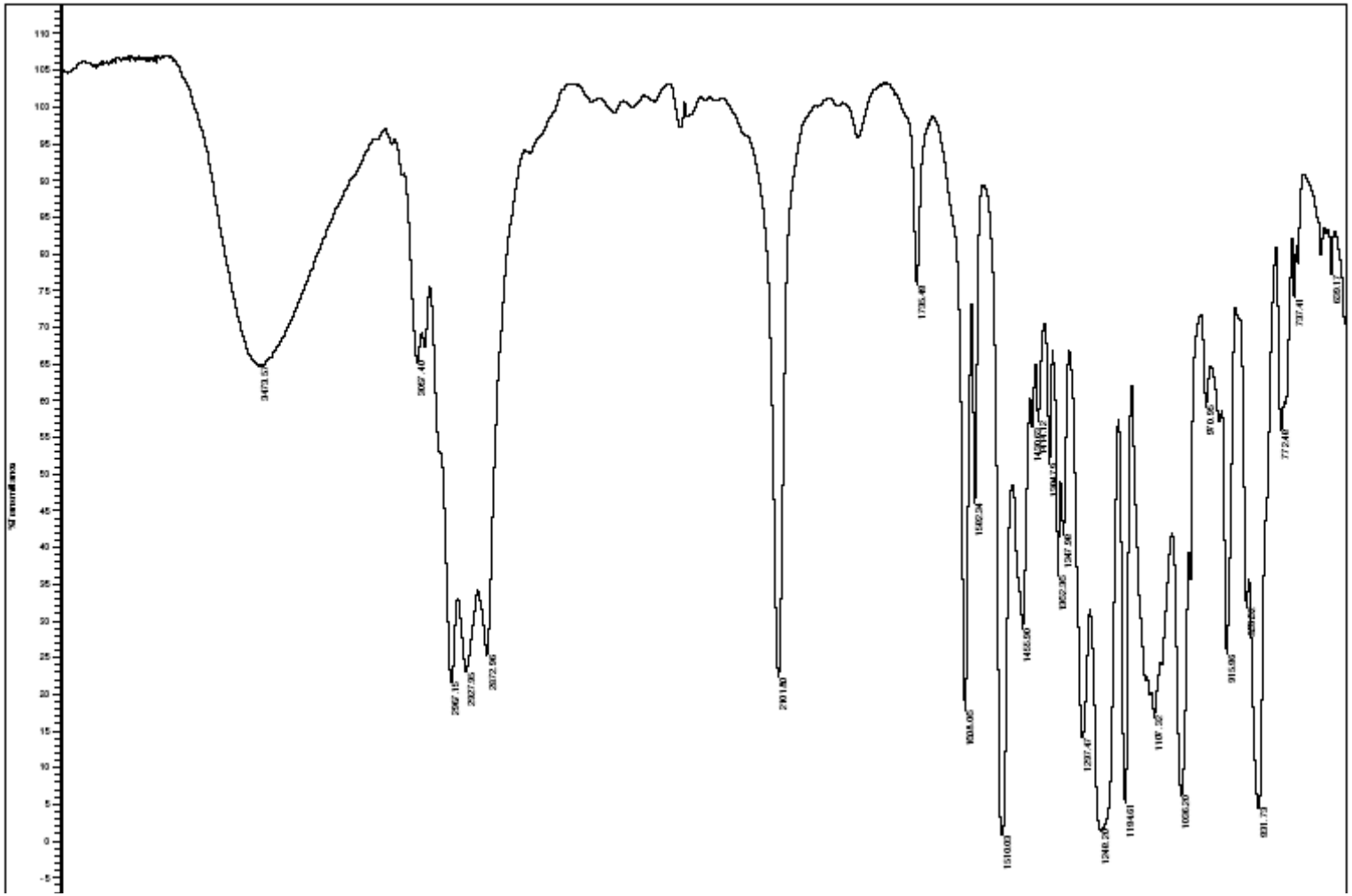

Figure 58: IR spectrum of **20**.

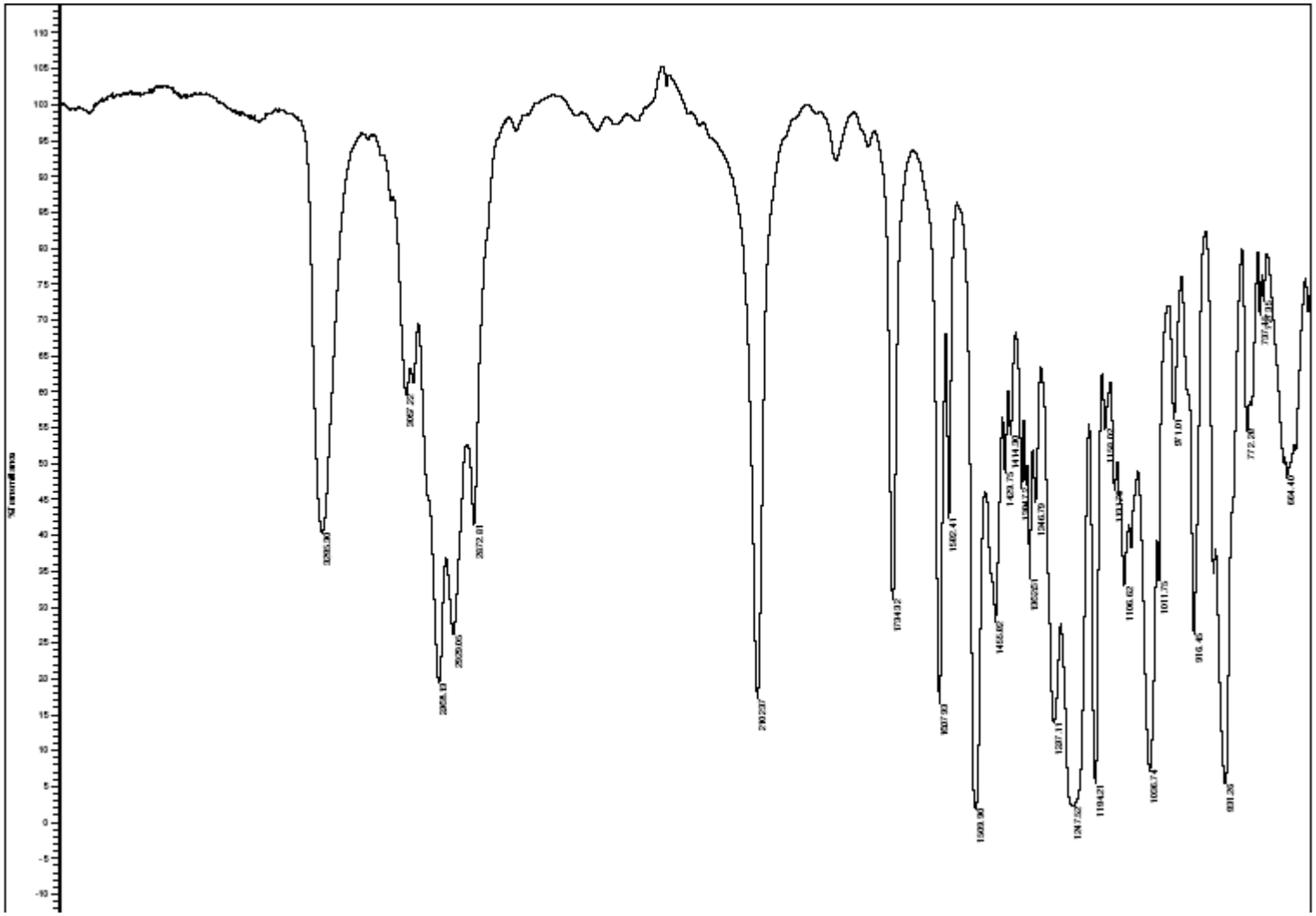

Figure 59: IR spectrum of **21**.

Appendix B

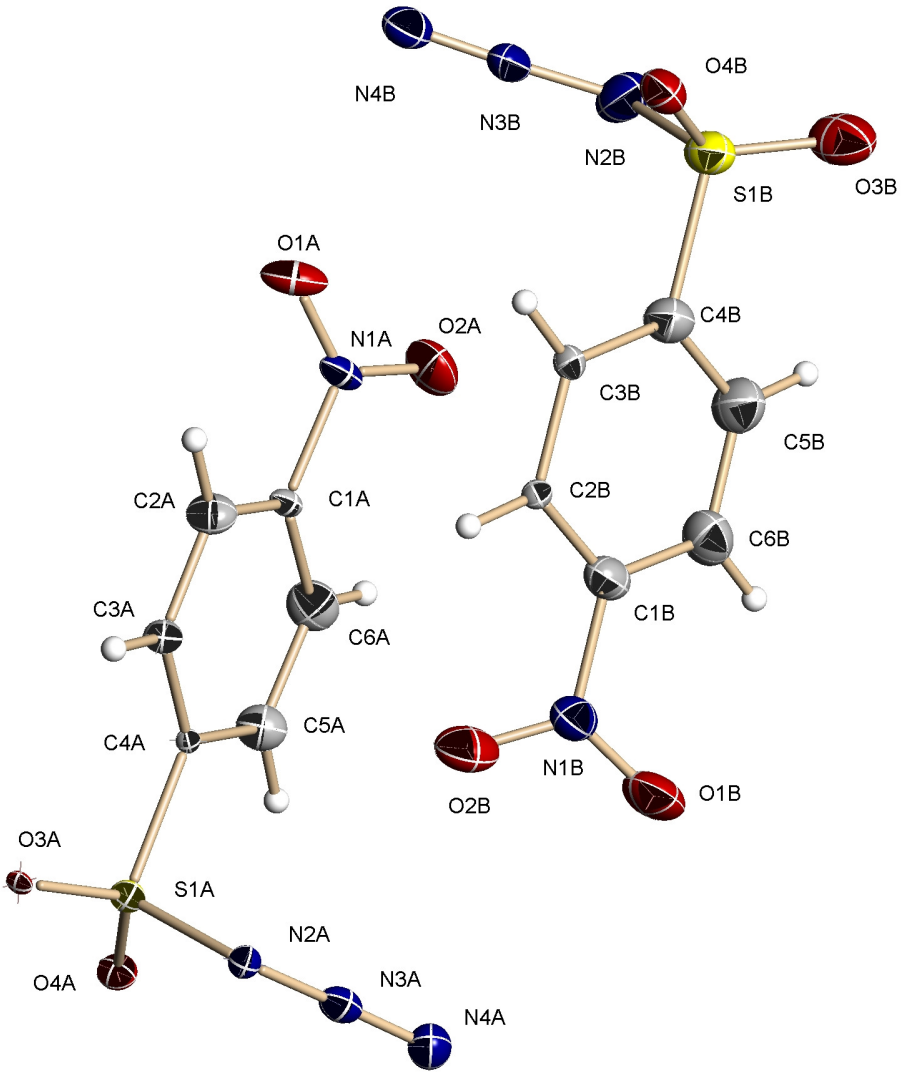
N4B
N3B
O4B
N2B
S1B
O3B
O1A
N1A
O2A
C4B
C3B
C5B
C2A
C1A
C2B
C6B
C3A
C6A
C1B
C5A
C4A
N1B
O1B
O2B
O3A
S1A
N2A
O4A
N3A
N4A

Table 1. Crystal data and structure refinement for 07mz179m:

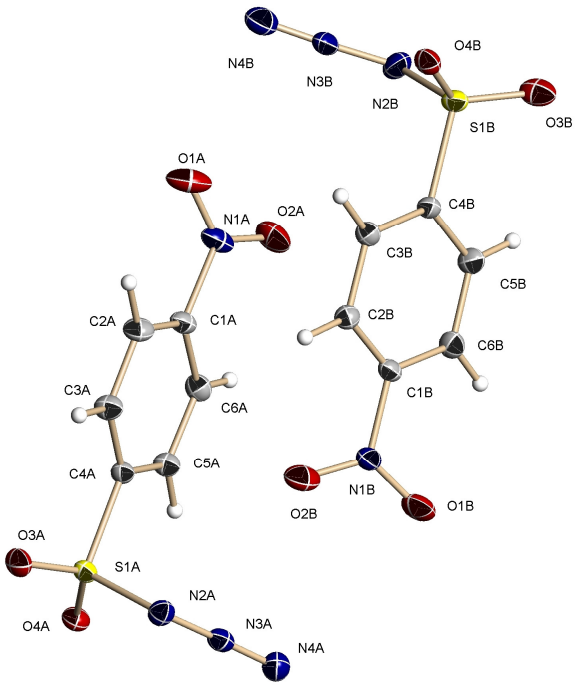

Identification code: 07mz179m
Empirical formula: C6 H4 N4 O4 S
Formula weight: 228.19
Temperature: 100(2) K
Wavelength: 0.71073 Å
Crystal system: Orthorhombic
Space group: $Pna2_1$
Unit cell dimensions:
a = 15.9258(9) Å, α = 90°
b = 10.7124(6) Å, β = 90°
c = 10.2493(6) Å, γ = 90°
Volume, Z: 1748.57(17) $Å^3$, 8
Density (calculated): 1.734 Mg/m^3
Absorption coefficient: 0.371 mm^{-1}
F(000): 928
Crystal size: 0.60 × 0.49 × 0.46 mm
Crystal shape, colour: block, colourless
θ range for data collection: 2.29 to 28.26°
Limiting indices: $-21 \le h \le 21$, $-14 \le k \le 14$, $-13 \le l \le 13$
Reflections collected: 17470
Independent reflections: 4335 (R(int) = 0.0218)
Completeness to θ = 28.26°: 100.0 %
Absorption correction: multi-scan
Max. and min. transmission: 0.843 and 0.802
Refinement method: Full-matrix least-squares on F^2
Data / restraints / parameters: 4335 / 1 / 271
Goodness-of-fit on F^2: 1.062
Final R indices [$I>2\sigma(I)$]: R1 = 0.0240, wR2 = 0.0643
R indices (all data): R1 = 0.0241, wR2 = 0.0645
Absolute structure parameter: 0.01(4)
Largest diff. peak and hole: 0.204 and −0.342 e × $Å^{-3}$

Refinement of F^2 against ALL reflections. The weighted R-factor wR and goodness of fit are based on F^2, conventional R-factors R are based on F, with F set to zero for negative F^2. The threshold expression of $F^2 > 2\sigma(F^2)$ is used only for calculating R-factors

Treatment of hydrogen atoms:
All hydrogen atoms were placed in calculated positions and were refined with an

isotropic displacement parameter 1.2 times that of the adjacent carbon atom.

Table 2. Atomic coordinates [× 10^4] and equivalent isotropic displacement parameters [$Å^2$ × 10^3] for 07mz179m. U(eq) is defined as one third of the trace of the orthogonalized U_{ij} tensor.

	x	y	z	U(eq)
C(1A)	5216(1)	2612(1)	3711(1)	18(1)
C(2A)	5178(1)	1360(1)	4038(2)	21(1)
C(3A)	5535(1)	988(1)	5216(1)	20(1)
C(4A)	5932(1)	1881(1)	5981(1)	15(1)
C(5A)	5975(1)	3137(1)	5626(1)	18(1)
C(6A)	5601(1)	3511(1)	4466(1)	20(1)
N(1A)	4807(1)	2999(1)	2478(1)	24(1)
N(2A)	5586(1)	1526(1)	8560(1)	19(1)
N(3A)	5449(1)	2639(1)	8914(1)	19(1)
N(4A)	5278(1)	3581(1)	9299(1)	24(1)
O(1A)	4639(1)	2187(1)	1685(1)	35(1)
O(2A)	4648(1)	4110(1)	2334(1)	35(1)
O(3A)	6550(1)	112(1)	7443(1)	22(1)
O(4A)	7020(1)	2309(1)	7810(1)	20(1)
S(1A)	6380(1)	1420(1)	7477(1)	15(1)
C(1B)	3253(1)	3587(1)	5360(1)	17(1)
C(2B)	3127(1)	2467(1)	4708(1)	18(1)
C(3B)	2711(1)	2501(1)	3516(1)	17(1)
C(4B)	2455(1)	3651(1)	3024(1)	16(1)
C(5B)	2588(1)	4769(1)	3688(1)	20(1)
C(6B)	2990(1)	4738(1)	4892(1)	20(1)
N(1B)	3689(1)	3560(1)	6631(1)	20(1)
N(2B)	2742(1)	4063(1)	448(1)	26(1)
N(3B)	3104(1)	3085(1)	45(1)	24(1)
N(4B)	3455(1)	2280(1)	-383(1)	30(1)
O(1B)	3620(1)	4469(1)	7348(1)	29(1)
O(2B)	4095(1)	2615(1)	6895(1)	28(1)
O(3B)	1433(1)	4812(1)	1446(1)	28(1)
O(4B)	1617(1)	2514(1)	1197(1)	20(1)
S(1B)	1949(1)	3725(1)	1495(1)	18(1)

All esds (except the esd in the dihedral angle between two l.s. planes) are estimated using the full covariance matrix. The cell esds are taken into account individually in the estimation of esds in distances, angles and torsion angles; correlations between esds in cell parameters are only used when they are defined by crystal symmetry. An approximate (isotropic) treatment of cell esds is used for estimating esds involving l.s. planes.

Table 3. Bond lengths [Å] and angles [deg] for 07mz179m.

C(1A)-C(6A)	1.3796(19)	O(1A)-N(1A)-O(2A)	124.48(13)
C(1A)-C(2A)	1.3832(18)	O(1A)-N(1A)-C(1A)	117.74(12)
C(1A)-N(1A)	1.4808(17)	O(2A)-N(1A)-C(1A)	117.78(12)
C(2A)-C(3A)	1.3928(19)	N(3A)-N(2A)-S(1A)	112.43(9)
C(2A)-H(2A)	0.9500	N(4A)-N(3A)-N(2A)	173.99(14)
C(3A)-C(4A)	1.3890(17)	O(3A)-S(1A)-O(4A)	121.43(6)
C(3A)-H(3A)	0.9500	O(3A)-S(1A)-N(2A)	102.96(6)
C(4A)-C(5A)	1.3952(16)	O(4A)-S(1A)-N(2A)	109.33(6)
C(4A)-S(1A)	1.7611(12)	O(3A)-S(1A)-C(4A)	109.33(6)
C(5A)-C(6A)	1.3897(18)	O(4A)-S(1A)-C(4A)	107.99(6)
C(5A)-H(5A)	0.9500	N(2A)-S(1A)-C(4A)	104.51(6)
C(6A)-H(6A)	0.9500	C(6B)-C(1B)-C(2B)	123.87(13)
N(1A)-O(1A)	1.2208(18)	C(6B)-C(1B)-N(1B)	117.72(11)
N(1A)-O(2A)	1.2260(17)	C(2B)-C(1B)-N(1B)	118.40(11)
N(2A)-N(3A)	1.2647(16)	C(1B)-C(2B)-C(3B)	118.01(12)
N(2A)-S(1A)	1.6868(12)	C(1B)-C(2B)-H(2B)	121.0
N(3A)-N(4A)	1.1171(17)	C(3B)-C(2B)-H(2B)	121.0
O(3A)-S(1A)	1.4278(9)	C(2B)-C(3B)-C(4B)	118.75(12)
O(4A)-S(1A)	1.4361(9)	C(2B)-C(3B)-H(3B)	120.6
C(1B)-C(6B)	1.3873(18)	C(4B)-C(3B)-H(3B)	120.6
C(1B)-C(2B)	1.3887(17)	C(3B)-C(4B)-C(5B)	122.59(12)
C(1B)-N(1B)	1.4765(17)	C(3B)-C(4B)-S(1B)	119.70(9)
C(2B)-C(3B)	1.3896(17)	C(5B)-C(4B)-S(1B)	117.71(9)
C(2B)-H(2B)	0.9500	C(6B)-C(5B)-C(4B)	118.91(12)
C(3B)-C(4B)	1.3924(17)	C(6B)-C(5B)-H(5B)	120.5
C(3B)-H(3B)	0.9500	C(4B)-C(5B)-H(5B)	120.5
C(4B)-C(5B)	1.3935(16)	C(1B)-C(6B)-C(5B)	117.85(12)
C(4B)-S(1B)	1.7643(14)	C(1B)-C(6B)-H(6B)	121.1
C(5B)-C(6B)	1.3897(19)	C(5B)-C(6B)-H(6B)	121.1
C(5B)-H(5B)	0.9500	O(1B)-N(1B)-O(2B)	124.70(13)
C(6B)-H(6B)	0.9500	O(1B)-N(1B)-C(1B)	118.09(11)
N(1B)-O(1B)	1.2250(16)	O(2B)-N(1B)-C(1B)	117.22(11)
N(1B)-O(2B)	1.2312(16)	N(3B)-N(2B)-S(1B)	111.66(10)
N(2B)-N(3B)	1.2654(19)	N(4B)-N(3B)-N(2B)	174.42(15)
N(2B)-S(1B)	1.6963(13)	O(3B)-S(1B)-O(4B)	121.28(6)
N(3B)-N(4B)	1.1172(19)	O(3B)-S(1B)-N(2B)	103.46(7)
O(3B)-S(1B)	1.4254(10)	O(4B)-S(1B)-N(2B)	109.44(6)
O(4B)-S(1B)	1.4340(9)	O(3B)-S(1B)-C(4B)	109.32(6)
		O(4B)-S(1B)-C(4B)	108.48(6)
		N(2B)-S(1B)-C(4B)	103.37(6)

C(6A)-C(1A)-C(2A)	124.09(12)
C(6A)-C(1A)-N(1A)	118.56(12)
C(2A)-C(1A)-N(1A)	117.34(12)
C(1A)-C(2A)-C(3A)	118.01(12)
C(1A)-C(2A)-H(2A)	121.0
C(3A)-C(2A)-H(2A)	121.0
C(4A)-C(3A)-C(2A)	118.56(12)
C(4A)-C(3A)-H(3A)	120.7
C(2A)-C(3A)-H(3A)	120.7
C(3A)-C(4A)-C(5A)	122.64(12)
C(3A)-C(4A)-S(1A)	118.84(10)
C(5A)-C(4A)-S(1A)	118.51(9)
C(6A)-C(5A)-C(4A)	118.69(11)
C(6A)-C(5A)-H(5A)	120.7
C(4A)-C(5A)-H(5A)	120.7
C(1A)-C(6A)-C(5A)	117.97(12)
C(1A)-C(6A)-H(6A)	121.0
C(5A)-C(6A)-H(6A)	121.0

Table 4. Anisotropic displacement parameters [$Å^2 \times 10^3$] for 07mz179m. The anisotropic displacement factor exponent takes the form: $-2\pi^2 [(h\,a^*)^2 U11 + ... + 2\,h\,k\,a^*\,b^*\,U12]$

	U11	U22	U33	U23	U13	U12
C(1A)	15(1)	26(1)	14(1)	3(1)	-1(1)	0(1)
C(2A)	21(1)	24(1)	19(1)	-2(1)	-4(1)	-5(1)
C(3A)	23(1)	17(1)	19(1)	0(1)	-2(1)	-2(1)
C(4A)	16(1)	17(1)	13(1)	1(1)	0(1)	1(1)
C(5A)	19(1)	17(1)	18(1)	1(1)	-2(1)	-2(1)
C(6A)	21(1)	18(1)	20(1)	4(1)	-1(1)	0(1)
N(1A)	18(1)	37(1)	18(1)	7(1)	-3(1)	-3(1)
N(2A)	21(1)	20(1)	17(1)	1(1)	2(1)	0(1)
N(3A)	17(1)	23(1)	15(1)	3(1)	-2(1)	-1(1)
N(4A)	25(1)	25(1)	24(1)	0(1)	1(1)	3(1)
O(1A)	39(1)	45(1)	20(1)	5(1)	-11(1)	-14(1)
O(2A)	39(1)	39(1)	29(1)	10(1)	-8(1)	10(1)
O(3A)	26(1)	16(1)	24(1)	2(1)	-4(1)	4(1)
O(4A)	18(1)	22(1)	19(1)	0(1)	-3(1)	-2(1)
S(1A)	16(1)	15(1)	15(1)	2(1)	-2(1)	1(1)
C(1B)	14(1)	22(1)	14(1)	-2(1)	-1(1)	-2(1)
C(2B)	18(1)	17(1)	18(1)	1(1)	0(1)	1(1)
C(3B)	19(1)	16(1)	17(1)	-2(1)	0(1)	0(1)
C(4B)	17(1)	16(1)	13(1)	-1(1)	-1(1)	-1(1)
C(5B)	26(1)	14(1)	19(1)	-1(1)	-1(1)	-1(1)
C(6B)	23(1)	17(1)	19(1)	-4(1)	1(1)	-3(1)
N(1B)	16(1)	29(1)	16(1)	0(1)	-1(1)	-3(1)
N(2B)	36(1)	25(1)	16(1)	1(1)	2(1)	-8(1)
N(3B)	20(1)	36(1)	15(1)	1(1)	-3(1)	-7(1)
N(4B)	21(1)	46(1)	22(1)	-2(1)	-2(1)	0(1)
O(1B)	34(1)	31(1)	22(1)	-8(1)	-8(1)	-4(1)
O(2B)	25(1)	38(1)	23(1)	1(1)	-6(1)	6(1)
O(3B)	36(1)	20(1)	26(1)	0(1)	-9(1)	6(1)
O(4B)	23(1)	18(1)	19(1)	-3(1)	-3(1)	-2(1)
S(1B)	23(1)	16(1)	14(1)	0(1)	-3(1)	0(1)

Table 5. Hydrogen coordinates ($\times 10^4$) and isotropic displacement parameters ($Å^2 \times 10^3$) for 07mz179m.

	x	y	z	U(eq)
H(2A)	4916	772	3477	26
H(3A)	5508	142	5490	24
H(5A)	6256	3724	6167	21
H(6A)	5609	4361	4201	23
H(2B)	3319	1700	5065	21
H(3B)	2604	1753	3046	20
H(5B)	2407	5539	3325	23

H(6B)	3081	5481	5378	24

Table 6. Torsion angles [deg] for 07mz179m.

C(6A)-C(1A)-C(2A)-C(3A)	1.3(2)
N(1A)-C(1A)-C(2A)-C(3A)	-177.85(12)
C(1A)-C(2A)-C(3A)-C(4A)	-1.8(2)
C(2A)-C(3A)-C(4A)-C(5A)	1.0(2)
C(2A)-C(3A)-C(4A)-S(1A)	179.60(11)
C(3A)-C(4A)-C(5A)-C(6A)	0.53(19)
S(1A)-C(4A)-C(5A)-C(6A)	-178.08(10)
C(2A)-C(1A)-C(6A)-C(5A)	0.2(2)
N(1A)-C(1A)-C(6A)-C(5A)	179.35(12)
C(4A)-C(5A)-C(6A)-C(1A)	-1.12(19)
C(6A)-C(1A)-N(1A)-O(1A)	163.84(13)
C(2A)-C(1A)-N(1A)-O(1A)	-16.97(19)
C(6A)-C(1A)-N(1A)-O(2A)	-17.24(18)
C(2A)-C(1A)-N(1A)-O(2A)	161.95(13)
N(3A)-N(2A)-S(1A)-O(3A)	167.36(10)
N(3A)-N(2A)-S(1A)-O(4A)	36.98(11)
N(3A)-N(2A)-S(1A)-C(4A)	-78.41(11)
C(3A)-C(4A)-S(1A)-O(3A)	22.62(12)
C(5A)-C(4A)-S(1A)-O(3A)	-158.72(10)
C(3A)-C(4A)-S(1A)-O(4A)	156.63(10)
C(5A)-C(4A)-S(1A)-O(4A)	-24.70(12)
C(3A)-C(4A)-S(1A)-N(2A)	-87.04(11)
C(5A)-C(4A)-S(1A)-N(2A)	91.63(11)
C(6B)-C(1B)-C(2B)-C(3B)	-0.1(2)
N(1B)-C(1B)-C(2B)-C(3B)	179.65(11)
C(1B)-C(2B)-C(3B)-C(4B)	1.09(18)
C(2B)-C(3B)-C(4B)-C(5B)	-1.0(2)
C(2B)-C(3B)-C(4B)-S(1B)	178.48(10)
C(3B)-C(4B)-C(5B)-C(6B)	-0.2(2)
S(1B)-C(4B)-C(5B)-C(6B)	-179.65(10)
C(2B)-C(1B)-C(6B)-C(5B)	-1.1(2)
N(1B)-C(1B)-C(6B)-C(5B)	179.20(11)
C(4B)-C(5B)-C(6B)-C(1B)	1.15(19)
C(6B)-C(1B)-N(1B)-O(1B)	17.52(17)
C(2B)-C(1B)-N(1B)-O(1B)	-162.24(12)
C(6B)-C(1B)-N(1B)-O(2B)	-162.90(13)
C(2B)-C(1B)-N(1B)-O(2B)	17.34(17)
N(3B)-N(2B)-S(1B)-O(3B)	-158.62(10)
N(3B)-N(2B)-S(1B)-O(4B)	-28.04(12)
N(3B)-N(2B)-S(1B)-C(4B)	87.39(11)
C(3B)-C(4B)-S(1B)-O(3B)	154.50(11)
C(5B)-C(4B)-S(1B)-O(3B)	-26.01(13)
C(3B)-C(4B)-S(1B)-O(4B)	20.30(13)
C(5B)-C(4B)-S(1B)-O(4B)	-160.21(10)
C(3B)-C(4B)-S(1B)-N(2B)	-95.81(12)
C(5B)-C(4B)-S(1B)-N(2B)	83.68(11)

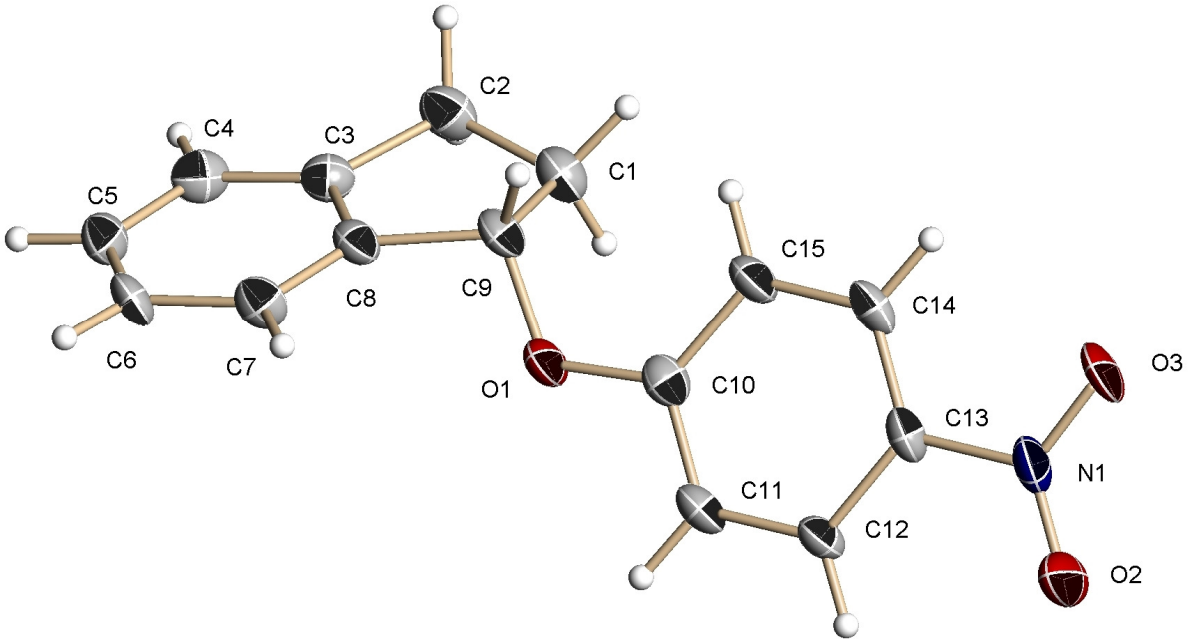
C2
C4
C3
C1
C5
C15
C14
C8
C9
C6
C7
O1
C10
O3
C13
N1
C11
C12
O2

Table 1. Crystal data and structure refinement for 07mz178m:

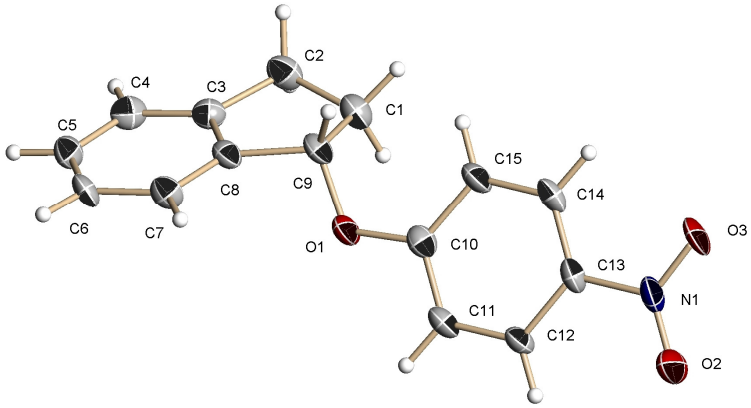

Identification code: 07mz178m
Empirical formula: C15 H13 N O3
Formula weight: 255.26
Temperature: 100(2) K
Wavelength: 0.71073 Å
Crystal system: Triclinic
Space group: P-1
Unit cell dimensions:
a = 7.730(2) Å, α = 65.663(6)°
b = 9.343(2) Å, β = 88.623(7)°
c = 9.997(3) Å, γ = 72.046(7)°
Volume, Z: 621.4(3) Å^3, 2
Density (calculated): 1.364 Mg/m^3
Absorption coefficient: 0.096 mm^{-1}
F(000): 268
Crystal size: 0.56 × 0.20 × 0.09 mm
Crystal shape, colour: plate, colourless
θ range for data collection: 2.25 to 26.37°
Limiting indices: $-9 \le h \le 9$, $-10 \le k \le 11$, $0 \le l \le 12$
Reflections collected: 10284
Independent reflections: 2665 (R(int) = not defined)
Completeness to θ = 26.37°: 97.2 %
Absorption correction: multi-scan
Max. and min. transmission: 1 and 0.629
Refinement method: Full-matrix least-squares on F^2
Data / restraints / parameters: 2665 / 0 / 173
Goodness-of-fit on F^2: 1.265
Final R indices [$I>2\sigma(I)$]: R1 = 0.1091, wR2 = 0.2234
R indices (all data): R1 = 0.1305, wR2 = 0.2362
Largest diff. peak and hole: 0.463 and -0.384 e × Å^{-3}

Refinement of F^2 against ALL reflections. The weighted R-factor wR and goodness of fit are based on F^2, conventional R-factors R are based on F, with F set to zero for negative F^2. The threshold expression of $F^2 > 2\sigma(F^2)$ is used only for calculating R-factors

Comments:
The crystal under investigation was found to be non-merohedrally twinned. The

orientation matrices for the two components were identified using the program Cell_Now, and the two components were integrated using Saint, resulting in a total of 10284 reflections. 4032 reflections (2399 unique ones) involved component 1 only (mean I/sigma = 6.7), 4042 reflections (2397 unique ones) involved component 2 only (mean I/sigma = 6.3), and 2210 reflections (1455 unique ones) involved both components (mean I/sigma = 9.4). The exact twin matrix identified by the integration program was found to be -0.99981 -0.00082 0.00260, -0.72347 1.00106 -0.75378, -0.00720 0.00650 -1.00155.

The data were corrected for absorption using twinabs, and the structure was solved using direct methods with only the non-overlapping reflections of component 1. The structure was refined using the hklf 5 routine with all reflections of component 1 (including the overlapping ones) below a d-spacing threshold of 0.8, resulting in a BASF value of 0.472(4).

Treatment of hydrogen atoms:

All hydrogen atoms were placed in calculated positions and were refined with an isotropic displacement parameter 1.2 times that of the adjacent carbon atom.

Table 2. Atomic coordinates [× 10^4] and equivalent isotropic displacement parameters [Å^2 × 10^3] for 07mz178m. U(eq) is defined as one third of the trace of the orthogonalized U_{ij} tensor.

	x	y	z	U(eq)
C(1)	2080(8)	1418(8)	4318(7)	33(1)
C(2)	2806(8)	2436(8)	4913(7)	35(1)
C(3)	4272(7)	2870(7)	3922(6)	28(1)
C(4)	5594(8)	3527(7)	4112(6)	31(1)
C(5)	6742(7)	3893(7)	3007(7)	31(1)
C(6)	6599(7)	3635(7)	1753(6)	29(1)
C(7)	5299(7)	2935(7)	1601(6)	29(1)
C(8)	4154(7)	2566(6)	2680(6)	26(1)
C(9)	2653(7)	1811(7)	2738(6)	28(1)
C(10)	2340(7)	-409(7)	2222(6)	28(1)
C(11)	3209(7)	-1794(7)	1956(6)	28(1)
C(12)	2200(7)	-2653(7)	1678(6)	25(1)
C(13)	291(7)	-2083(7)	1644(6)	26(1)
C(14)	-578(7)	-705(7)	1907(6)	28(1)
C(15)	428(7)	130(7)	2218(7)	31(1)
N(1)	-778(6)	-2961(6)	1304(5)	31(1)
O(1)	3454(5)	345(5)	2487(4)	30(1)
O(2)	16(6)	-4220(6)	1131(5)	42(1)
O(3)	-2472(5)	-2377(5)	1187(5)	39(1)

All esds (except the esd in the dihedral angle between two l.s. planes) are estimated using the full covariance matrix. The cell esds are taken into account individually in the estimation of esds in distances, angles and torsion angles; correlations between esds in cell parameters are only

used when they are defined by crystal symmetry. An approximate (isotropic) treatment of cell esds is used for estimating esds involving l.s. planes.

Table 3. Bond lengths [Å] and angles [deg] for 07mz178m.

C(1)-C(2)	1.544(8)	C(3)-C(4)-H(4)	121.2
C(1)-C(9)	1.555(8)	C(5)-C(4)-H(4)	121.2
C(1)-H(1A)	0.9900	C(6)-C(5)-C(4)	122.4(5)
C(1)-H(1B)	0.9900	C(6)-C(5)-H(5)	118.8
C(2)-C(3)	1.526(8)	C(4)-C(5)-H(5)	118.8
C(2)-H(2A)	0.9900	C(5)-C(6)-C(7)	119.0(5)
C(2)-H(2B)	0.9900	C(5)-C(6)-H(6)	120.5
C(3)-C(8)	1.393(8)	C(7)-C(6)-H(6)	120.5
C(3)-C(4)	1.396(8)	C(8)-C(7)-C(6)	119.3(5)
C(4)-C(5)	1.397(8)	C(8)-C(7)-H(7)	120.3
C(4)-H(4)	0.9500	C(6)-C(7)-H(7)	120.3
C(5)-C(6)	1.383(8)	C(7)-C(8)-C(3)	121.3(5)
C(5)-H(5)	0.9500	C(7)-C(8)-C(9)	128.1(5)
C(6)-C(7)	1.399(8)	C(3)-C(8)-C(9)	110.6(5)
C(6)-H(6)	0.9500	O(1)-C(9)-C(8)	106.9(4)
C(7)-C(8)	1.379(7)	O(1)-C(9)-C(1)	113.1(5)
C(7)-H(7)	0.9500	C(8)-C(9)-C(1)	104.2(4)
C(8)-C(9)	1.521(7)	O(1)-C(9)-H(9)	110.8
C(9)-O(1)	1.440(6)	C(8)-C(9)-H(9)	110.8
C(9)-H(9)	1.0000	C(1)-C(9)-H(9)	110.8
C(10)-O(1)	1.359(7)	O(1)-C(10)-C(11)	115.7(5)
C(10)-C(11)	1.391(8)	O(1)-C(10)-C(15)	123.7(5)
C(10)-C(15)	1.407(7)	C(11)-C(10)-C(15)	120.5(5)
C(11)-C(12)	1.382(8)	C(12)-C(11)-C(10)	120.3(5)
C(11)-H(11)	0.9500	C(12)-C(11)-H(11)	119.9
C(12)-C(13)	1.402(7)	C(10)-C(11)-H(11)	119.9
C(12)-H(12)	0.9500	C(11)-C(12)-C(13)	118.7(5)
C(13)-C(14)	1.384(8)	C(11)-C(12)-H(12)	120.7
C(13)-N(1)	1.460(7)	C(13)-C(12)-H(12)	120.7
C(14)-C(15)	1.376(8)	C(14)-C(13)-C(12)	121.1(5)
C(14)-H(14)	0.9500	C(14)-C(13)-N(1)	120.2(5)
C(15)-H(15)	0.9500	C(12)-C(13)-N(1)	118.6(5)
N(1)-O(2)	1.228(6)	C(15)-C(14)-C(13)	120.3(5)
N(1)-O(3)	1.241(6)	C(15)-C(14)-H(14)	119.9
		C(13)-C(14)-H(14)	119.9
C(2)-C(1)-C(9)	106.7(5)	C(14)-C(15)-C(10)	119.1(5)
C(2)-C(1)-H(1A)	110.4	C(14)-C(15)-H(15)	120.5
C(9)-C(1)-H(1A)	110.4	C(10)-C(15)-H(15)	120.5
C(2)-C(1)-H(1B)	110.4	O(2)-N(1)-O(3)	122.8(5)
C(9)-C(1)-H(1B)	110.4	O(2)-N(1)-C(13)	119.5(4)
H(1A)-C(1)-H(1B)	108.6	O(3)-N(1)-C(13)	117.7(5)
C(3)-C(2)-C(1)	103.5(4)	C(10)-O(1)-C(9)	119.1(4)
C(3)-C(2)-H(2A)	111.1		
C(1)-C(2)-H(2A)	111.1		
C(3)-C(2)-H(2B)	111.1		
C(1)-C(2)-H(2B)	111.1		
H(2A)-C(2)-H(2B)	109.0		
C(8)-C(3)-C(4)	120.2(5)		
C(8)-C(3)-C(2)	111.4(5)		
C(4)-C(3)-C(2)	128.4(5)		
C(3)-C(4)-C(5)	117.7(5)		

Table 4. Anisotropic displacement parameters [$Å^2 \times 10^3$] for 07mz178m. The anisotropic displacement factor exponent takes the form: $-2\pi^2 [(h a^*)^2 U11 + ... + 2 h k a^* b^* U12]$

	U11	U22	U33	U23	U13	U12
C(1)	25(3)	41(3)	33(3)	-15(3)	6(2)	-12(2)
C(2)	30(3)	45(4)	32(3)	-20(3)	7(3)	-12(3)
C(3)	28(3)	28(3)	27(3)	-11(2)	2(2)	-6(2)
C(4)	32(3)	35(3)	28(3)	-16(2)	-3(2)	-7(2)
C(5)	21(3)	32(3)	40(3)	-14(3)	-1(2)	-9(2)
C(6)	17(3)	39(3)	34(3)	-15(3)	10(2)	-13(2)
C(7)	28(3)	38(3)	23(3)	-15(2)	6(2)	-11(2)
C(8)	18(3)	28(3)	29(3)	-11(2)	3(2)	-5(2)
C(9)	15(2)	35(3)	34(3)	-14(3)	2(2)	-7(2)
C(10)	21(3)	33(3)	27(3)	-11(2)	0(2)	-8(2)
C(11)	17(2)	37(3)	27(3)	-13(2)	5(2)	-7(2)
C(12)	16(2)	32(3)	30(3)	-16(2)	4(2)	-6(2)
C(13)	20(3)	36(3)	26(3)	-12(2)	5(2)	-15(2)
C(14)	19(2)	43(3)	23(3)	-13(2)	8(2)	-14(2)
C(15)	17(3)	38(3)	41(3)	-20(3)	7(2)	-8(2)
N(1)	23(2)	43(3)	38(3)	-20(2)	10(2)	-20(2)
O(1)	16(2)	37(2)	42(2)	-22(2)	5(2)	-10(2)
O(2)	24(2)	48(3)	68(3)	-37(2)	7(2)	-16(2)
O(3)	15(2)	53(3)	56(3)	-25(2)	9(2)	-18(2)

Table 5. Hydrogen coordinates ($\times 10^4$) and isotropic displacement parameters ($Å^2 \times 10^3$) for 07mz178m.

	x	y	z	U(eq)
H(1A)	730	1738	4284	40
H(1B)	2617	215	4965	40
H(2A)	1819	3453	4825	41
H(2B)	3339	1767	5961	41
H(4)	5709	3719	4963	38
H(5)	7654	4335	3122	37
H(6)	7373	3930	1006	35
H(7)	5207	2715	764	35
H(9)	1595	2621	1971	34
H(11)	4502	-2150	1965	33
H(12)	2789	-3612	1514	30
H(14)	-1874	-333	1873	33
H(15)	-161	1057	2427	37

Table 6. Torsion angles [deg] for 07mz178m.

C(9)-C(1)-C(2)-C(3)	-18.7(6)
C(1)-C(2)-C(3)-C(8)	13.6(6)
C(1)-C(2)-C(3)-C(4)	-167.8(5)
C(8)-C(3)-C(4)-C(5)	1.4(8)
C(2)-C(3)-C(4)-C(5)	-177.1(6)
C(3)-C(4)-C(5)-C(6)	0.4(8)
C(4)-C(5)-C(6)-C(7)	-2.1(8)
C(5)-C(6)-C(7)-C(8)	2.0(8)
C(6)-C(7)-C(8)-C(3)	-0.3(8)
C(6)-C(7)-C(8)-C(9)	179.8(5)
C(4)-C(3)-C(8)-C(7)	-1.4(8)
C(2)-C(3)-C(8)-C(7)	177.3(5)
C(4)-C(3)-C(8)-C(9)	178.5(5)
C(2)-C(3)-C(8)-C(9)	-2.8(6)
C(7)-C(8)-C(9)-O(1)	50.7(7)
C(3)-C(8)-C(9)-O(1)	-129.1(5)
C(7)-C(8)-C(9)-C(1)	170.7(5)
C(3)-C(8)-C(9)-C(1)	-9.2(6)
C(2)-C(1)-C(9)-O(1)	133.0(5)
C(2)-C(1)-C(9)-C(8)	17.3(6)
O(1)-C(10)-C(11)-C(12)	179.8(5)
C(15)-C(10)-C(11)-C(12)	0.3(8)
C(10)-C(11)-C(12)-C(13)	1.2(8)
C(11)-C(12)-C(13)-C(14)	-1.1(8)
C(11)-C(12)-C(13)-N(1)	178.0(5)
C(12)-C(13)-C(14)-C(15)	-0.4(8)
N(1)-C(13)-C(14)-C(15)	-179.6(5)
C(13)-C(14)-C(15)-C(10)	1.8(8)
O(1)-C(10)-C(15)-C(14)	178.7(5)
C(11)-C(10)-C(15)-C(14)	-1.8(8)
C(14)-C(13)-N(1)-O(2)	-177.1(5)
C(12)-C(13)-N(1)-O(2)	3.7(8)
C(14)-C(13)-N(1)-O(3)	3.6(8)
C(12)-C(13)-N(1)-O(3)	-175.6(5)
C(11)-C(10)-O(1)-C(9)	178.5(5)
C(15)-C(10)-O(1)-C(9)	-2.0(8)
C(8)-C(9)-O(1)-C(10)	-168.5(5)
C(1)-C(9)-O(1)-C(10)	77.4(6)